Effects of diallyl trisulfide-induced oxidative stress on proliferation, morphology and cell death in cancer cells

By Nibha Surajlal

Submitted in fulfilment of the requirements for the degree

MSc: Human Physiology

In the Department of Physiology
School of Medicine
Faculty of Health Sciences
University of Pretoria
Pretoria

Supervisor: Dr Michelle Helen Visagie
Department of Physiology
University of Pretoria

Co-supervisor: Prof Annie Joubert
Department of Physiology
University of Pretoria

Co-supervisor: Prof Friede Wenhold
Department of Human Nutrition
University of Pretoria

Abstract

Literature indicates that garlic possesses antiproliferative- and antimitotic activity due to containing organosulfur compounds including diallyl trisulfide (DATS). However, the role of reactive oxygen species (ROS) in the antiproliferative- and antimitotic effects exerted by DATS remains elusive. The role of oxidative stress in the effects induced by DATS on cell proliferation, the induction of oxidative stress morphology, cell cycle progression and mitochondrial membrane potential was investigated in this study, as well as the role of some possible sources of oxidative stress as induced by DATS, including dysregulation of antioxidant enzymes including superoxide dismutase (SOD) and catalase were also investigated in breast (MDA-MB-231)- and lung cancer cells (A549). Experiments were conducted in the presence or absence of the ROS scavenger, N-acetyl cystein (NAC) to determine if DATS is dependant on ROS as well as in the presence of sodium azide (SA), N, N-dimethyl thiourea (DMTU), 2-(4-Carboxyphenyl)-4,4,5,5-tetramethylimidazoline-1-oxyl-3-oxide (Carboxy-PTIO), D-Mannitol (Mannitol), Tiron and Trolox which scavange scavenge $O_2^{\bullet}$, H_2O_2, •NO, •OH, O_2^{-}, and $HO_2^{\bullet}$ respectively, to determine the dependency of the effects of DATS on specific ROS. Exposure to 100 µM DATS for 24 h in the MDA-MB-231 cell line reduced cell growth by 36%; this was abolished in the presence of 2 mM NAC. Co-exposure to SA (6 mM), DMTU (8 mM), Carboxy-PTIO (8 µM), Mannitol (80 mM), Tiron (6 mM) or Trolox (40 µM) with 100 µM DATS for 24 h restored cell growth. Exposure of A549 cells to 300 µM DATS for 24 h reduced cell growth by 42% which in the presence of 2 mM NAC was restored. In addition, co-exposure to SA (10 mM), DMTU (8 mM), Carboxy-PTIO (6 µM), Mannitol (20mM), Tiron (2 mM) or Trolox (20 µM) with 300 µM DATS for 24 h also restored cell growth. Fluorescent microscopy demonstrated an increase in H_2O_2 production by 67% in the MDA-MB-231 cell line after 24 h. In the A549 cell line, H_2O_2 production increased by 14%, 16%, and 18% after 48 h of exposure. After 24 h exposure to 100 µM DATS in the MDA-MB-231 cell line cell rounding increased to 46 cells from 5. Cell rounding induced by DATS was significantly inhibited by NAC to 9 and to 8, 5, 16, 12 and to 10 by SA, DMTU, Carboxy-PTIO, Mannitol and Tiron. After exposure of the A549 cells to 300 µM DATS for 24 h cell rounding increased from 4 to 45 which was decreased to 3 by NAC, and to 9, 27, 33, 38, 23 and 23 by SA, DMTU, Carboxy-PTIO, Mannitol, Tiron and Trolox. Cell cycle analysis indicated that exposure to 100 µM DATS in the MDA-MB-231 cell line for 24 h increased the quantity

of cells occupying the sub-G_1 phase by 17% which was decreased to a 1% increase by NAC. After exposure of the A549 cells to 300 µM DATS for 24 h the percentage of cells in the G_2M phase increased by 34% which was restored to 19% by NAC. Exposure of the MDA-MB-231 cells to 100 µM DATS for 24 h resulted in a 1.75-fold increase in mitochondrial membrane potential depolarisation; however, after co-treatment with NAC this decreased to a 1.68-fold change. Exposure of the A549 cells to 300 µM DATS for 24 h resulted in an increase in mitochondrial membrane potential depolarisation to 2.71-fold which was reduced to 1.22-fold after co-treatment with NAC. After 24 h exposure of the MDA-MB-231 cells to 100 µM DATS the percentage of SOD inhibition was recorded as 73% compared to cells propagated in growth medium (63%). After exposure of the A549 cell line to 300 µM DATS for 24 h a significant decrease in SOD inhibition was observed from 85% in cells propagated in growth medium to 79%. After exposure of the MDA-MB-231 cells to 100 µM DATS for 24 h a 40% decrease in catalase enzyme activity was observed relative to cells in growth medium. After exposure of the A549 cells to 300 µM DATS for 24 h catalase activity was decreased by 24%. This study contributes further understanding to the role of oxidative stress in the effects exerted by DATS and other naturally occuring small organosulfur compounds on proliferation, morphology and cell death indution in cancer cell lines. Additionally this study provides insight into the role of specific ROS in the effects of DATS; as well as the modulation of endogenous sources of ROS by DATS, such as SOD, catalase and mitochondrial membrane potential depolarisation.

Key words: Diallyl Trisulfide, DATS, Reactive Oxygen Species, Organosulfur Compound, Phytomedicine

Table of Contents

List of Abbreviations

Abbreviation	Definition
ADAM	A Disintegrin and metalloproteases
AIF	Apoptosis-inducing factor
AP-1	Activator protein-1
Apaf-1	Apoptotic protease activating factor 1
APC	Anaphase promoting complex
ASK-1	Apoptosis signal-regulating kinase-1
ATM	Ataxia telangiectasia mutated
ATR	Ataxia telangiectasia and rad3-related protein
ATP	Adenosine triphosphate
ATR	Ataxia telangiectasia and Rad3 related protein
Bad	Bcl-2 associated agonist of cell death
BAK	B-cell 2 homologue antagonist killer
BAX	B-cell lymphoma associated X
Bcl-2	B-cell lymphoma
Bcl-xL	B-cell lymphoma extra large
BH3	B-cell lymphoma 3 homologue
Bid	BH3 interacting-domain death agonist
Bim	Bcl-2 like protein 11
Carboxy-PTIO	2-(4-Carboxyphenyl)-4,4,5,5-tetramethylimidazoline-1-oxyl-3-oxide
CAD	Carbamoyl-phosphate synthetase 2, aspartate transcarbamylase, and dihydroorotase
CCCP	Carbonyl cyanide *m*-chlorophenylhydrazone
Cdc27	Cell division cycle protein-27
Cdc25C	Cell division cycle 25C protein
Cdh1	Cadherin-1

CDK	Cyclin-dependent kinase
CDK1	Cyclin-dependent kinase-1
CDKI	CDK inhibitors
Chk1	Checkpoint kinase-1
c-Myc	Cellular-Myc proto-oncogene
DADS	Diallyl disulfide
DAS	Diallyl sulfide
DATS	Diallyl trisulfide
DCFDA	2,7-Dichlorofluoresceindiacetate
DR4/5	Death receptor 4/5
DHE	Dihydroethidium
DMEM	Dulbecco's minimum essential medium
DMSO	Dimethyl sulphoxide
DMTU	N,N-dimethylthiourea
DNA	Deoxyribonucleic acid
DUOX	Dual oxidases
EMBS	(8R,13S,14S,17S)-2-Ethyl-13-methyl-7,8,9,11,12,13,14,15,16,17-decahydro-6H-cyclopenta[a]phenanthrane-3,17-diyl bis(sulphamate)
ER	Estrogen receptor
ETC	Electron transport chain
FADD	Fas-associated protein with death domain
Fas	First apoptosis signal
FasL	Fas ligand
FCS	Foetal calf serum
GLUT	Glucose Transporter
GSH	Glutathione peroxidise
GST	Glutathione-S-transferase

HER	Human epidermal growth factor-receptor
IKK	IκB kinase
IL-6	Interleukin-6
JC-1	5',6,6'-Tetrachloro-1,1',3,3'-tetraethylbenzimidazolylcarbocyanine iodide
c-JNK	*c*-Jun-terminal kinase
JNK	Jun-terminal kinase
Keap1	Kelch-like ECH-associated protein 1
MAPK	Mitogen-activated protein kinase
MAP3K	MAP kinase kinases
MAP2K	MAP kinase kinases
MDM2	Mouse double minute 2
MKK	MAP kinase
mTOR	Mechanistic target of rapamycin
NAC	N-acetyl cystein
NF-κB	Nuclear factor-kappa B
NOX	NADPH oxidases
nmol	Nano-moles
NOXA	Phorbol-12-myristate-13-acetate-induced protein 1
NQO	NAD(P)H quinone oxidoreductase
Nrf2	Nuclear factor erythroid 2-related factor 2
p38 MAPK	p38 mitogen activated protein kinase
PBS	Phosphate buffer solution
PI3K	Phosphatidylinositol 3-kinase
PR	Progesterone receptor
PTP1B	Protein tyrosine phosphatase 1B
PUMA	p53 Upregulated modulator of apoptosis
ROS	Reactive oxygen species

SOD	Superoxide dismutase
TBARS	Thiobarbituric acid reactive substances
Tiron	Sodium 4,5-dihydroxybenzene-1,3-disulfonate
TNF- α	Tumour necrosis factor-α
TRAF2	TNF-receptor-associated factor 2
TRAIL-R1	TNF-related apoptosis-inducing ligand-receptor 1
Trolox	6-Hydroxy- 2, 5, 7, 8-tetramethylchromane-2-carboxylic acid

List of Figures

List of Tables

µM) in the presence of the scavengers SA (10 mM), DMTU (8 mM), Carboxy-PTIO (6 µM), Mannitol (20mM), Tiron (2 mM) and Trolox (20 µM) after 24 h of exposure.

Table 11: The representative images of cell cycle progression in MDA-MB-231 cells after 24 h of exposure to DATS (10 µM, 50 µM, 100 µM and 150 µM) in the presence and absence of NAC (2 mM).

Table 12: The representative images of cell cycle progression in MDA-MB-231 cells after 48 h of exposure to DATS (10 µM, 50 µM, 100 µM and 150 µM) in the presence and absence of NAC (2 mM).

Table 13: The representative images of cell cycle progression in MDA-MB-231 cells after 24 h of exposure to DATS (50 µM and 100 µM) and SA (6mM), DMTU (8 mM), Carboxy-PTIO (8 µM), Mannitol (80 mM), Tiron (6 mM) and Trolox (40 µM).

Table 14: Table displaying the representative images of cell cycle progression in A549 cells after 24 h of exposure to DATS (100 µM, 200 µM, 300 µM and 400 µM) in the presence and absence of NAC (2 mM).

Table 15: Table displaying the representative images of cell cycle progression in A549 cells after 48 h of exposure to DATS (100 µM, 200 µM, 300 µM and 400 µM) in the presence and absence of NAC (2 mM).

Table 16: The representative images of cell cycle progression in A549 cells after 24 h of exposure to DATS (100 µM, 300 µM) and SA (10 mM), DMTU (8 mM), Carboxy-PTIO (6 µM), Mannitol (20 mM), Tiron (2 mM) and Trolox (20 µM).

Table 17: Representative images displaying the amount of green fluorescence demonstrating mitochondrial membrane potential after 24 h exposure of MDA-MB-231 cells to DATS (10 µM, 50 µM, 100 µM and 150 µM) in the presence and absence of NAC.

Table 18: Representative images displaying the amount of green fluorescence demonstrating mitochondrial membrane potential after 24 h exposure of MDA-MB-231 cells to DATS (10 µM, 50 µM, 100 µM and 150 µM) in the presence of SA (6mM), DMTU (8 mM), Carboxy-PTIO (8 µM), Mannitol (80 mM), Tiron (6 mM) and Trolox (40 µM).

Table 19: Representative images displaying the amount of green fluorescence as a result of the mitocapture assay after 24 h exposure of the A549 cells to DATS (100 µM, 200 µM, 300 µM and 400 µM) in the presence and absence of NAC.

Table 20: Representative images displaying the amount of green fluorescence as a result of the mitocapture assay after 24 h exposure of A549 cells to DATS (100 µM, 200 µM, 300 µM and 400 µM) in the presence and absence of NAC.

1. Background

1.1 Cancer epidemiology

Cancer is a well-recognised global health concern where the number of new diagnoses and the mortality rate are expected to increase dramatically in the next decade. In addition, 62% of cancer-related deaths occur in economically developing countries of which 50% take place in Western- and Northern Africa (1). In sub-Saharan Africa the estimated cancer incidence rate is 128.2 out of 100 000 people which is higher than what is found in medium- and low human development index countries. In addition, the cancer mortality rate is estimated to be 87.1 per 100 000 people in sub-Saharan Africa. Breast cancer is the most commonly diagnosed cancer in sub-Saharan Africa accounting for 16.1% of the cancer incidences and 12.4% of the cancer related deaths, while lung cancer accounts for 2.8% of cancer incidences and 3.9% of cancer related deaths in sub-Saharan Africa (2). Moreover, breast cancer is the most frequently diagnosed type of cancer in women worldwide. In addition, the frequency of triple negative breast cancer diagnosed in Africa is estimated to be 27% and in South Africa it is estimated to be 14% of all cancer diagnoses (3). Furthermore, the number of cancer diagnoses and mortality rates are still expected to increase, with cancer-related deaths expected to be approximately 28 million by 2040 (4). By the year 2050, the number of elderly cancer patients (80 years and older) are expected to increase from 143 to 426 million with an estimated 7 million new cancer diagnoses made within this age group in 2050 accounting for 22% of all projected new diagnoses (5).

Current anticancer treatment strategies are associated with possibly severe side effects including hair loss, nausea, fatigue, pain, anaemia, emesis and a weakened immune system which might result in patient non-compliance. Additionally, synthetic medicine is often an expensive form of treatment (6-10). Due to the above-mentioned reasons, there has been a shift towards research involving plant-derived medicinal compounds also known as phytomedicines that may potentially be more cost effective and possibly exert less severe side effects that could effectually complement- or substitute current therapy (10). The latter includes research into bioactive naturally occurring small molecule organosulfur compounds which have demonstrated antiviral, antibacterial, immune modulatory, anti-inflammatory- and anticancer activity such as the garlic derived diallyl trisulfide (DATS), which was investigated in this study (11). However, the mechanism of action exerted by DATS is not completely understood (12).

1.2 Garlic

Garlic (*Allium sativum*) is one of the most widely researched plants for medicinal purposes and has been used for therapeutic purposes for over 4000 years for its antimicrobial-, antithrombotic-, hypolipidemic- and anticancer activity. In addition, literature further suggests that consumption of garlic potentially reduces the risk of developing myeloma, gastric-, colorectal-, endometrial-, lung- and prostate cancer with the consumption of as little as 20 g (wet weight) of garlic per day reportedly being associated with a decreased risk of developing gastric cancer (12). In a meta-analysis of the effect of garlic consumption on the risk of developing gastric cancer, participants who consumed garlic at least once a day had a 35% decreased risk of developing gastric cancer (13).

Garlic has also been shown to decrease lipid peroxidation which refers to oxidative damage induced by free radicals to lipid containing molecules including the phospholipids present in the lipid bilayer of the cell membrane. Lipid peroxidation was demonstrated in hamsters with induced buccal pouch carcinogenesis treated with 250 mg of garlic per kg orally 3 times a week. It was observed that after 14 weeks of treatment with 250 mg garlic 3 times a day, the TBARS decreased to 3.32 nmol compared to 4.22 nmol in hamsters not treated with garlic (14). In addition, literature suggests that several of the beneficial effects of garlic are due to the biologically active sulfur compounds present in garlic, that are responsible for inducing phase II metabolising enzymes such as glutathione-S-transferases (GSTs) referring to detoxifying enzymes that remove destructive electrophiles by means of conjugating them with glutathione (15). Oral administration of diallyl-sulfide (DAS) (400 mg/kg) in mice models exhibited a 149% increase in GST activity after 24 h when compared to mice not exposed to DAS (16). In addition, garlic derived-DAS, diallyl disulfide (DADS) and diallyl trisulfide (DATS) have been shown to increase the expression of NAD(P)H quinone oxidoreductase (NQO) which is involved in the detoxification of quinone metabolites of benzopyrene, a commonly occurring carcinogen found in car exhaust fumes, smoke from wood fires, tobacco and charred foods (17).

Literature demonstrates that garlic exerts anti-carcinogenic effects with the most prominent bioactive compounds within it being the organosulfur compounds including DAS, DADS and DATS; of which DATS is the most potent followed by DADS and then DAS likely due to the presence of the double and triple bonds which allow DADS and DATS to conjugate easier (18,12,15). The current study was conducted in order to unravel the role of oxidative stress in the effects exerted by the bioactive compound DATS, present in garlic, in a triple negative metastatic breast cancer cell line and a lung cancer cell line.

1.3 Diallyl trisulfide

DATS is formed by the hydrolysis and oxidation of γ-glutamyl-S-alk(en)yl-L-cysteine to S-alk(en)yl-L-cysteine sulfoxide (alliin) which is stored in the garlic clove. When the clove is crushed or chewed, vaculoes containing an enzyme, allinase, are ruptured. Subsequently, allinase is released resulting in the conversion of alliin to allicin which rapidly breaks down into DAS, DADS and DATS as illustrated in figure 1 (12). The amount of allicin found in natural garlic is approximately 2.5 mg/g which translates to 5–20 mg per clove, which is then deconstructed into 30–100 µg/g DAS, 530–610 µg/g DADS and 900–1100 µg/g DATS, respectively (12,19).

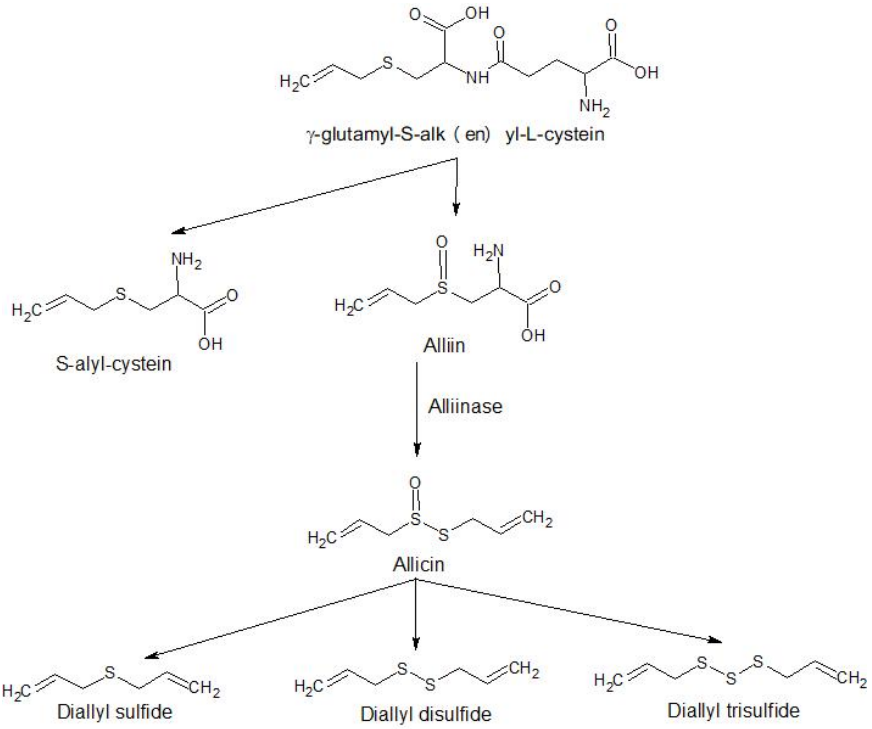

Figure 1: DATS Formation within a garlic clove from the precursor molecule γ-glutamyl-S-alk(en)yl-L-cysteine (figure created by Nibha Surajlal using ChemSketch version 14, ACD/Labs, Toronto, Canada).

Previous studies have demonstrated that, among these garlic-derived organosulfur compounds, DATS exerts the most potent antiproliferative effect in cancer cells, as shown in a study conducted on prostate cancer cells (PC-3 and DU145) where cells were treated with DATS, DADS and DAS for 24 h. Cell growth assessed using a sulforhodamine B assay demonstrated that proliferation decreased to 50% after exposure to 22 µM DATS and 35 µM DADS, whereas exposure to DAS at the highest

conecntration (40 µM) resulted in 97% cell growth (15). In addition, exposure to DATS (100 µM) for 6 h in lung cancer cells (A549) resulted in decreased cell growth to 60% when compared to cells propagated in growth medium (20). Proliferation studies have also demonstrated that exposure to 40 µM DATS decreases cell growth in triple negative MDA-MB-231 breast cancer cells in a dose-dependent manner to 43% cell growth after 24 h of exposure. Furthermore, exposure to DATS (40 µM) for 24 h has been shown to inhibit the expression of A disintegrin and metalloproteases (ADAM) -10 and -17 by 80%. ADAM -10 and -17 are involved in the cleavage of cell surface molecules leading to the activation of the notch signalling pathway which regulates cell proliferation and differentiation in breast cancer triple negative MDA-MB-231 cells (21). In another study looking at the effect of DATS on the cell migration of triple negative breast cancer (MDA-MB-231 and HS 578T) it was found that exposure to DATS (20 µM) reduced cell migration to 55% (22). Furthermore, antiproliferative activity has been confirmed in several other tumourigenic cell lines including of colon cancer (HT-29) (23), prostate cancer (PC-3) (24), gastric carcinoma (AGS) (25), alveolar adenocarcinoma (A549) (26) and glioma cells (U87MG and T89G) (27). However, the signalling mechanism utilised by DATS in cancer cells in order to induce antiprolioferative activity, antimitotic activity and induction of cell death remains elusive (12). Furthermore, it is also speculated that the prominent antiproliferative activity exerted by DATS compared to its organosulfur counterparts is due to DATS owning the most sulfur bonds resulting in DATS being more stable than DADS and DAS (28, 29).

1.4 Reactive oxygen species

Reactive oxygen species (ROS) are produced within cells due to energy production within the mitochondria including the electron transport chain and the nitric oxide synthase reaction, and non-mitochondrial sources, namely Fenton's reaction, peroxisomal beta oxidation and respiratory bursts of phagocytosis (30). The resulting ROS are responsible for the regulation of important pro-survival cellular pathways including the phosphatidylinositol 3-kinase (PI3K)- and mitogen activated protein kinase (MAPK) pathways (31). However, an excess in ROS is potentially harmful to the body and results in oxidative stress and oxidative damage culminating in deoxyribonucleic acid (DNA)-, protein- and lipid damage (32). In order to regulate a level of ROS which supports cell survival and to prevent excessive accumulation of ROS, the level of ROS is modulated by the antioxidant enzymes including SOD, catalase and glutathione peroxidase (GSH) (30). The generation of excessive and harmful ROS stems from the superoxide radical (O_2^-) and the singlet oxygen radical ($O_2^{\bullet}$) from which other damaging ROS can be derived. In addition, a major source of oxygen radicals is the electron transport chain (ETC) whereby energy is produced in the form of adenosine triphosphate (ATP) within the mitochondria (33). In this process, oxygen is reduced to H_2O; however, incomplete reduction of oxygen does frequently occur resulting in production of the O_2^- radical which is dismutated to H_2O_2 by SOD which can cause membrane-, DNA-, and protein damage. In addition, H_2O_2 can be reduced to the toxic hydroxyl radical (•OH) which leads to oxidative damage by reacting with a range of metabolites such as Fe^{2+} ions, lipids, and proteins. Therefore, an increase in mitochondrial activity can result in increased ROS production, particularly by means of the generation of O_2^-, and subsequent damage to the mitochondrial membrane and mitochondrial DNA. In addition, other oxidative enzymes also contribute to ROS generation including NADPH oxidases (NOX) and dual oxidases (DUOX) (34).

Cancer cells exhibit increased glucose uptake primarily via an increase in the glucose transporter (GLUT) enzymes GLUT-1 and GLUT-3 when compared to non-carcinogenic cells since most types of cancer cells favour aerobic glycolysis. This is due to glycolysis providing rapid energy generation, which is favourable when rapid growth and proliferation is occurring, when compared to oxidative phosphorylation which the mitochondrial ETC is a part of, however, oxidative phosphorylation does continue to occur and contributes to ROS production via increased mitochondrial activity and the resulting production of O_2^- (35). This increased aberrant metabolic rate present in most types of cancer cells is termed the Warburg effect, and results in increased energy- and ROS production (36). However, the increased ROS is counteracted by elevated production of ROS scavengers including SOD which is responsible for the conversion of $O_2^{\bullet}$ and O_2^- to H_2O_2 as well as catalase and GSH which convert H_2O_2 to water, this is depicted in figure 2 (37).

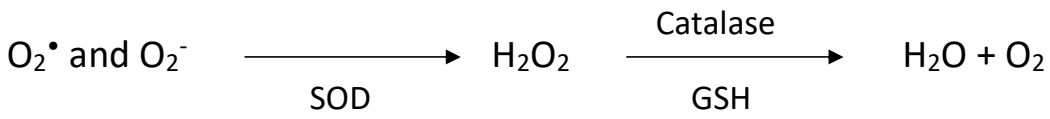

Figure 2: Formation of water (H_2O) and Oxygen (O_2) from the singlet oxygen radical ($O_2^{\bullet}$) and superoxide radical (O_2^-) through the antioxidant enzymes superoxide dismutase (SOD), glutathione peroxidase (GSH) and catalase (Image created by Nibha Surajlal using Microsoft® Office Word 2010 (Microsoft Corporation, United States of America).

The increased level of ROS activity is used to promote the pro-survival signalling pathways and the oxidation and inactivation of phosphatases including protein tyrosine phosphatase 1B (PTP1B) which inhibits the survival PI3K pathway (38). This abberent regulation of ROS compared to non-tumourigenic-and differentiated cells makes ROS a possible target for cancer therapeutic treatment. Previous studies have shown that several types of cancer cell lines including the triple negative metastatic breast cancer MDA-MB-231 cell line are dependent on ROS for proliferation which was confirmed when a ROS scavenger, N-acetyl cystein (NAC) inhibited proliferation (39). However, administration of antioxidants does not successfully modulate ROS activity in cancer cells since the antioxidants do not effectively target the specific ROS production sites and subsequently can affect chemotherapy that is dependent on ROS production. Due to the inefficacy of antioxidants, alternative methods of ROS-targeted cancer treatment is required (38).

ROS acts in a biphasic manner where the quantity of ROS determines the affect either resulting in increased signalling of survival pathways or the induction of apoptosis. Increased oxidative stress due to upregulated ROS production or a decrease in antioxidant activity results in inhibition of tumour growth and induction of apoptosis (40). ROS-dependent apoptosis is mediated by apoptosis signal-regulating kinase 1 (ASK-1), activation of p38 mitogen activated protein kinase (p38 MAPK) and jun terminal kinases (JNK). Furthermore, p38 MAPK and JNK induce the upregulation of pro-apoptotic signalling through the activation of the genes including B-cell lymphoma 3 homologue (BH3) interacting-domain death agonist (Bid), Bcl-2-like protein 11 (Bim) and p53 in addition to inhibition of the anti-apoptotic proteins such as B-cell lymphoma (Bcl-2) and B-cell lymphoma extra-large (Bcl-xL) resulting in apoptosis. Thus, more research is required on compounds that manipulate ROS culminating in decreased cell growth and induction of cell death in tumourigenic cells (38).

1.5 Cell cycle progression

The cell cycle consists of the longer interphase period and mitosis. Interphase is divided into growth phase 1 or the G_1 phase where the cell might enter senescence (G_0 phase) or receive growth signals or mitogens that initiate entry into the next phase, the synthesis phase, or S phase when the cell is undergoing DNA replication; this is followed by the G_2 phase or the second growth phase during which the cell is preparing to enter the mitosis phase or M phase wherein the cell will divide into daughter cells; this process is illustrated in figure 3. Progression through the cell cycle is driven by the cyclin dependant kinase (CDK) enzymes and their association with the correct cyclin in order to be activated (41). In the event of DNA damage such as DNA double stranded breaks enzymes such as ataxia telangiectasia mutated (ATM) and ataxia telangiectasia and rad3-related (ATR) are recruited and results in phosphorylation of many substrates including the p53 gene and checkpoint kinase 1- and 2 (Chk1- and 2) in order to halt cell division and initiate DNA damage repair mechanisms, this may result in slower cell division or cell cycle arrest in the G_1- or G_2 phase of the cell cycle. In order for the cells to enter the G_1 phase of the cell cycle and pass through the retinoblastoma/E2F transcription factor checkpoint which causes growth inhibition if the cellular conditions to enter the G_1 phase are not met, after which the cell is committed to undergo a cycle of cell division. Cell cycle arrest in the G_1 phase can be caused by ATM and ATR related phosphorylation of p53 and mouse double minute 2 protein (MDM2) which result in the accumulation of the p53 protein and the subsequent activation of p21 genes for CDK inhibitors, to prevent the association of CDK2 and cyclin E which is necessary for progression into the S phase of the cell cycle along with the association of cyclin D and CDK4/6, this is assisted by phosphorylation of the CDK4/6-cyclin E complex by CHK1 and 2 leading to downregulation of the complex. The inhibition of CDK2 prevents the recruitment of cell division cycle protein 45 to the DNA, this protein is required to recruit DNA polymerase α which is an important protein for the synthesis of new DNA strands, thus this inhibits the S phase of the cell cycle which additionally requires the association of CDK2 with cyclin A. The G_2-M checkpoint can prevent the cell from entering mitosis by inhibiting the activation of the CDK1-cyclin B complex, this can be achieved by phosphorylation of ATM/ATR or CHK1/CHK2 or the transcription of CDK inhibitors via the p21 gene (42,35).

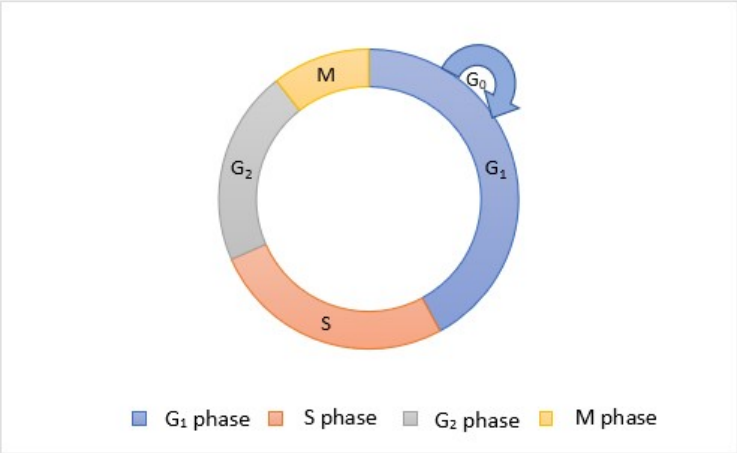

Figure 3: The phases of the cell cycle as a cell might progress through it including senescence (G_0) growth phase 1 (G_1), synthesis phase (S), growth phase 2 (G_2) and mitosis (M). (Figure created by Nibha Surajlal using Microsoft® Office Word 2010 (Microsoft Corporation, United States of America)).

1.6 DATS and cell cycle progression

Previous research regarding the effects of DATS on the cell cycle progression indicated that exposure to DATS results in a G_2M phase arrest by means of an increase in ROS, one suggested pathway for this is the degradation of ferritin by the activation of JNK and an increase in the labile iron pool, this redox active iron then reacts with the superoxide radical and H_2O_2 to form •OH and $HO_2^{\bullet}$ in PC-3 prostate cancer cells (43,44). The generation of excessive ROS including •OH and $HO_2^{\bullet}$ are responsible for cellular DNA damage and therefore exposure to DATS is also associated with an increase in DNA damage checkpoint proteins including Chk1 and ATR, which recognize persistent single stranded DNA and phosphorylates Chk1 which subsequently phosphorylates the regulatory points on CDK1 resulting in CDK1 inhibition and G_2M cell cycle arrest (45). The increased ROS generation by DATS results in phosphorylation of the amino-acid serine-216 which causes the inhibition of cell division cycle 25C protein (Cdc25C) which is responsible for the dephosphorylation of inhibitory sites of CDK1 preventing CDK1 activation and therefore preventing CDK1 from binding with cyclin B and may be responsible for the G_2M arrest and cell death induction (46). However, cells do gradually regain CDK1 activity as shown by DU145 cells being able to escape the G_2M phase arrest after 24 h possibly due to reversal of the inhibition of cyclin B-CDK1 as demonstrated in a prostate cancer cell line (DU145) cell line after 8 h exposure to 40 µM DATS. In addition, exposure to DATS (20 µM and 40 µM) for 8 h and 16 h in colon cancer cells (HCT 116) and prostate cancer cells (LNCaP) resulted in a dose- and time dependant increase in cells experiencing a G_2M cell cycle arrest. Furthermore, the effect of DATS on the components of the anaphase promoting complex (APC) was

investigated in this study, the APC is required for a cell to exit mitosis and upon investigation it was discovered that DATS induced phosphorylation of major subunits of the APC including cell division cycle protein 27 (Cdc27), and Cadherin-1 (Cdh1), preventing the formation of the APC and subsequently promoting the cell cycle arrest caused by DATS (47).

1.7 Apoptosis

Apoptosis is a form of controlled cell death that is used to regulate tissue sizes, tissue shape and to maintain body structures (48). Morphological hallmarks of apoptosis include withdrawal of a cell from its surrounding cells, blebbing of the plasma membrane, condensation of the nucleus and cytoplasm, margination of the condensed chromatin, fragmentation of the nucleus and formation of apoptotic bodies (49).

Apoptosis takes place by means of the intrinsic pathway involving the mitochondria, the death receptor-mediated extrinsic pathway, the endoplasmic reticulum pathway and the caspase-independent pathway (50 ,45).

1.7.1 Extrinsic pathway

The extrinsic pathway is stimulated by the interaction of the death receptors with their ligands including first apoptosis signal (Fas) found on the cell membrane. The Fas ligand (FasL) binds to the Fas receptor which results in the recruitment of a Fas receptor adaptor molecule, Fas-associated protein with death domain (FADD), which is responsible for the cleavage of procaspase-8 into caspase-8 and therefore caspase-3 activation leading to activation of the execution pathway, depicted in figure 4, other death receptors include tumour necrosis factor-receptor 1 (TNF-receptor 1), TNF-related apoptosis-inducing ligand receptor 1 (TRAIL-R1) and TRAIL-R2 (50).

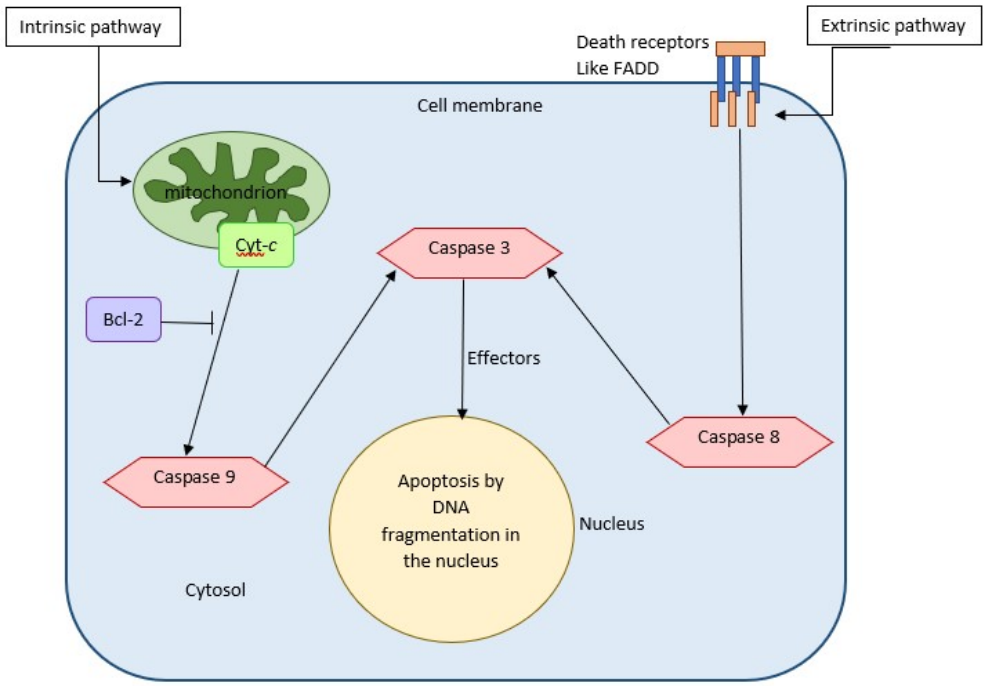

Figure 4: A brief schematic of the extrinsic and intrinsic apoptotic pathways including B cell lymphoma 2 (Bcl-2), cytochrome *c* (Cyt-*c*) and Fas-associated protein with death domain (Image created by Nibha Surajlal using Microsoft® Office Word 2010 (Microsoft Corporation, United States of America)).

1.7.2 Intrinsic pathway

The intrinsic pathway is activated by intracellular stress including oxidative- and DNA damage that is potentially is a result of increased ROS quantities. The latter results in the activation of pro-apoptotic proteins from the BH3 family which results in the subsequent oligomerization of B-cell lymphoma associated X (BAX) and B-cell 2 homologue antagonist killer (BAK) directly or indirectly (45). Activation of the BAX and BAK oligomer results in depolarisation of the mitochondrial membrane and the subsequent release of cytochrome *c* which binds to apoptotic protease activating factor 1 (Apaf-1) and pro-caspase 9 to form the apoptosome. The apoptosome activates initiator caspase-9 which subsequently activates caspase-3, and -6 and -7 leading to apoptosis which results in the release of apoptotic proteins including apoptosis inducing factor (AIF), endonuclease G and carbamoyl-phosphate synthetase 2, aspartate transcarbamylase, and dihydroorotase (CAD) from the mitochondria (51). AIF is translocated into the nucleus resulting in stage 1 peripheral chromatin condensation and DNA fragmentation, endonuclease G also moves into the nucleus to cleave nuclear chromatin. After CAD cleavage by caspase 3, it then also moves into the nucleus to cause oligonucleosomal DNA fragmentation and stage 2 condensation (52). In addition, the tumour suppressor protein p53 plays a key role in the regulation of the Bcl-2 family of regulatory proteins

including anti-apoptotic like B cell lymphoma 2 (Bcl-2) and B-cell lymphoma extra-large (Bcl-xL) which inhibit the release of cytochrome *c* and are neutralised by BCL2 associated agonist of cell death (Bad) and some are pro-apoptotic like BAX and BAK (45). The p53 initiated Bcl-2 family member proteins, and the p53 upregulated modulator of apoptosis (PUMA) and phorbol-12-myristate-13-acetate-induced protein 1 (NOXA) are also important pro-apoptotic proteins of the p53 pathway and result in the increased expression of BAX by PUMA and NOXA inhibits anti-apoptotic Bcl-2 family member proteins (45,51,52).

Both the extrinsic- and intrinsic apoptotic pathways converge at the execution pathway which is initiated by execution caspases resulting in the activation of cytoplasmic endonuclease- and proteases to degrade nuclear- and cytoskeletal material- and proteins. The most important executioner caspase is caspase 3 which can be activated by the initiator caspases 8-, 9- and 10, additionally caspase 3 is responsible for the reorganising of the cytoskeleton into apoptotic bodies and the activation of cytoplasmic endonucleases- and proteases (53).

1.7.3 Jun terminal kinases mediated apoptosis

JNKs family of the mitogen-activated protein kinase (MAPK) superfamily are involved in various cell signalling pathways regulating cell proliferation, differentiation and apoptosis depending on the respective stimuli. Variants of JNKs are encoded mainly by 3 genes JNK1-, 2- and 3 and form the last group of the MAP kinases, which have 3 subgroups including MAP kinase kinase kinases (MAP3Ks), the MAP kinase kinases (MAP2Ks) and the MAP kinases (MAPKs). Activation of these JNKs is primarily caused by MAP kinase kinase (MKK) 4- or 7 and the activated JNKs can then activate apoptotic signalling through the upregulation of pro-apoptotic genes such as p53 and p73 or by modulating mitochondrial pro- or anti-apoptosis proteins including *c*-Jun which is a pro-apoptotic protein. In addition to the MKKs activation of JNKs, the activation of JNKs can be initiated by various stimuli including ROS that activate JNKs via activation of ASK1 by TNF-receptor-associated factor 2 (TRAF2) and TRAF6. Activated JNKs will move into the nucleus where the JNKs will phosphorylate *c*-Jun resulting in the formation of activator protein 1 (AP-1) which subsequently leads to the transcription of various pro-apoptotic proteins including BAK, tumour necrosis factor α (TNF-α) and FasL. Another mechanism used by JNKs to cause apoptosis is the phosphorylation of the transcription factors p53- and p73 and the subsequent transcription of pro-apoptotic proteins such as PUMA and BAX. JNKs are also capable of relocating to the mitochondria where they can cause the cleavage of Bid to form tBid which activates BAX. Another mechanism of apoptosis induction through JNKs is that they have also been shown to activate Bim which leads to BAX- and BAK activation and inhibition of Bcl-2- and Bcl-xL anti-apoptotic proteins (53).

1.8 DATS and cell death

Literature indicates that cell death induced by DATS is associated with the intrinsic apoptotic pathway and increased activation of JNK, an apoptosis regulating protein which is activated by ASK1. Activation of JNK induced apoptosis is caused by the release of ASK1 which is usually bound by thioredoxin and glutaredoxin, forming a protein complex. The increased oxidative stress caused by DATS causes oxidation of thioredoxin and glutaredoxin culminating in the release of activated ASK1 (53). The release of activated ASK1 due to increased H_2O_2 induced by DATS was demonstrated in MDA-MB-231 cells which were transfected with an adenoviral vector carrying a His-tagged glutaredoxin gene and an HA tagged ASK1 gene, that were exposed to DATS. Cells propagated in growth medium exhibited a ratio of 0.6 between glutaredoxin to ASK1; however, after exposure to 10- and 80 µM DATS for 1 h the ratio was 0.1, indicating that ASK1 was not associated with glutaredoxin after treatment with DATS confirms that DATS induces the release of ASK1 from the glutaredoxin and thioredoxin complex and subsequently induces cell death (54). Another study conducted in estrogen-dependent MCF-7 breast cancer cells demonstrated that exposure to 10 µM-, 25 µM- and 50 µM DATS for 12 h resulted in stimulation of JNK and activation of the AP-1 transcription factor which is involved in the regulation of the Jun (c-Jun, Jun D and Jun B) and fos (c-Fos, FosB, Fra-1 and Fra-2) protein families (55). Upregulated expression of the pro-apoptotic p53 protein is also induced by DATS and is associated with decreased expression of the p53 negative regulator, mouse double minute 2 (MDM2), therefore affecting the downstream targets of p53 resulting in the induction of apoptosis in colon cancer cells (HCT 116) and prostate cancer cells (LNCaP) (47). In addition, exposure to DATS also results in increased phosphorylation of the JNK pathway downstream pro-apoptotic protein, Bim target. DATS induced apoptosis is also linked to depolarisation of the mitochondrial membrane and the release of cytochrome *c* which forms a complex with apoptotic protease activating factor-1 (Apaf-1) to initiate caspase dependant apoptosis through activation of caspases 9- and 3 (12, 56). In addition, DATS exposure also leads to a decrease in the activity of cell survival pathways displayed by a decrease in the DNA binding ability of AP-1 and decreased expression of nuclear factor kappa B (NF-κB) in MDA-MB-231- and HS578t breast cancer cells, other survival proteins regulated through DATS to inhibit cell survival include cellular Myc proto-oncogene (c-Myc), mechanistic target of rapamycin (mTOR), TNF-α, interleukin 6 (IL-6) and IκB kinase (IKK) (12, 57).

The role of oxidative stress in the effects induced by DATS on cell proliferation, morphology, cell cycle progression, mitochondrial membrane potential and the possible modulation of the antioxidant enzymes, SOD and catalase in a human alveolar basal epithelial adenocarcinoma cell line

(A549) and a triple negative breast cancer cell line (MDA-MB-231) was investigated in this study. Data obtained from this study provided knowledge regarding the role of oxidative stress in the effects exerted by DATS and other small naturally occurring sulphur-containing bioactive compounds culminating in antiproliferative activity and induction of cell death in cancer cells. In addition, the involvement of different ROS species, namely hydrogen peroxide (H_2O_2), •OH, nitric oxide (•NO), peroxyl radical ($HO_2^{\bullet}$), singlet oxygen ($O_2^{\bullet}$), and the superoxide anion (O_2^{-}), was also investigated in the influence exerted by DATS. This study will further the understanding of the mechanism of action utilised by DATS in cancer cells.

2. Aim

The aim of this study was to determine if the mode of action exerted by DATS culminating in antiproliferative effects and the induction of cell death in triple negative breast cancer cells (MDA-MB-231) and alveolar adenocarcinoma cells (A549), is dependent on oxidative stress and the excessive production of ROS.

3. Objectives

The objectives of this study were as follows, and is illustrated in figure 5:

1. To determine if the antiproliferative effects of DATS in a triple negative breast cancer cell line (MDA-MB-231) and alveolar adenocarcinoma cell line (A549) were dependent on the generation of ROS. This was done by demonstrating the effects of DATS on cell growth in the presence or absence of NAC by means of crystal violet staining (spectrophotometry).

2. To determine which ROS are required for the antiproliferative effects exerted by DATS in a triple negative breast cancer cell line (MDA-MB-231) and an alveolar adenocarcinoma cell line (A549). This was done by demonstrating the effects of DATS on cell growth in the presence or absence of various ROS scavengers by means of crystal violet staining (spectrophotometry).

3. To quantify the production of H_2O_2 and O_2^- induced by DATS in a triple negative breast cancer cell line (MDA-MB-231) and alveolar adenocarcinoma cell line (A549) by utilizing 2,7-dichlorofluoresceindiacetate (DCFDA) and dihydroethidium (DHE) staining (fluorescent microscopy).

4. To determine if the cell rounding effect induced by DATS is dependent on the production of ROS. This was shown by means of light microscopy after cells were exposed to DATS in the presence or absence of NAC and the specific ROS scavengers.

5. To determine if the antimitotic activity induced by DATS is dependent on ROS production. This was accomplished by establishing the influence of DATS on the progression of the cell cycle and the induction of cell death in the presence or absence of NAC and the specific ROS scavengers by means of flow cytometry.

6. To determine if ROS modulation by DATS induced disruption of the mitochondrial membrane potential in the presence or absence of NAC and specific ROS scavengers by using the mitoprobe assay (flow cytometry).

7. To determine if the ROS-dependent effects of DATS are due to an alteration of antioxidant enzyme activity by performing a SOD assay and catalase assay (spectrophotometry).

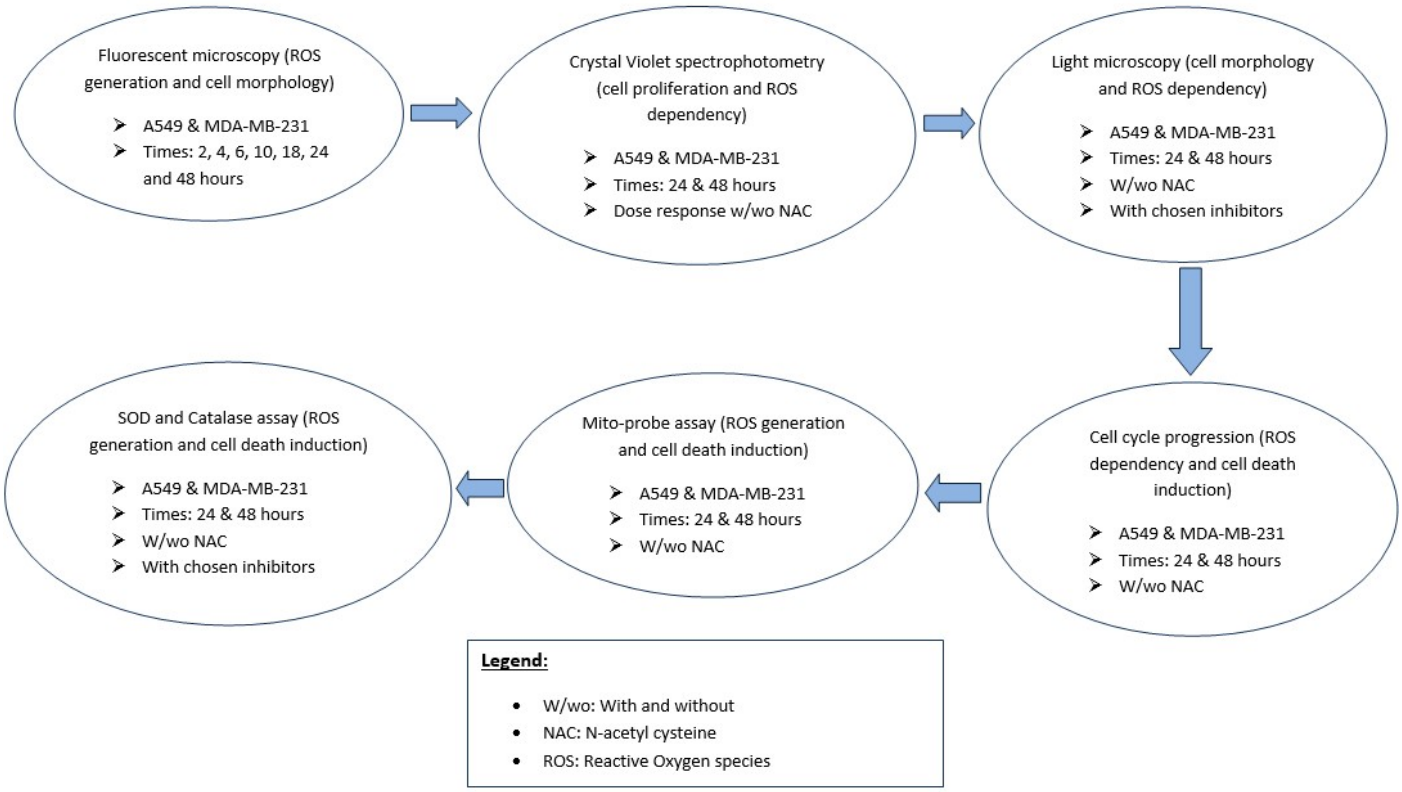

Figure 5: Conceptual framework of this study's objectives.

4. Materials and Methods

4.1.1. Cell lines

The MDA-MB-231 cell line that was used in this study is a commercially available triple negative breast cancer cell line. These cells do not contain estrogen receptors (ER), progesterone receptors (PR) or human epidermal growth factor receptors (HER) (58). This cell line was obtained from the American Type Culture Collection (Manassas, Virginia, United States of America) from a metastatic adenocarcinoma site (59). The MDA-MB-231 cells were cultured in 75 cm^2 tissue flasks in Dulbecco's Modified Eagle Medium (DMEM) containing 10% heat-inactivated fetal calf serum (FCS) (56°C, 30 min), 100 U/ ml penicillin G, 100 mg/ml streptomycin and fungizone (250 mg/l) in a humified atmosphere at 37°C and 5% CO_2.

The A549 cell line is an alveolar adenocarcinoma cell line with increased expression of the nuclear factor erythroid 2-related factor 2 (Nrf2) gene (60, 61). This leads to increased expression of the Nrf2 transcription factor which results in the upregulation of genes involved in oxidative stress resistance as well as chemoresistance (62). This cell line was obtained from the American Type Culture Collection (Manassas, Virginia, United States of America). These cells were cultured in DMEM containing 10% heat-inactivated FCS (56°C, 30 min), 100 U/ ml penicillin G, 100 mg/ml streptomycin and fungizone (250 mg/l) a humified atmosphere at 37°C and 5% CO_2 in 75 cm^2 tissue flasks.

4.1.2. Reagents

The crystal violet stain was provided and manufactured by Merc and Co., Inc. (Kenilworth, New Jersey, United States of America). The propidium iodide, DHE, DCFDA, DATS, NAC, sodium 4,5-dihydroxybenzene-1,3-disulfonate (Tiron), 6-hydroxy- 2, 5, 7, 8-tetramethylchromane-2-carboxylic acid (Trolox), 2-(4-Carboxyphenyl)-4,4,5,5-tetramethylimidazoline-1-oxyl-3-oxide (Carboxy-PTIO), N, N-dimethylthiourea (DMTU), sodium azide (SA) and D-Mannitol was supplied by Sigma Chemical Co. (St. Louis Missouri, United States of America). The SOD activity assay kit and the human catalase activity kit simplestep were purchased from Abcam plc. (Cambridge. England. United Kingdom). The Mitoprobe JC-1 assay kit was provided by Thermo Fisher Scientific Co. (Waltham. Massachusetts, United States of America). Appropriate controls were used in all experiments, including a negative control where cells were propagated in complete growth medium as well as vehicle-treated cells where the growth medium had equal volumes of the vehicle dimethyl sulphoxide (DMSO) as the DATS-treated cells. The final dilution of the DMSO did not exceed 0.05% (v/v).

4.2. Methods

4.2.1. Cell proliferation

4.2.1.1. Cell number determination using crystal violet staining (spectrophotometry)

Crystal violet staining was used to investigate the effect of DATS on proliferation in the presence or absence of NAC to determine if oxidative stress is required for the antiproliferative activity exerted by DATS. Furthermore, experiments were conducted in the presence of various scavengers specific for certain ROS (Table 1), to determine which ROS if any are necessary for the activity exerted by DATS resulting in decreased cell density. The crystal violet staining technique involves a triphenylmethane cation dye a DNA intercalating agent which binds to the DNA present in the cell nuclei of proliferating cells resulting in a purple staining. This technique is used to quantify the number of proliferating cells growing in a monolayer (63).

Spectrophotometry is conducted using a spectrophotometer which transmits light through a sample at a specified wavelength that is optimised for absorption of the colour of the stain and detects the amount of light absorbed as a function of the light intensity for a specific wavelength. Cellular samples which are unstained appear colourless or transparent, because light passes easily through cells and is minimally absorbed, therefore a stain, such as the crystal violet, is employed to stain the DNA of cells a certain colour which allows for the absorption of light (64). This method applies two laws, the first is Lambert's law which states that the proportion of light absorbed by a colour will remain constant regardless of the intensity of the light. The second law is Beer's law which dictates that the absorbance of light is directly proportional to the concentration of the medium it is passing through as well as the thickness or path length of the medium. This means that different spectrophotometers which may emit light at different intensities can give comparable results and that the absorbance of light through a sample is affected by the density of the sample. Thus, an increase in cell numbers will correlate with an increase in the absorbance detected (65).

The MDA-MB-231- and A549 cells were seeded into 96 well plates at a density of 5000 cells per well and plates were incubated for 24 h at 37°C and 5% CO_2 in a humified atmosphere to allow the cells to attach to the plate. Cells were then exposed to 10 µM - 150 µM DATS since previous studies demonstrated that exposure to DATS in this concentration range demonstrated a dose-response with respect to antiproliferative activity in tumorigenic cell lines (63). Furthermore, cells were exposed to DATS in the presence or absence of NAC (0.5 mM - 30 mM) to investigate if the antiproliferative activity induced by DATS was dependent on the production of ROS, this dose range was chosen since previous studies indicated a concentration of 20 mM was suitable to negate the effect of sulphur compounds on proliferation (66). DATS-exposed cells were incubated with

scavengers for specific ROS including DMTU, D-Mannitol, Carboxy-PTIO, Trolox, SA and finally Tiron the scavenger of the superoxide anion (O_2^-) at various concentration ranges as indicated in table 1.

Table 1: Scavengers for specific reactive oxygen species

Reactive oxygen species	**Inhibitor**	**Concentration**
Hydrogen peroxide (H_2O_2)	N, N-dimethyl thiourea (DMTU)	1-10 mM (67)
Hydroxyl radical (•OH)	D-Mannitol	20-100 mM (68,69)
Nitric oxide (•NO)	2-(4-Carboxyphenyl)-4,4,5,5-tetramethylimidazoline-1-oxyl-3-oxide (Carboxy-PTIO)	1-10 µM (70)
Peroxyl radical ($HO_2^•$)	Trolox	10-100 µM (71)
Singlet oxygen ($O_2^•$)	Sodium azide (SA)	1-10 mM (72)
Superoxide anion (O_2^-)	Tiron	1-10 mM (73)

The plates were incubated for 24 h, 48 h and 72 h at 37°C and 5% CO_2 since previous studies demonstrated that DATS exhibited optimal antiproliferative effects in tumorigenic cell lines at these exposure periods (66). Subsequently, medium was discarded, and 1% glutaraldehyde solution (100 µl) was used to fix the cells for 15 minutes at room temperature. The glutaraldehyde was then discarded, and 0.1% crystal violet stain (100 µl) was added to the wells for 30 minutes at room temperature. The crystal violet was then washed out of the plates with distilled water and the plates were left to dry overnight. The dye was solubilised using 0.2% triton X-100 (200 µl). The absorbencies were read using an EPOCH Microplate Reader (Biotek Instruments, Inc. (Winooski, Vermont, United States of America)) at a wavelength of 570 nm. The data obtained was analysed using Microsoft® Excel 2010 (Microsoft Corporation, Washington, United Sates of America).

4.2.2. Oxidative stress

4.2.2.1. H_2O_2 generation using 2,7-dichlorofluoresceindiacetate (fluorescent microscopy)

The effect of DATS on H_2O_2 production was used as an indicator of oxidative stress which was quantified using DCFDA and fluorescent microscopy. DCFDA is a non-fluorescent probe which is deacetylated by esterase enzymes after entering the cell and is oxidised when it comes into contact with H_2O_2 to generate its green, fluorescent derivative, 2,7-dichlorofluorescein (DCF). The resulting fluorescent DCF was quantified and used to investigate the production of H_2O_2 after exposure to DATS at different concentrations and time intervals (74).

The MDA-MB-231- and A549 cells were seeded in 24 well plates at a density of 20 000 cells per well and incubated for 24 h in a humified atmosphere at 37°C and 5% CO_2 to allow for attachment. The cells were then exposed to DATS 10 µM, 50 µM, 100 µM and 150 µM for the MDA-MB-231 cells and 100 µM, 200 µM, 300 µM and 400 µM for the A549 cell line since previous studies demonstrated that exposure to DATS in this concentration range demonstrated a dose-response with respect to antiproliferative activity in tumorigenic cell lines (57). Cells were then incubated for various time periods (2 h – 48 h) in a humified atmosphere at 37°C and 5% CO_2 in order to determine when the optimal effect of DATS was observable. The positive control included cells exposed to H_2O_2 (1% made in distilled water) and cells were incubated for 5 minutes. Thereafter, the H_2O_2 solution was removed. Subsequently, samples were washed with phosphate buffer solution (PBS) and incubated with 20 µM DCFDA for 20 minutes at 37°C and 5% CO_2. Samples were then washed with PBS (0.5 ml) after which an additional 500 µl of PBS was added to each well. Zeiss Axiovert CFL40 microscope, Zeiss Axiovert MRm monochrome camera (Zeiss, Oberkochen, Germany) and Zeiss filter 9 were used to capture the images of DCFDA-stained (green) cells. Fluorescence images were analyzed using Image J software developed by the National Institutes of Health (Bethesda, Maryland, United States of America). The fluorescent intensity of at least 100 cells were evaluated per condition in each experiment using image J software.

4.2.2.2. O_2^- generation using dihydroethidium (fluorescent microscopy)

The effect that DATS has on the production of the O_2^- radical was used as an additional indication of oxidative stress induction and this was measured using DHE. The fluorescent dye, DHE, fluoresces blue within the cytosol of cells until it reacts with the O_2^- radical to form hydroxyethidium, a red fluorescent dye that intercalates into the nucleus of the cells staining cells red. This florescence was used to indicate the presence of the O_2^- radical (75).

The MDA-MB-231- and A549 cells were seeded at a density of 20 000 cells per well in 24 well plates and incubated for 24 h to allow for attachment. The MDA-MB-231 cells were then treated with 10 µM, 50 µM, 100 µM and 150 µM of DATS and the A549 cells were treated to 100 µM, 200 µM, 300 µM and 400 µM of DATS and incubated for various time periods (2h - 48 h) in a humified atmosphere at 37°C and 5% CO_2. Cells were then washed with PBS and stained for 45 minutes using 10 µM of DHE at 37°C and with 5% CO_2. Cells were subsequently washed in PBS after which an additional 500 µl of PBS was added to each well. Images of the red stained cells were captured using the Zeiss Axiovert CFL40 microscope, Zeiss Axiovert MRm monochrome camera (Zeiss, Oberkochen, Germany) and Zeiss filter 15. The fluorescent intensity of at least 100 cells per sample were analyzed using Image J software.

4.2.3. Cell Morphology

4.2.3.1. Morphology observation using light microscopy

Light microscopy was used to evaluate the effects of DATS on cell rounding and morphology. The MDA-MB-231 cells and A549 cells was seeded in 24 well plates with 20 000 cells per well. Plates were incubated in a humified atmosphere at 37°C with 5% CO_2 for 24 h to allow for cell attachment. Cells were exposed to DATS (10 µM - 150 µM for the MDA-MB-231 cells and 100 µM – 400 µM for the A549 cell line) in the presence and absence of NAC and the selected ROS scavengers including SA (6 mM), DMTU (8 mM), Carboxy-PTIO (8 µM), Mannitol (80 mM), Tiron (6 mM) and Trolox (40 µM) for the MDA-MB-231 cell line and SA (10 mM), DMTU (8 mM), Carboxy-PTIO (6 µM), Mannitol (20 mM), Tiron (2 mM) and Trolox (20 µM). A positive control was included for both cell lines by exposing the cells to 0.5 µM of (8R,13S,14S,17S)-2-ethyl-13-methyl-7,8,9,11,12,13,14,15,16,17-decahydro-6H-cyclopenta[a]phenanthrane-3,17-diyl bis-sulphamate (EMBS). Cells were incubated at 37˚C and 5% CO_2 for 24- and 48 h in a humidified atmosphere. Thereafter, an Axiovert 40 CFL microscope (Zeiss, Oberkochen, Germany) was used to capture images for each condition. For data analysis, at least 100 cells were counted at random per sample, and the number of rounded cells and normal cells were recorded for each sample thrice. This experiment was conducted at least three times.

4.2.4. Cell cycle progression and cell death induction

4.2.4.1. Cell cycle analysis using propidium iodide staining (flow cytometry)

The effect of DATS on cell cycle progression and the induction of apoptosis was evaluated using flow cytometry and propidium iodide (PI) staining in the presence and absence of the ROS scavenger, NAC (2mM), as well as SA (6mM), DMTU (8 mM), Carboxy-PTIO (8 µM), Mannitol (80 mM), Tiron (6 mM) and Trolox (40 µM) for the MDA-MB-231 cell line and SA (10 mM), DMTU (8 mM), Carboxy-PTIO (6 µM), Mannitol (20mM), Tiron (2 mM) and Trolox (20 µM) for the A549 cell line. Once cells are permeabilized, PI binds and intercalates into the DNA of a cell, the amount of PI within a cell can therefore be used as a representation of the amount of DNA present within each cell and this was analysed using a flow cytometer. The amount of DNA quantified in each cell correlates with the stages of the cell cycle (G_1, S, G_2 and M) that the cells are in which can be used to analyse the cell cycle progression (76).

The MDA-MB-231- and A549 cells were seeded at a density of 1 000 000 cells per T25 cm^2 tissue culture flask and cells were incubated in a humified atmosphere at 37°C and 5% CO_2 for 24 h to allow for the cells to attach. Subsequently, cells were exposed to DATS (10 µM - 150 µM for the MDA-MB-231 cells and 100 µM – 400 µM for the A549 cells) in the presence or absence of NAC and various

selected ROS scavengers for 24- and 48 h. The positive control included cells exposed to 0.5 µM of EMBS and all samples were incubated at 37°C with 5% CO_2 in a humified atmosphere. Upon termination cells were trypsinized and centrifuged for 3 minutes at 300 x *g* and resuspended in 1 ml growth medium. The samples were then centrifuged for 5 minutes at 300 x *g* and the supernatant was removed. The pellet was resuspended in ice-cold PBS containing 0.1% FCS. Thereafter, 4 ml of 70% ethanol was added in a drop-wise manner and samples were kept at 4°C for at least 24 h. Cells were centrifuged at 300 x *g* for 5 minutes and the supernatant was removed. Cells were resuspended in 1 ml PBS containing PI (40 µg/ml), ribonuclease A (100 µg/ml) and triton X-100 (0.1%) and incubated at 37°C for 45 minutes. PI fluorescence was measured with the Gallios flow cytometer (Beckman Coulter, Inc. (Brea, California, United States of America)) available from The Department of Immunology, University of Pretoria, South Africa. Data from the cell debris (particles smaller than apoptotic bodies) and clumps of 2 or more cells were removed from further analysis. Cell cycle distributions were calculated using Kaluza and Kaluza C analysis software from Beckman Coulter (Brea, California, United States of America) by assigning relative DNA content per cell to sub-G_1-, G_1-, S- and G_2M phases.

4.2.5. Mitochondrial membrane integrity

4.2.5.1. Mitochondrial membrane potential depolarisation determination using a mitoprobe assay (flow cytometry)

The influence of DATS on the mitochondrial membrane potential was evaluated by utilising 5',6,6'-tetrachloro-1,1',3,3'-tetraethylbenzimidazolylcarbocyanine iodide (JC-1), a fluorescent cyanine dye which can distinguish between energized polarised mitochondrial membrane potentials and mitochondrial membrane potentials which are not polarised. The dye emits an orange red fluorescent signal when found outside the mitochondria when depolarisation has not occurred, compared to the JC-1 monomers which aggregate within the mitochondria once depolarisation of the mitochondrial membrane has occurred which emit a green, fluorescent signal (77).

The MDA-MB-231- and A549 cells were seeded in T25 cm^2 flasks at a density of 1 000 000 cells per flask and incubated for 24 h in a humified atmosphere at 37°C with 5% CO_2 to allow for attachment to the surface of the flask. The cells were exposed to DATS (10 µM - 150 µM for the MDA-MB-231 cells and 100 µM – 400 µM for the A549 cells) for 24- and 48 h in a humified atmosphere at 37°C with 5% CO_2. Cells were trypsinized and resuspended in 1 ml growth medium. The positive control comprised of cells exposed to 50 mM carbonyl cyanide m-chlorophenylhydrazone (CCCP) (supplied by manufacturer) for 5 minutes at 37°C with 5% CO_2 according to the suppliers' instructions (Thermo Fisher Scientific Co. (Waltham. Massachusetts, United States of America)). All samples were then

stained with 200 µM JC-1 (10 µl) and incubated for 30 minutes at 37°C with 5% CO_2. Samples were then centrifuged at 300 x *g* for 3 minutes, and the supernatant removed. The cells were resuspended and washed in PBS (2 ml), samples were then centrifuged at 300 x *g* for 3 minutes and the supernatant removed. PBS (500 µl) was then added to each sample and the amount of green fluorescence was measured using the Gallios flow cytometer (Beckman Coulter, Inc. (Brea, California, United States of America)) available from The Department of Immunology, University of Pretoria, South Africa. Samples were analysed using Kaluza and Kaluza C analysis software from Beckman Coulter (Brea, California, United States of America).

4.2.6. Antioxidant activity

4.2.6.1. Superoxide dismutase assay (spectrophotometry)

The influence of DATS on SOD activity was assessed and was used as an indicator with regards to the effect DATS exerts on the innate antioxidant defence mechanism. SOD is an endogenous enzyme responsible for converting O_2^- and $O_2^{\bullet}$ into H_2O_2. Therefore, quantification of SOD was used as an indication regarding the effect of DATS on the antioxidant activity in MDA-MB-231- and A549 cells and whether aberrant ROS production is due to DATS modulating the SOD enzyme activity. In this assay the cells are treated with WST-1 working solution (provided by Abcam plc. (Cambridge. England. United Kingdom)) which is reduced by SOD into a formazan dye which can be measured. The formation of the dye correlates to the inhibition of the enzyme xanthine oxidase that is caused by SOD (30).

The MDA-MB-231- and A549 cells were seeded at 1 000 000 cells per T25 cm^2 tissue culture flask and incubated for 24 h in a humified atmosphere at 37°C with 5% CO_2 to allow for attachment to the flask. The cells were then exposed to DATS (10 µM - 150 µM for the MDA-MB-231 cells and 100 µM – 400 µM for the A549 cells), for 24 h and 48 h at 37°C with 5% CO_2. Subsequently, the cells were scraped and placed in ice-cold 0.1 M Tris buffer (pH of 7.4) consisting of triton X-100 (0.5%), β-mercaptoethanol (5 mM) and phenylmethylsulfonyl fluoride (0.1 mg/ml). Samples were then centrifuged for 5 minutes at 14 000 x *g* at 4°C and the supernatant was collected as samples in eppendorf tubes and kept on ice. Subsequently, 20 µl of each sample was transferred to corresponding wells in a 96 well plate and WST-1 working solution (200 µl) (provided by Abcam plc. (Cambridge. England. United Kingdom)), and 200 µl enzyme working solution (provided by Abcam plc. (Cambridge. England. United Kingdom)) were added to each sample. The samples were then mixed and incubated for 20 minutes at room temperature. The absorbance was measured then measured at 450 nm using an EPOCH Microplate Reader (Biotek Instruments, Inc. (Winooski,

Vermont, United States of America). The data obtained was analysed using Microsoft® Excel 2010 (Microsoft Corporation, Washington, United Sates of America).

4.2.6.2. Catalase assay (spectrophotometry)

The effects of DATS on the antioxidant activity of the cells were assessed by quantifying the presence of the catalase enzyme within the cells. Catalase is responsible for the conversion of H_2O_2 produced by SOD into water and oxygen (30). Therefore, quantification of catalase was used as an indication of the effect of DATS on antioxidant activity within the cells and whether an increase in ROS after exposure to DATS corelates to reduced activity of the catalase enzyme.

MDA-MB-231- and A549 cells were seeded at a density of 1 000 000 cells per T25 cm^2 tissue culture flask and incubated for 24 h in a humified atmosphere at 37°C with 5% CO_2 to allow for attachment. After which cells were exposed to DATS (10 µM - 150 µM for the MDA-MB-231 cells and 100 µM – 400 µM for the A549 cells) for 24- and 48 h at 37°C with 5% CO_2. Cells were scraped using a cell scraper and placed in ice-cold 0.1 M Tris buffer solution (pH 7.4) containing triton X-100 (0.5%), β-mercaptoethanol (5 mM) and phenylmethylsulfonyl fluoride (0.1 mg/ml). Subsequently, samples were centrifuged at 14 000 x *g* for 5 minutes at 4°C. The supernatant was discarded, and the samples were transferred to new eppendorf tubes and samples were kept on ice. Afterwards, WST working solution (200 µl) (provided by Abcam plc. (Cambridge. England. United Kingdom)), dilution buffer (20 µl) (provided by Abcam plc. (Cambridge. England. United Kingdom)) and enzyme working solution (200 µl) (provided by Abcam plc. (Cambridge. England. United Kingdom)) was added to each well. Subsequently, the samples were mixed and incubated for 20 minutes at 37°C. Subsequently, the solution (100 µl) was transferred into a new plate and the absorbance measured at 570 nm using an EPOCH Microplate Reader (Biotek Instruments, Inc. (Winooski, Vermont, United States of America).

5. Statistics

Quantitative data was obtained from spectrophotometry (cell proliferation), light microscopy (cell rounding), fluorescent microscopy (ROS production), flow cytometry (cell cycle progression and mitoprobe assay) and enzyme-linked immunosorbent assays (SOD and catalase activity). Qualitative data was obtained from light- and fluorescent microscopy. Three independent repeats were conducted for each method conducted in this study. Statistical analysis include means with their associated standard error and 95% confidence intervals which were provided for categorical variables (p-value < 0.05). The data was compared to the negative control samples including cells propagated in growth medium and vehicle-treated cells. Data was evaluated using Microsoft® Excel 2010 (Microsoft Corporation, Washington, United Sates of America). Data is statistically analysed for significance using the factorial design approach of analysis of variance (ANOVA)-single model. This was followed by comparing DATS-treated cells in the absence of the ROS scavengers with DATS-treated cells in the presence of the ROS scavengers to determine if the scavengers had an effect on the impact DATS had on both cell lines over different time periods. Flow cytometry analysis involved at least 10 000 events and was repeated three times. Fluorescent images were analysed using Image J software developed by the National Institutes of Health (Bethesda, Maryland, United States of America). The fluorescent intensity of at least 100 cells was evaluated per condition in each experiment. Furthermore, 100 cells were counted for light microscopy per condition; these included rounded and not rounded cells.

6. Results

6.1 Cell proliferation (crystal violet): spectrophotometry

A crystal violet assay in combination with spectrophotometry was used to evaluate the effect of DATS on cell proliferation over 24 h- and 48 h in the presence and absence of the ROS scavenger NAC as well as scavengers for individual ROS. The crystal violet stain is a triphenylmethane cation dye which acts as a DNA intercalating agent that binds to the DNA within cell nuclei and resulting in a purple staining. When solubilised, the dye intensity can be used to quantify cell density of proliferating cells growing in a monolayer since the absorbance directly correlates with cell number with an increase in dye intensity indicating higher cell density (63). This assay was used to establish the dependency of the mechanism of action of DATS on ROS and the relevance of the different ROS after 24 h- and 48 h of exposure as well as to determine the concentrations of DATS and the ROS scavengers to be used for subsequent experiments.

The effect of DATS on cell growth was first established in both cell lines to determine what the optimal exposure period and DATS concentration was. Exposure to DATS at 10 µM – 150 µM in the MDA-MB-231 cell line resulted in a dose-dependent and time-dependant decrease in cell growth to 84%, 81%, 74%, 70%, 64%, 60%, and 53% after exposure to 10 µM-, 25 µM-, 50 µM-, 75 µM-, 100 µM-, 125 µM- and 150 µM DATS after 24 h, when compared to cells propagated in complete growth medium, this is depicted in figure 6. After 48 h exposure to these concentrations, cell growth in the MDA-MB-231 cell line was decreased to 84%, 62%, 57%, 53%, 56%, 51% and 45% respectively, when compared to cells propagated in complete growth medium which is depicted in Figure 7. The representative doses of DATS chosen for further experiments in the MDA-MB-231 cell line include 10 µM-, 50 µM-, 100 µM- and 150 µM to represent the full dose response range exerted by DATS. In addition, this study utilised 100 µM DATS where cells were co-exposed with DATS and the individual scavengers for specific ROS, since exposure to 100 µM DATS demonstrated optimal antiproliferative activity as seen in figures 6 and 7. Subsequently, cells were exposed to DATS (100 µM) in the presence and absence of different concentrations of NAC to determine the optimal NAC concentration whereby cell growth was maximally restored. It was observed that at 1.5 mM, 1.75 mM and 2mM NAC cell growth reached 100%, 92% and 105% respectively, after 24 h of exposure when compared to cells propagated in growth medium. After 48 h of exposure to DATS (100 µM) in the presence of 1.75 mM and 2 mM NAC cell growth had reached 101% and 108%, respectively. After exposure to the higher concentrations of NAC, cell growth decreased significantly for both time

periods, therefore a concentration of 2 mM NAC was selected as this completely restored cell growth when compared to cells exposed to only DATS (100 µM) for 24 h (64%) and 48 h (56%) illustrated in figure 8. The MDA-MB-231 cells were also treated with NAC (2 mM) in conjunction with DATS (10 µM-, 25 µM-, 50 µM-, 75 µM-, 100 µM-, 125 µM- and 150 µM) to confirm the dependency of the effect of DATS on ROS. After 24 h of co-exposure, cell growth in the presence of DATS (10 µM-, 25 µM-, 50 µM-, 75 µM-, 100 µM-, 125 µM- and 150 µM) and NAC was 110%, 107%, 106%, 108%, 96%, 99%, and 97% respectively, when compared to cells propagated in growth medium alone, demonstrating a significant (*p*-value < 0.05) increase in cell growth when compared to cells exposed to DATS alone as illustrated in figure 6. Similarly, after 48 h of co-exposure cell growth was observed to be 100%, 107%, 108%, 104%, 99%, 99% and 88% when compared to cells propagated in growth medium alone, also demonstrating a significant (*p*-value < 0.05) increase in cell growth when compared to cells exposed to DATS alone as observed in figure 7.

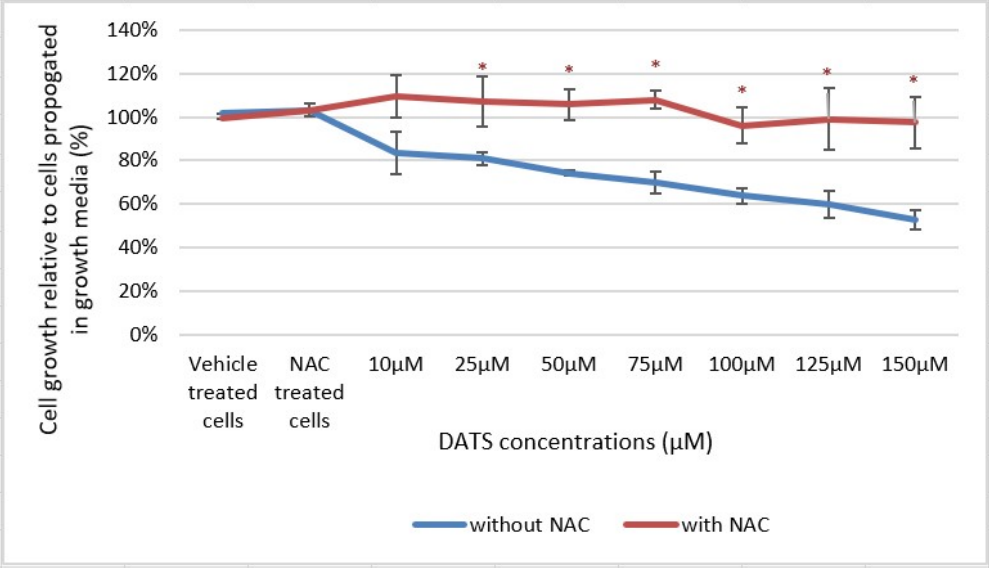

Figure 6: Spectrophotometry data of crystal violet staining intensity in MDA-MB-231 cells demonstrating the effect of diallyl trisulfide (DATS) (10 µM, 25 µM, 50 µM, 75 µM, 100 µM, 125 µM and 150 µM) on proliferation in the presence or absence of N-acetyl cysteine (NAC) (2 mM) compared to cells propagated in complete growth medium for 24 h. Statistical significance was calculated using an ANOVA test with a *p*-value < 0.05 indicating statistical significance of data compared to cells propagated in DATS alone without NAC and is indicated by an *.

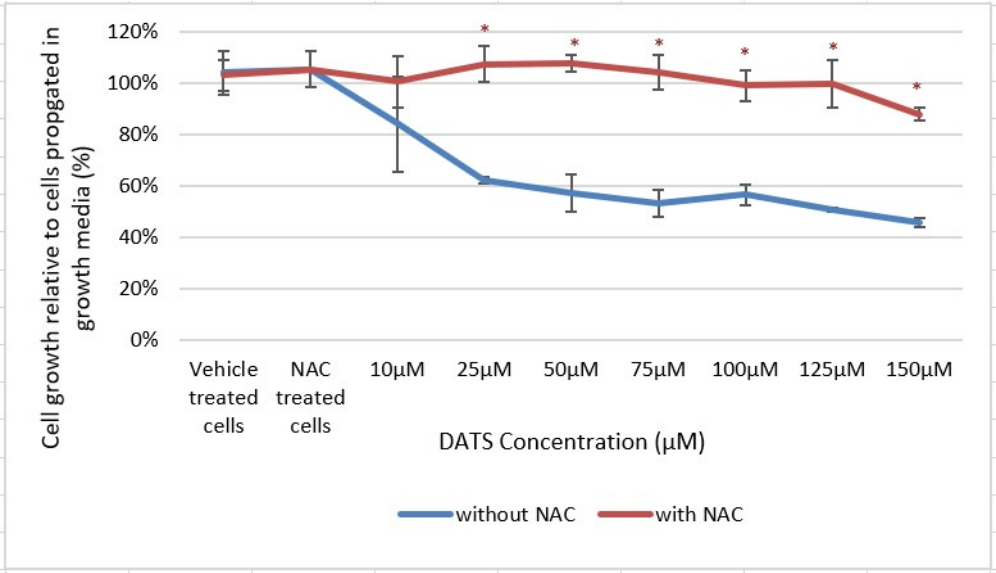

Figure 7: Spectrophotometry data of crystal violet staining intensity in MDA-MB-231 cells demonstrating the effect of diallyl trisulfide (DATS) (10 µM, 25 µM, 50 µM, 75 µM, 100 µM, 125 µM and 150 µM) on proliferation in the presence or absence of N-acetyl cysteine (NAC) (2 mM) compared to cells propagated in complete growth medium for 48 h. Statistical significance was calculated using an ANOVA test with a *p*-value < 0.05 indicating statistical significance of data compared to cells propagated in DATS alone without NAC and is indicated by an *.

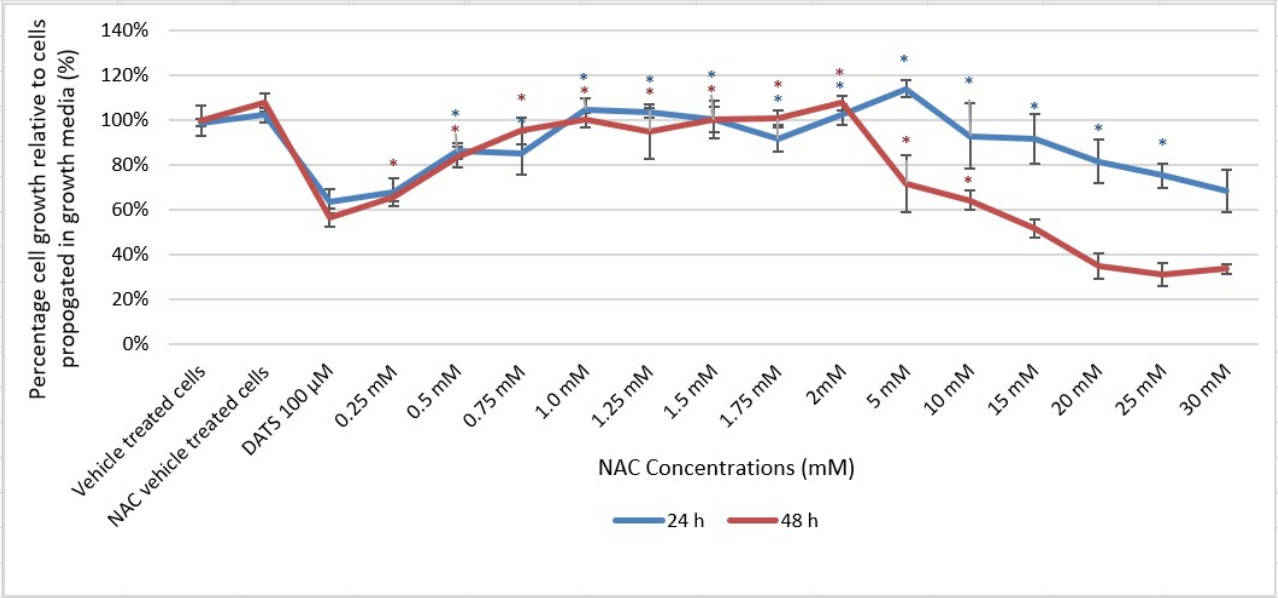

Figure 8: Crystal violet spectrophotometry results showing the effect of different doses of N-acetyl cysteine (NAC) (0.25 mM - 30 mM) with a NAC vehicle of 30 mM in the presence of diallyl trisulfide (DATS) (100 µM) for 24- and 48 h of exposure in the MDA-MB-231 cell line in order to determine the appropriate concentration of NAC for further experiments. Statistical significance was calculated using an ANOVA test with a *p*-value < 0.05 indicating statistically significant increases in cell growth when compared to cells exposed to 100 µM DATS and is indicated by an *.

Data demonstrated that the A549 cell line was more resistant to the antiproliferative effects exerted by DATS and required exposure to a higher concentration-range. Thus, an alternative concentration range of DATS was selected (10 µM– 400 µM) to determine an effective concentration range for all subsequent experiments. It was decided that a dose range of 100 µM, 150 µM, 200 µM, 250 µM, 300 µM and 400 µM would be used for the A549 cell line for treatment with NAC and to mirror the concentration range used for the MDA-MB-231 cell line, this was chosen as cell growth at concentrations lower than 100 µM remained above 80% and only below this dose did the effects of DATS become apparent as is illustrated in figure 9.

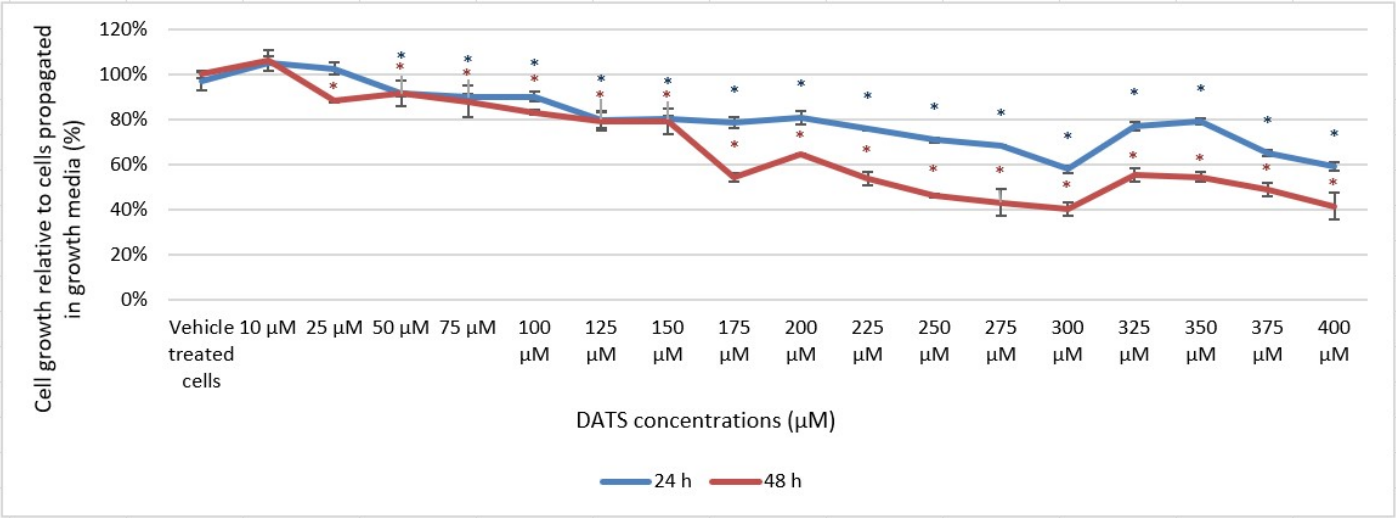

Figure 9: Crystal violet spectrophotometry results showing the effect of different doses of diallyl trisulfide (DATS) (10 µM - 400 µM) on the A549 cell line in order to ascertain the effective concentration range of DATS for 24 h and 48 h exposure. Statistical significance was calculated using an ANOVA test with a *p*-value < 0.05 indicating statistical significance of data compared to cells propagated growth medium alone and is indicated by an *.

The effect of DATS on cell growth of the A549 cells exhibited time- and dose-dependent antiproliferative activity as demonstrated by a decrease in cell growth to 90%, 80%, 81%, 71%, 58% and 59% after exposure to DATS (100 µM, 150 µM, 200 µM, 250 µM, 300 µM and 400 µM) for 24 h, when compared to cells propagated in growth medium, this is illustrated in figure 10. Similarly, after 48 h of treatment with DATS (100 µM, 150 µM, 200 µM, 250 µM, 300 µM and 400 µM), cell growth was reduced to 83%, 79%, 64%, 46%, 40% and 41%, respectively when compared to cells propagated in growth medium as illustrated in figure 11. The representative doses of DATS chosen for further experiments in the A549 cell line included 100 µM, 200 µM, 300 µM and 400 µM to represent the full dose response range exerted by DATS. In addition, this study utilised 300 µM DATS where cells were exposed to DATS in the presence or absence and the individual scavengers for specific ROS, since exposure to 300 µM DATS demonstrated optimal antiproliferative activity.

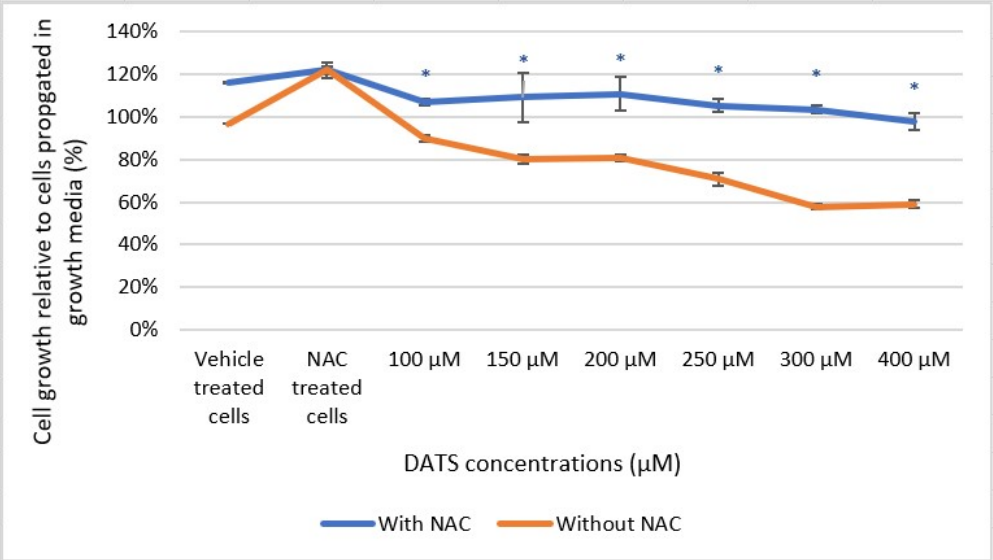

Figure 10: Spectrophotometry results of crystal violet staining intensity in A549 cells demonstrating the effect of diallyl trisulfide (DATS) (100 µM, 150 µM, 200 µM, 250 µM, 300 µM, 350 µM and 400 µM) on proliferation in the presence or absence of N-acetyl cysteine (NAC) (2 mM) compared to cells propagated in complete growth medium for 24 h. Statistical significance was calculated using an ANOVA test with a *p*-value < 0.05 indicating statistical significance of data compared to cells propagated in DATS alone without NAC and is indicated by an *.

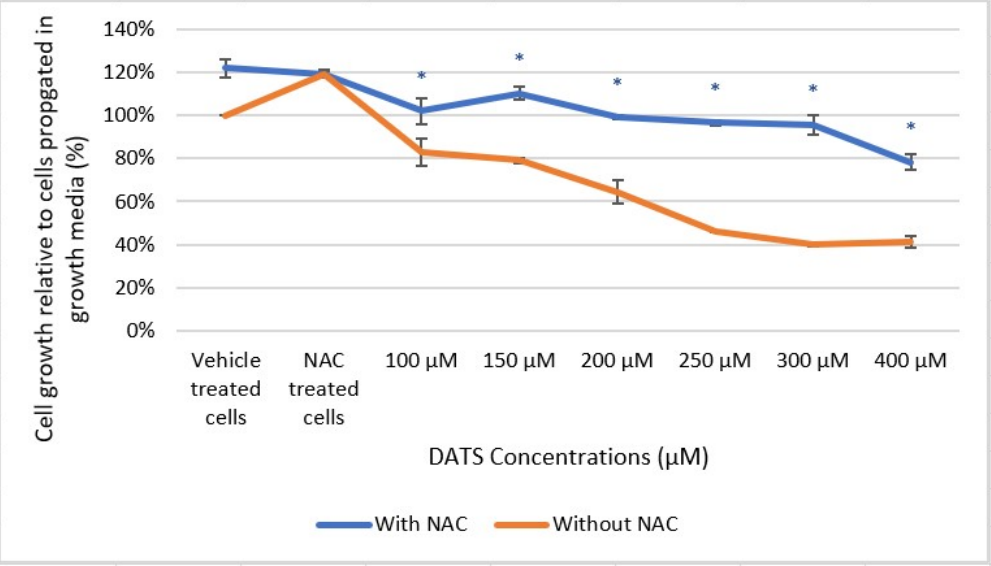

Figure 11: Spectrophotometry results of crystal violet staining intensity in A549 cells demonstrating the effect of diallyl trisulfide (DATS) (100 µM, 150 µM, 200 µM, 250 µM, 300 µM, 350 µM and 400 µM) on proliferation in the presence or absence of N-acetyl cysteine (NAC) (2 mM) compared to cells propagated in complete growth medium for 48 h. Statistical significance was calculated using an ANOVA test with a *p*-value < 0.05 indicating statistical significance of data compared to cells propagated in DATS alone without NAC and is indicated by an *.

The A549 cells were also exposed to DATS (300 µM) in the presence and absence of NAC (0.5 mM – 30 mM) to determine the optimal concentration of NAC that restored cell growth to that of cells propagated in media only. Exposure to DATS (300 µM) for 48 h in the presence of NAC (2-15 mM) restored cell growth and therefore, 2 mM NAC was selected for further experiments this is illustrated in figure 12. The A549 cells were also treated with DATS (100 µM, 150 µM, 200 µM, 250 µM, 300 µM, and 400 µM) in the presence of NAC (2 mM) to confirm that the effect of DATS on proliferation is dependent on the generation of excessive ROS. After 24 h of exposure to DATS (100 µM - 400 µM) in the presence of NAC (2 mM) cell growth was observed to be 107%, 109%, 111%, 105%, 103%, and 98% respectively when compared to cells propagated in growth medium as seen in figure 10. After 48 h of exposure to DATS (100 µM - 400 µM) in the presence of NAC (2 mM) cell growth was restored to 102%, 110%, 99%, 97%, 96%, and 78% when compared to cells propagated in growth medium alone, illustrated in figure 11. At both time periods cell growth was significantly (p-value < 0.05) increased by NAC when compared to cells exposed to DATS alone.

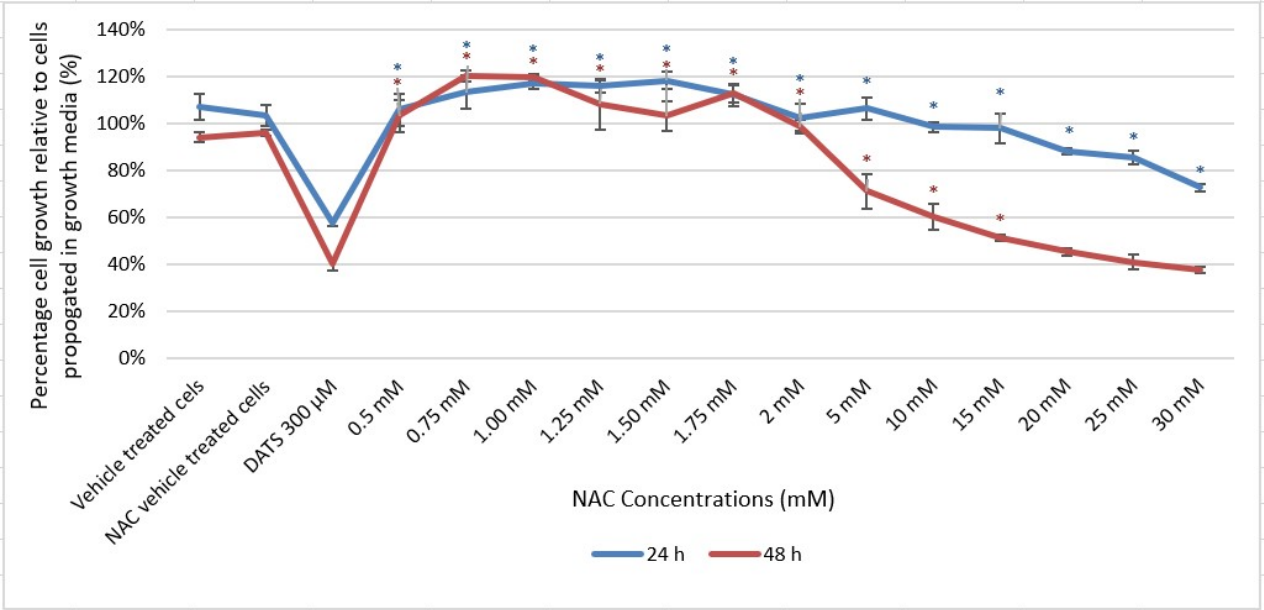

Figure 12: Crystal violet Spectrophotometry results showing the effect of different doses of N-acetyl cysteine (NAC) (0.25 mM - 30 mM) in the presence of diallyl trisulfide (DATS) (300 µM) for 24- and 48 h of exposure in the A549 cell line to determine the appropriate concentration of NAC. Statistical significance was calculated using an ANOVA test with a p-value < 0.05 indicating statistically significant increases in cell growth compared to cells propagated in 300 µM DATS and is indicated by an *.

Results thus indicated that NAC significantly inhibited the antiproliferative activity exerted by DATS and restored cell growth in both cell lines, thus scavengers of specific ROS were employed for further studies to evaluate the role of each ROS in the influence exerted by DATS on cell growth. This was accomplished by exposing MDA-MB-231 cells to DATS (100 µM) in the presence or absence of the scavengers specific for each ROS. In addition, a concentration-range was utilised for each scavenger to determine at what concentration cell growth was optimally restored, when compared to cells exposed to 100 µM DATS for 24 h and 48 h alone which resulted in 64% and 56% cell growth respectively, when compared to cells propagated in growth medium in the MDA-MB-231 cell line. However, Carboxy-PTIO restored cell growth in a dose-dependent manner to 88%, 98%, 95%, 98%, 106% and 108% at 1-, 2-, 4-, 6-, 8- and 10 µM Carboxy-PTIO compared to cells propagated in growth medium therefore, co-exposure with 8 µM (106%) was chosen for Carboxy-PTIO for all subsequent experiments for 24 h of exposure, as illustrated in figure 13. After exposure to Tiron in the presence of DATS (100 µM) for 24 h cell growth increased in a dose-dependent manner reaching cell growth of 92%, 92%, 98%, 106%, 106% and 113% at 1 mM, 2 mM, 4 mM, 6 mM, 8 mM and 10 mM respectively. A dose of 6 mM (106%) was selected for 24 h exposure to Tiron, as illustrated in figure 14. Exposure to DMTU in the presence of 100 µM DATS for 24 h resulted in cell growth of 85%, 94%, 99%, 100%, 100% and 101% at 1 mM, 2 mM, 4 mM, 6 mM, 8 mM and 10 mM DMTU, indicating a dose-dependent increase in cell growth after which a concentration of 8 mM DMTU was chosen (100% cell growth) for 24 h of exposure to DATS and DMTU for further experiments, as illustrated in figure 15. Exposure to SA in the presence of 100 µM DATS for 24 h resulted in cell growth of 92%, 92%, 98%, 99%, 106% and 109% at 1-, 2-, 4-, 6-, 8- and 10 mM respectively exhibiting a dose-dependent increase in cell growth, and 6 mM was chosen for further experiments at 24 h of exposure (99% cell growth), as illustrated in figure 16. After exposure to Mannitol with DATS 100 µM for 24 h, cell growth was increased in a dose-dependent manner to 73%, 76%, 85%, 90%, 98% and 94% at 10-, 20-, 40-, 60-, 80- and 100 mM respectively, therefore a dose of 80 mM (98% cell growth) was decided upon for 24 h exposure to DATS and Mannitol, as shown in figure 17. Finally, after exposure to Trolox in the presence of 100 µM DATS for 24 h a concentration of 40 µM was decided on (99% cell growth) for 24 h of exposure since cell growth reached 83%, 102%, 99%, 100%, 110% and 107% in a dose-dependent manner after exposure to DATS in the presence of 10 µM, 20 µM, 40 µM, 60 µM, 80 µM and 100 µM, respectively, depicted in figure 18.

After 48 h of exposure to 100 µM DATS alone, cell growth was observed to be 56% and subsequently, this concentration of DATS was used for exposure to DATS in the presence of the various inhibitors of ROS for 48 h in the MDA-MB-231 cell line. However, a significant increase (p-value < 0.05) in cell growth after 48 h of exposure to DATS (100 µM) with the inhibitors was

observed only for cells co-exposed to DATS in the presence of Carboxy-PTIO, Mannitol or Trolox and not for DMTU, SA and Tiron, as seen in figures 13 - 18. Therefore, the concentration chosen was 8 µM for Carboxy-PTIO (84% cell growth) since co-exposure to DATS in the presence of 1 µM, 2 µM, 4 µM, 6 µM, 8 µM and 10 µM resulted in cell growth of 63%, 65%, 81%, 74%, 84% and 81% indicating a dose-dependent increase in cell growth and that at 8 µM cell growth was optimally restored, illustrated in figure 13. Exposure to Mannitol in the presence of DATS 100 µM for 48 h of exposure increased cell growth to 77%, 81%, 90%, 75%, 85% and 100% in a dose-dependent manner at 10 mM, 20 mM, 40 mM, 60 mM, 80 mM and 100 mM therefore, a concentration of 100 mM for Mannitol (100% cell growth) was chosen, this is shown in figure 17. After 48 h exposure to Trolox with DATS 100 µM cell growth was increased in a dose-dependent manner to 57%, 53%, 70%, 75%, 87% and 65% at 10 µM, 20 µM, 40 µM, 60 µM, 80 µM and 100 µM, after which a concentration of 80 µM was decided upon for Trolox (87% cell growth), taken from figure 18. After 24 h and 48 h of exposure, all 6 scavengers either partially or completely restored cell growth when compared to cells exposed to only DATS (100 µM), and optimal doses of the scavengers were selected for further experiments including Carboxy-PTIO (8 µM), Tiron (6 mM), DMTU (8 mM), SA (6 mM), Mannitol (80 mM) and Trolox (40 µM) for 24 h exposure experiments and for 48 h experiments the selected concentrations for Carboxy-PTIO, Mannitol, and Trolox were 8 µM, 100 mM and 80 µM, respectively.

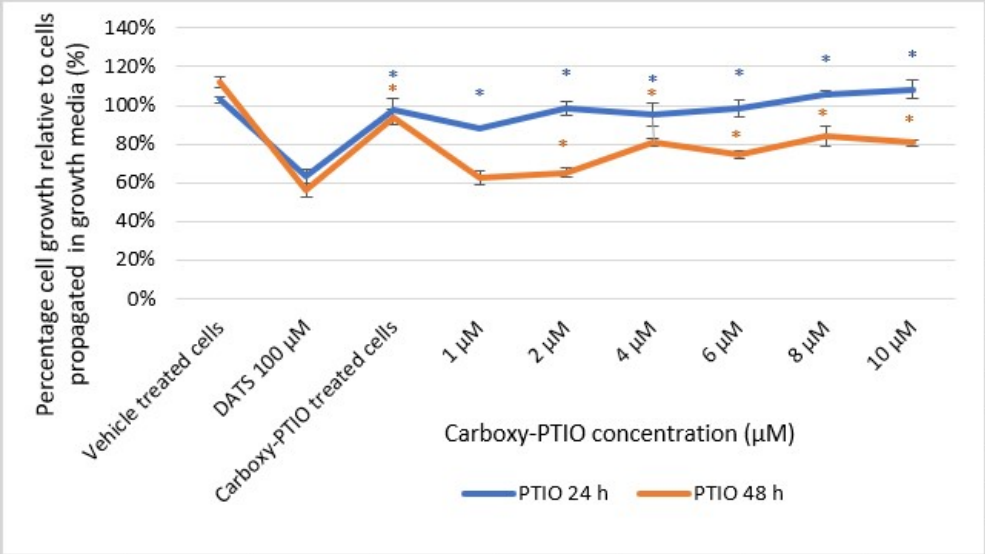

Figure 13: Spectrophotometry results of crystal violet staining intensity demonstrating the effect of different concentrations of 2-(4-Carboxyphenyl)-4,4,5,5-tetramethylimidazoline-1-oxyl-3-oxide (Carboxy-PTIO) with diallyl trisulfide (DATS) (100 µM) on the proliferation of MDA-MB-231 cells after 24 h and 48 h exposure. Statistical significance was calculated using an ANOVA test with a *p*-value < 0.05 indicating statistically significant increases in cell growth compared to cells exposed to DATS alone and is indicated by an *.

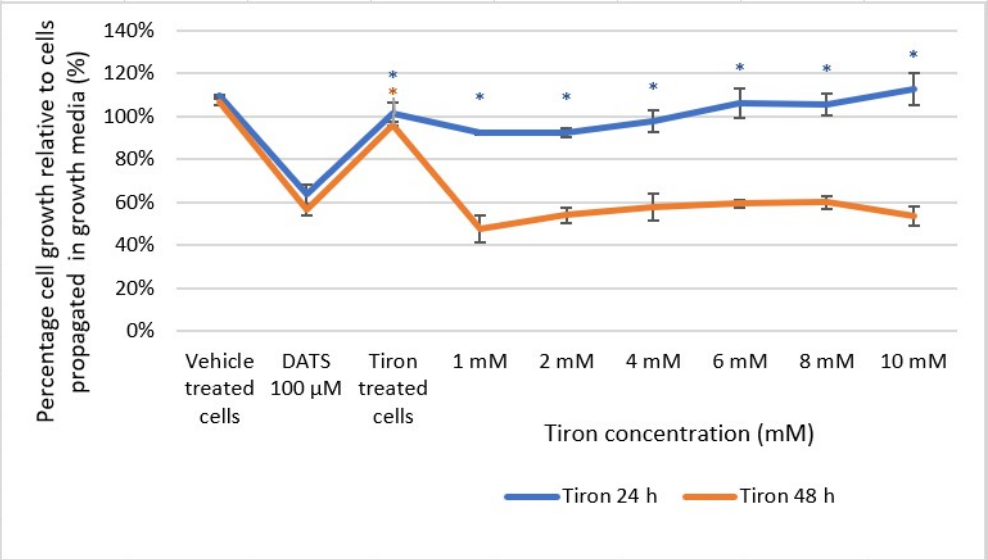

Figure 14: Spectrophotometry results of crystal violet staining intensity demonstrating the effect of different concentrations of Tiron with diallyl trisulfide (DATS) (100 µM) on the proliferation of MDA-MB-231 cells after 24 h and 48 h of exposure. Statistical significance was calculated using an ANOVA test with a *p*-value < 0.05 indicating statistically significant increases in cell growth compared to cells exposed to DATS alone and is indicated by an *.

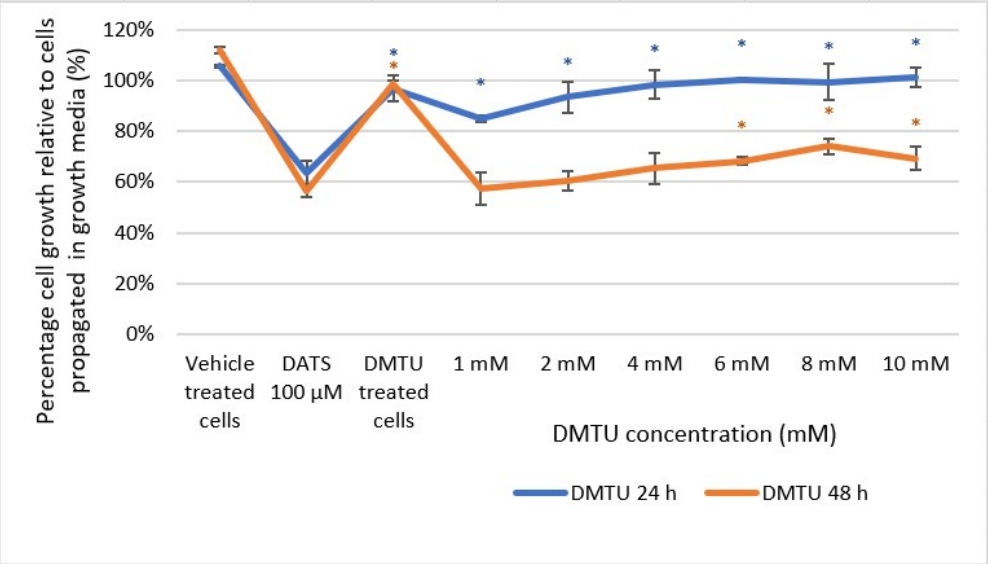

Figure 15: Spectrophotometry results of crystal violet staining intensity demonstrating the effect of different concentrations of N, N-dimethyl thiourea (DMTU) with diallyl trisulfide (DATS) (100 µM) on the proliferation of MDA-MB-231 cells after 24 h and 48 h of exposure. Statistical significance was calculated using an ANOVA test with a *p*-value < 0.05 indicating statistically significant increases in cell growth compared to cells exposed to DATS alone and is indicated by an *.

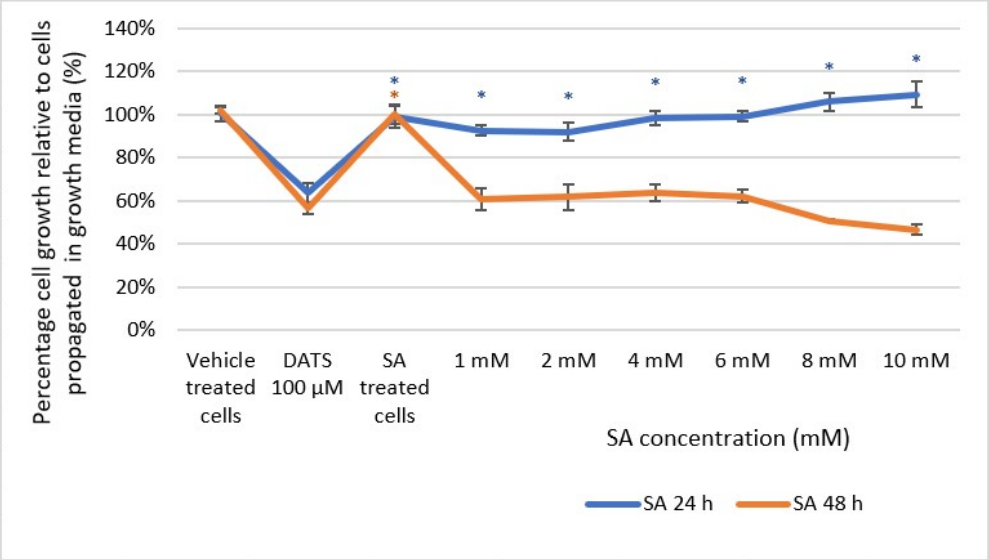

Figure 16: Spectrophotometry results of crystal violet staining intensity demonstrating the effect of different concentrations of sodium azide (SA) with diallyl trisulfide (DATS) (100 µM) on the proliferation of MDA-MB-231 cells after 24 h and 48 h of exposure. Statistical significance was calculated using an ANOVA test with a *p*-value < 0.05 indicating statistically significant increases in cell growth compared to cells exposed to DATS alone and is indicated by an *.

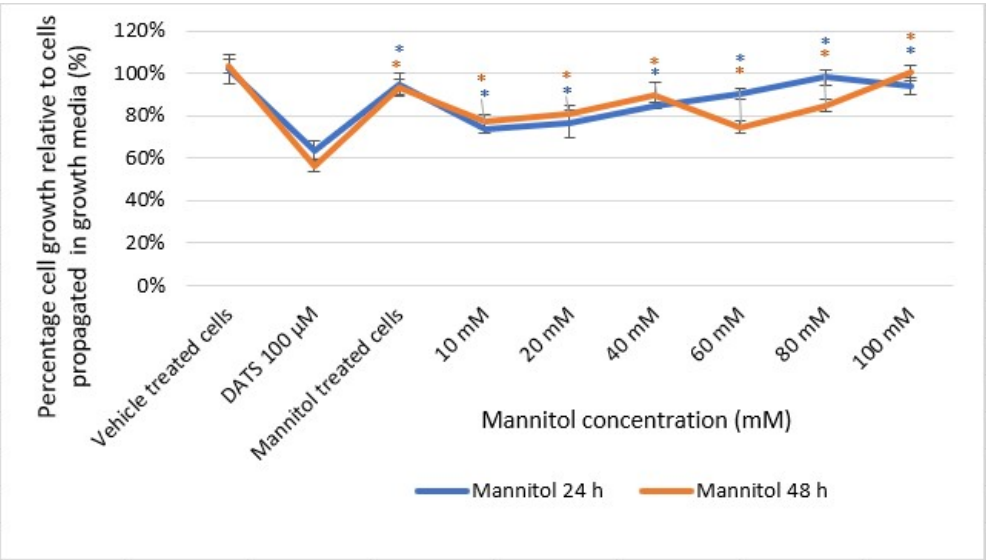

Figure 17: Spectrophotometry results of crystal violet staining intensity demonstrating the effect of different concentrations D-Mannitol (Mannitol) with diallyl trisulfide (DATS) (100 µM) on the proliferation of MDA-MB-231 cells after 24 h and 48 h exposure. Statistical significance was calculated using an ANOVA test with a *p*-value < 0.05 indicating statistically significant increases in cell growth compared to cells exposed to DATS alone and is indicated by an *.

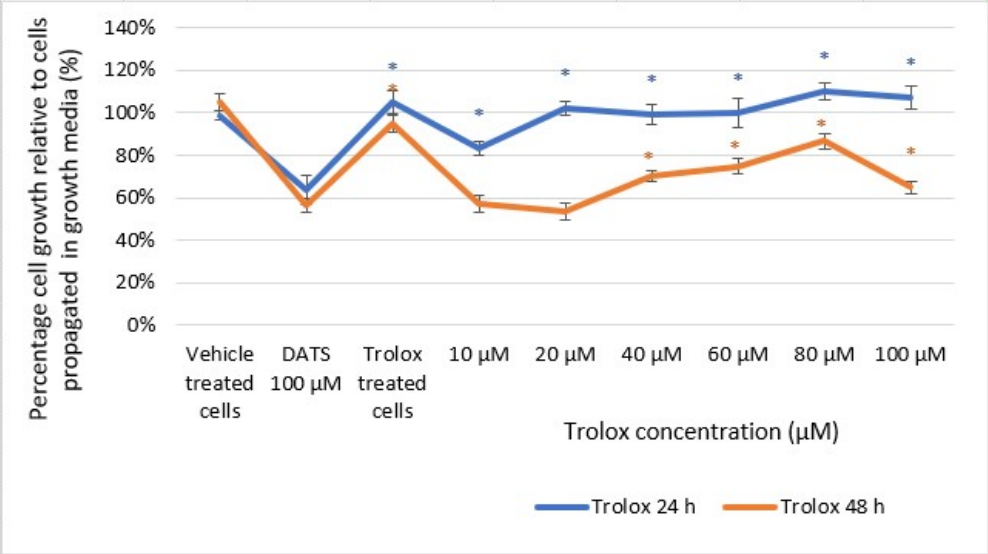

Figure 18: Spectrophotometry results of crystal violet staining intensity demonstrating the effect of different concentrations Trolox with diallyl trisulfide (DATS) (100 µM) on the proliferation of MDA-MB-231 cells after 24 h and 48 h exposure. Statistical significance was calculated using an ANOVA test with a *p*-value < 0.05 indicating statistically significant increases in cell growth compared to cells exposed to DATS alone and is indicated by an *.

Since NAC partially abolished the antiproliferative effects exerted by DATS in the A549 cell line, the role of ROS was evaluated on the antiproliferative activity exerted by DATS by using specific scavengers for ROS in the presence and absence of DATS (300 µM). After 24 h of exposure to the 6 scavengers, cell growth was partially-or completely restored when compared to cells exposed to 300 µM DATS alone which exhibited growth of 58% when compared to cells propagated in growth medium. After 24 h of exposure to 300 µM DATS in the presence of SA (10 mM) cell growth was observed at 103% compared to 58% when exposed to DATS (300 µM) alone. Exposure to DATS in the presence of 1 mM, 2 mM, 4 mM, 6 mM, and 8 mM SA resulted in cell growth of 70%, 82%, 83%, 90%, and 94% respectively indicating that SA inhibited the antiproliferative effects exerted by DATS in a dose-dependent manner, this is illustrated in figure 19. After exposure to DMTU in the presence of DATS (300 µM) a dose of 8 mM was chosen (97% cell growth) for 24 h exposure since co-exposure to DATS (300 µM) and DMTU (1 mM, 2 mM, 4 mM, 6 mM, 8 mM and 10 mM) significantly restored cell growth to 85%, 92%, 91%, 81%, 97% and 93% when compared to cells exposed to DATS alone (58%), depicted in figure 20. After exposure to DATS (300 µM) and Carboxy-PTIO for 24 h A concentration of 6 µM Carboxy-PTIO was decided upon (103% cell growth), as exposure to 1 µM, 2 µM, 4 µM, 8 µM and 10 µM Carboxy-PTIO in the presence of DATS resulted in cell growth of 87%, 91%, 97%, 103% 102% and 101% displaying a dose-dependent increase in cell growth, illustrated in

figure 21. Exposure to DATS (300 µM) with Tiron for 24 h also resulted in a dose-dependent increase in cell growth to 102%, 105%, 112%, 122%, 122% and 121% after exposure to 1 mM, 2 mM, 4 mM, 6 mM, 8 mM and 10 mM Tiron respectively, displaying a dose-dependent increase in cell growth; from this data a concentration of 2 mM Tiron was decided upon for further experiments at 24 h of exposure, this is observable in figure 22. After exposure to Mannitol in the presence of DATS 300 µM for 24 h, treatment with Mannitol at 10 mM, 20 mM, 40 mM, 60 mM, 80 mM and 100 mM resulted in cell growth of 101%, 96%, 115%, 104%, 111%, and 104% respectively. A concentration of 20 mM Mannitol was decided upon for further 24 h experiments, this illustrated in figure 23. Finally, after exposure to Trolox in the presence of DATS (300 µM) for 24 h cell growth was observed to be 94%, 114%, 111%, 116%, 116% and 118% after exposure to 10 µM, 20 µM, 40 µM, 60 µM, 80 µM and 100 µM Trolox respectively, displaying a dose-dependent increase in cell growth. From this data a concentration of 20 µM Trolox was selected (114% cell growth) for further 24 h experiments, depicted in figure 24. After 48 h of exposure to the scavengers Carboxy-PTIO, DMTU, SA, Tiron, Mannitol and Trolox at their highest concentrations respectively (10 µM, 10 mM, 10 mM, 10 mM, 100 mM and 100 µM) with DATS (300 µM) it was observed that cell growth had reached 66%, 64%, 58%, 61%, 76% and 84% respectively, indicating that 24 h exposure to the inhibitors in the presence of DATS (300 µM) was more effective than 48 h exposure therefore further experiments for this cell line were conducted at 24 h exposure times (Figures 19-24).

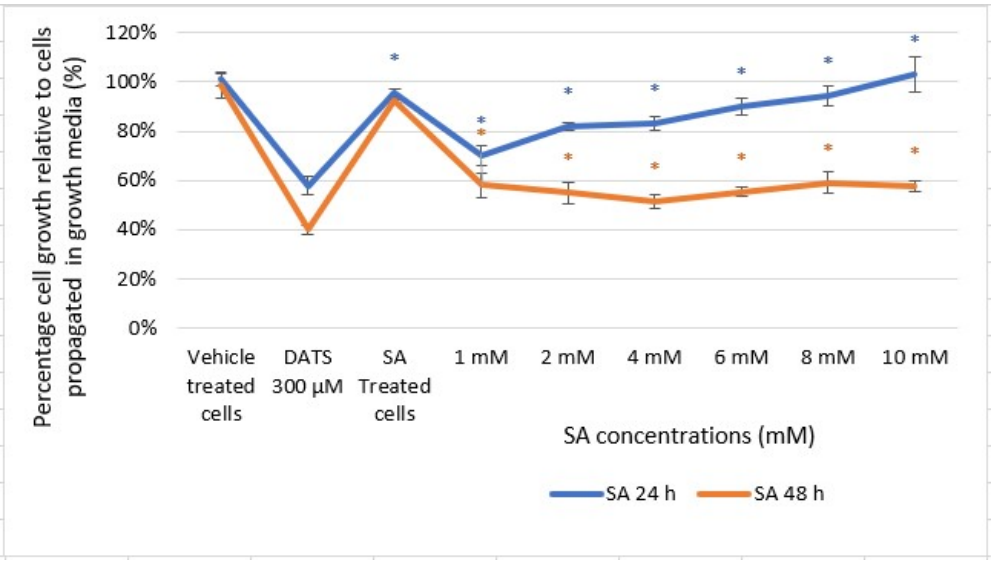

Figure 19: Spectrophotometry results of crystal violet staining intensity demonstrating the effect of different concentrations of sodium azide (SA) with diallyl trisulfide (DATS) (300 µM) on the proliferation of A549 cells after 24 h and 48 h of exposure. Statistical significance was calculated using an ANOVA test with a *p*-value < 0.05 indicating statistically significant increases in cell growth compared to cells exposed to DATS alone and is indicated by an *.

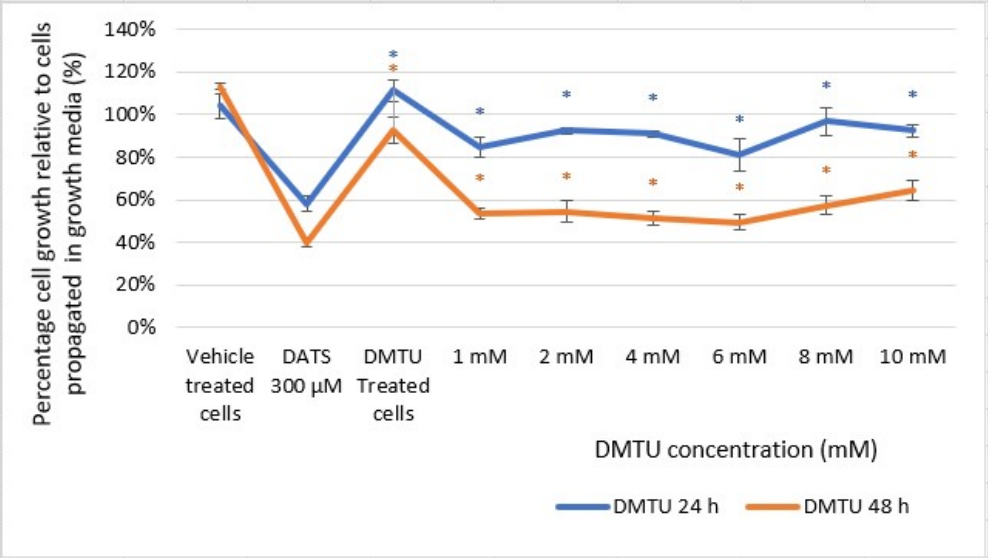

Figure 20: Spectrophotometry results of crystal violet staining intensity demonstrating the effect of different concentrations of N, N-dimethyl thiourea (DMTU) with diallyl trisulfide (DATS) (300 µM) on the proliferation of A549 cells after 24 h and 48 h of exposure. Statistical significance was calculated using an ANOVA test with a *p*-value < 0.05 indicating statistically significant increases in cell growth compared to cells exposed to DATS alone and is indicated by an *.

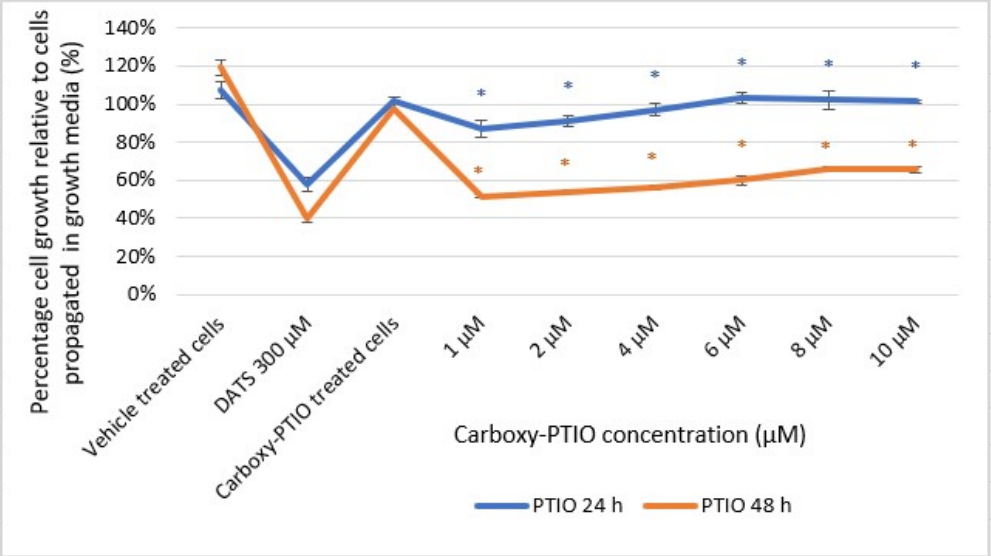

Figure 21: Spectrophotometry results of crystal violet staining intensity demonstrating the effect of different concentrations of 2-(4-Carboxyphenyl)-4,4,5,5-tetramethylimidazoline-1-oxyl-3-oxide (Carboxy-PTIO) with diallyl trisulfide (DATS) (300 µM) on the proliferation of A549 cells after 24 h and 48 h exposure. Statistical significance was calculated using an ANOVA test with a *p*-value < 0.05 indicating statistically significant increases in cell growth compared to cells exposed to DATS alone and is indicated by an *.

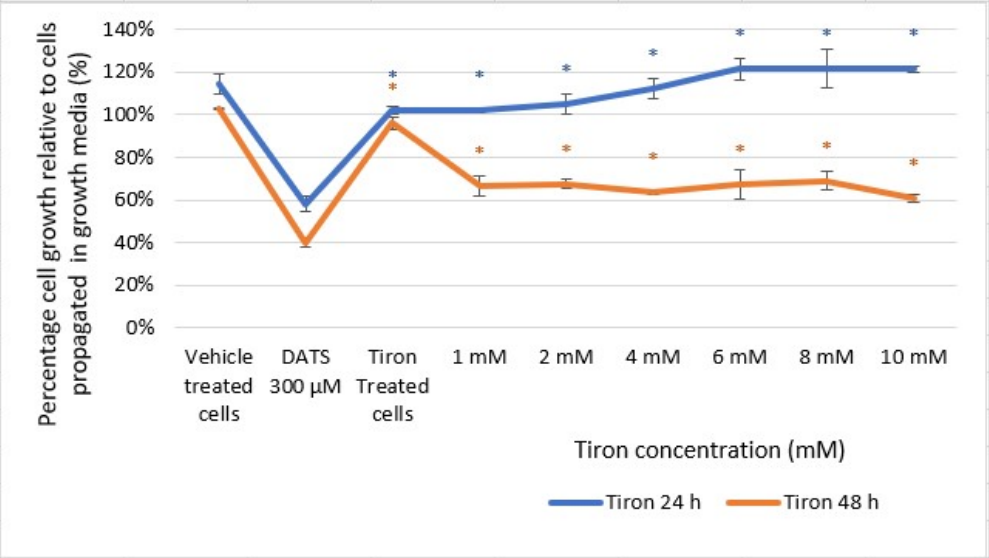

Figure 22: Spectrophotometry results of crystal violet staining intensity demonstrating the effect of different concentrations of Tiron with DATS (300 µM) on the proliferation of A549 cells after 24 h and 48 h exposure. Statistical significance was calculated using an ANOVA test with a *p*-value < 0.05 indicating statistically significant increases in cell growth compared to cells exposed to DATS alone and is indicated by an *.

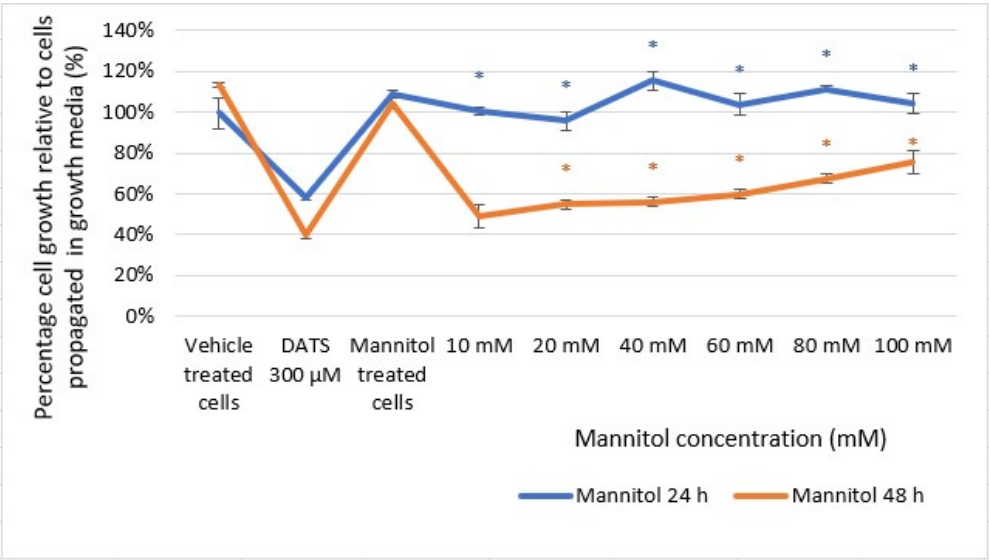

Figure 23: Spectrophotometry results of crystal violet staining intensity demonstrating the effect of different concentrations of D-Mannitol (Mannitol) with diallyl trisulfide (DATS) (300 µM) on the proliferation of A549 cells after 24 h and 48 h exposure. Statistical significance was calculated using an ANOVA test with a *p*-value < 0.05 indicating statistically significant increases in cell growth compared to cells exposed to DATS alone and is indicated by an *.

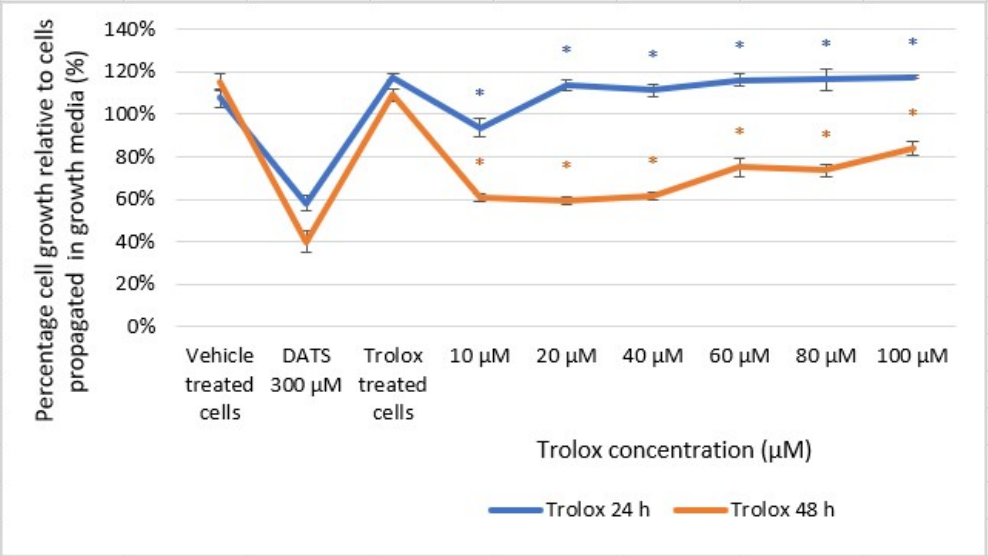

Figure 24: Spectrophotometry results of crystal violet staining intensity demonstrating the effect of different concentrations of Trolox with DATS (300 µM) on the proliferation of A549 cells after 24 h and 48 h exposure. Statistical significance was calculated using an ANOVA test with a *p*-value < 0.05 indicating statistically significant increases in cell growth compared to cells exposed to DATS alone and is indicated by an *.

6.2 H_2O_2 production using 2,7-dichlorofluoresceindiacetate: fluorescent microscopy

The effect of DATS on H_2O_2 production was used as an indicator of induced oxidative stress which was quantified using DCFDA, a non-fluorescent probe, which is oxidised by H_2O_2 to its fluorescent derivative, 2,7-dichlorofluorescein (DCF) staining the cells with a green fluorescence (74). Furthermore, to determine the temporal-dependent effects of DATS on the MDA-MB-231- and A549 cell lines, the cells were exposed to DATS for 2-, 4-, 6-, 10-, 24- and 48 h in order to determine when the effect of DATS was optimally observed.

The MDA-MB-231 cells were exposed to 10 µM-, 50 µM-, 100 µM- and 150 µM DATS, as suggested by the crystal violet data, for 2-, 4-, 6-, 10-, 24- and 48 h; however, only after exposure for 24- and 48 h was there a statistically significant (*p*-value < 0.05) increase observed in H_2O_2 production. Exposure for 24 h to 150 µM DATS demonstrated a significant (*p*-value < 0.05) increase in H_2O_2 generation to 167% when compared to cells propagated in complete growth medium (100%). Exposure to 100 µM- and 150 µM DATS for 48 h resulted in a significant increase in H_2O_2 production to 140% and 142% respectively, compared against cells propagated in growth medium, as illustrated in figure 25 and table 2. The A549 cells were exposed to DATS concentrations of 100 µM, 200 µM, 300 µM and 400 µM as suggested by the crystal violet data in a time study ranging 2-, 4-, 6-, 10-, 24 h- and 48 h,

however, no significant changes in H_2O_2 production was observed after exposure for 24 h. Furthermore, H_2O_2 production did increase in a statically significant (*p*-value < 0.05) manner after exposure for 48 h to 200 µM-, 300 µM- and 400 µM DATS as demonstrated with an increase in H_2O_2 generation to 114%, 116% and 118% respectively, when compared to cells propagated in growth medium as depicted in figure 26 and table 3. As observed the amount of oxidative stress was significantly increased only after 24 h and 48 h of exposure to DATS in the MDA-MB-231 cell line and only after 48 h in the A549 cell line, all subsequent experiments were therefore conducted after exposure to DATS for 24 h and 48 h.

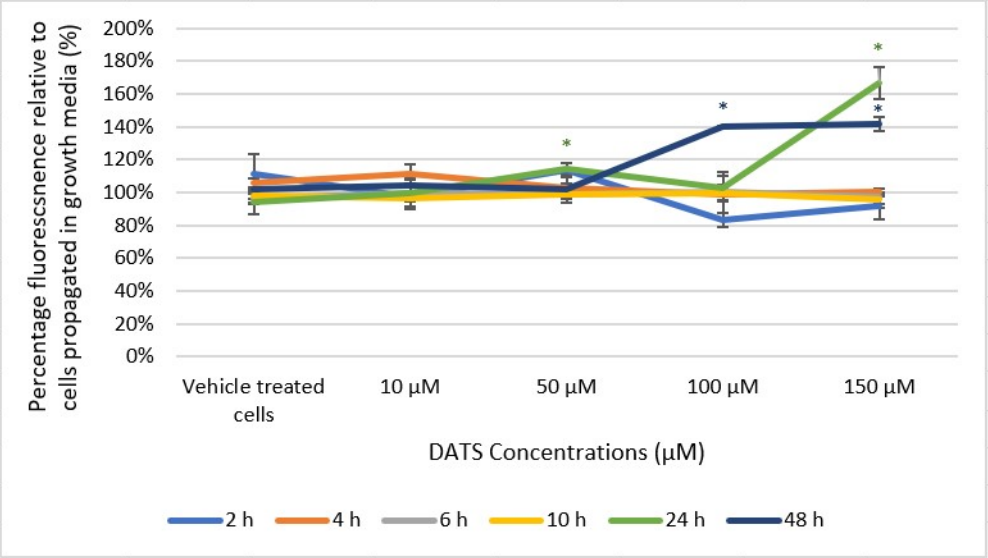

Figure 25: Fluorescent microscopy showing the 2,7-dichlorofluoresceindiacetate (DCFDA) staining results after the exposure of MDA-MB-231 cells to diallyl trisulfide (DATS) concentrations (10 µM, 50 µM, 100 µM and 150 µM) at various time intervals (2 h, 4 h, 6 h, 10 h, 24 h and 48 h). Statistical significance was calculated using an ANOVA test with a *p*-value < 0.05 indicating statistical significance of data compared to cells propagated in growth medium alone and is indicated by an *.

Table 2: Representative fluorescent images taken at **20X** magnification of MDA-MB-231 cells after exposure to diallyl trisulfide (DATS) (10 µM, 50 µM, 100 µM and 150 µM) at various time intervals (2 h, 4 h, 6 h, 10 h, 24 h and 48 h).

	2 h	4 h	6 h	10 h	24 h	48 h
Cells propagated in growth medium	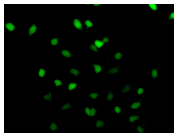	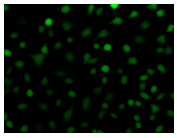	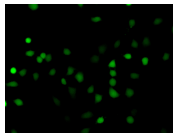	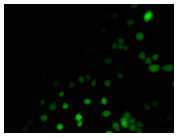	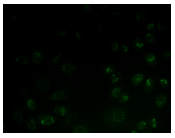	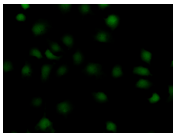
Vehicle-treated cells	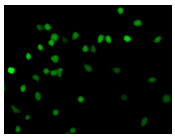	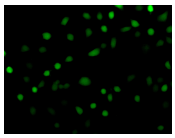	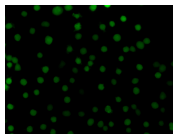	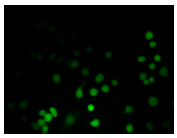	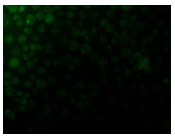	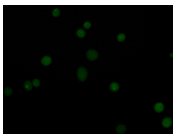
10 µM-treated cells	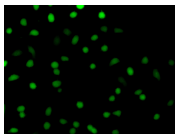	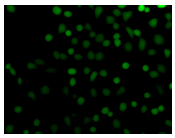	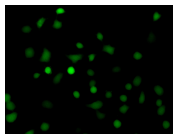	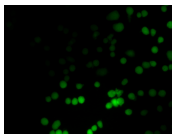	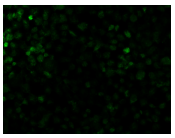	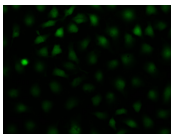
50 µM-treated cells	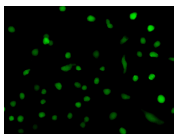	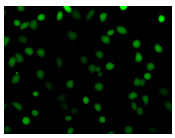	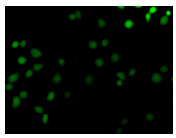	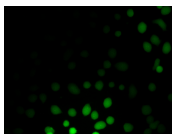	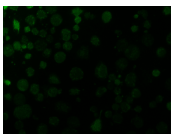	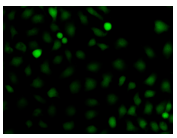
100 µM-treated cells	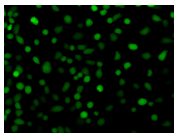	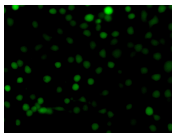	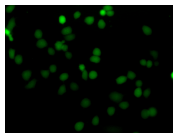	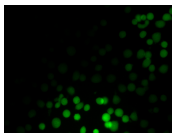	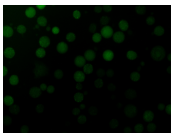	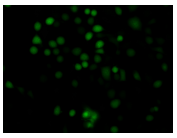
150 µM-treated cells	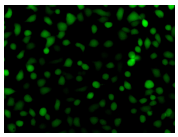	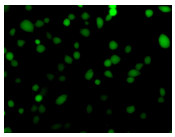	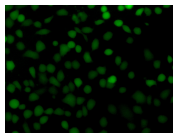	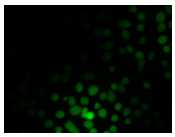	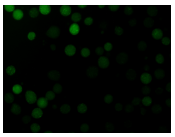	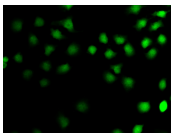

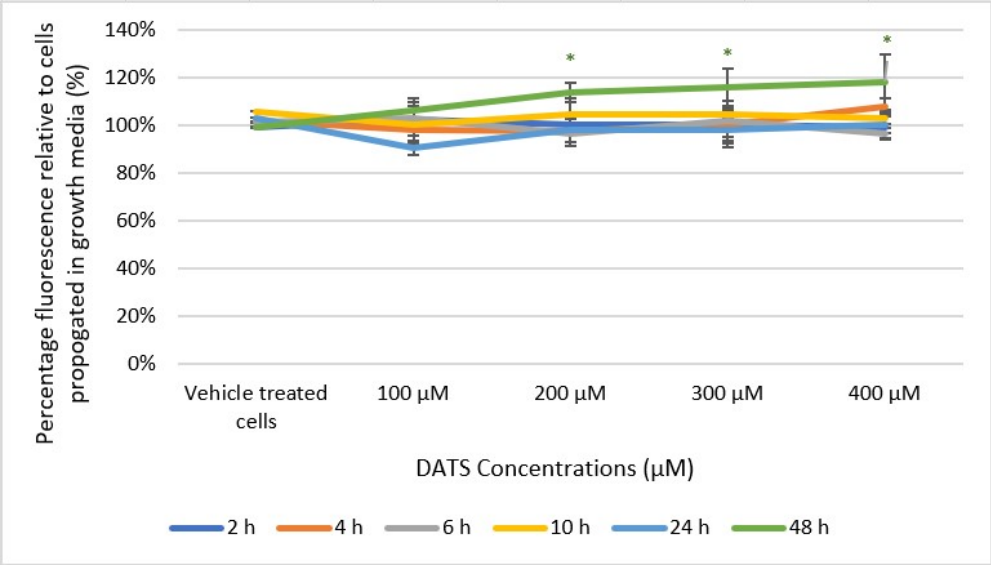

Figure 26: Fluorescent microscopy showing the 2,7-dichlorofluoresceindiacetate (DCFDA) staining results after the exposure of A549 cells to diallyl trisulfide (DATS) (100 µM, 200 µM, 300 µM and 400 µM) at various time intervals (2 h, 4 h, 6 h, 10 h, 24 h and 48 h). Statistical significance was calculated using an ANOVA test with a *p*-value < 0.05 indicating statistical significance of data compared to cells propagated in growth medium alone and is indicated by an *.

Table 3: Representative fluorescent images taken at 20X magnification of A549 cells after exposure to diallyl trisulfide (DATS) (100 µM, 200 µM, 300 µM and 400 µM) at various time intervals (2 h, 4 h, 6 h, 10 h, 24 h and 48 h).

	2 h	4 h	6 h	10 h	24 h	48 h
Cells propagated in growth medium	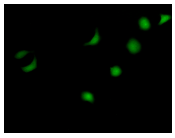	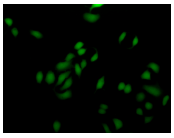	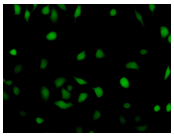	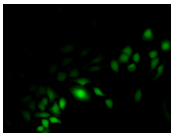	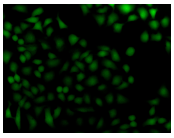	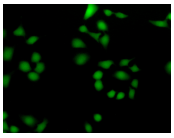
Vehicle-treated cells	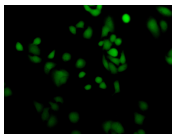	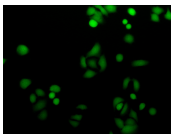	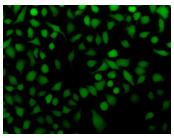	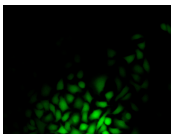	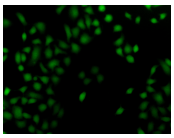	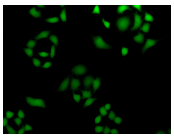
100 µM-treated cells	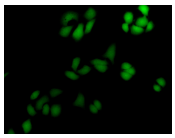	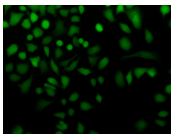	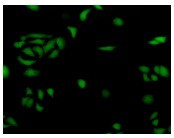	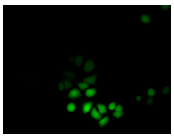	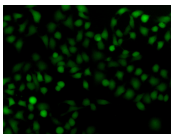	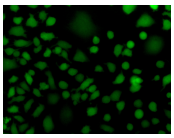
200 µM-treated cells	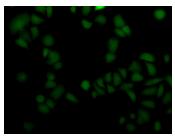	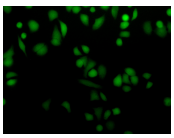	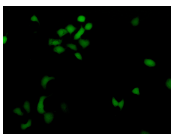	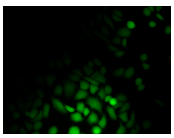	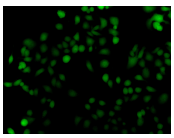	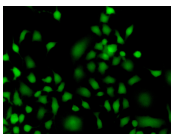
300 µM-treated cells	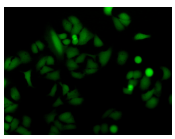	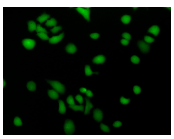	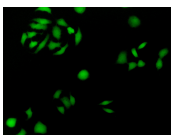	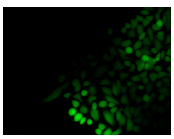	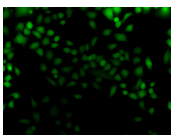	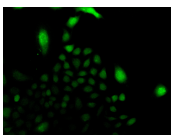
400 µM-treated cells	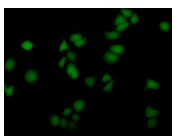	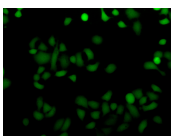	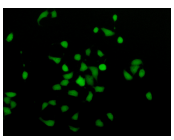	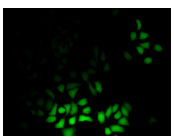	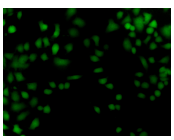	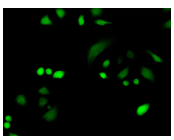

6.3 O_2^- production using dihydroethidium: fluorescent microscopy

The influence of DATS on the production of the O_2^- radical was also used as an additional indicator of oxidative stress induction and this was evaluated using DHE. The fluorescent dye, DHE, fluoresces blue within the cytosol of cells until it reacts with the O_2^- radical to form hydroxyethidium, a red fluorescent dye that intercalates into the nucleus of the cells staining the cells red. This florescence was used as an indicator to identify the presence of the O_2^- radical (75).

Fluorescent microscopy showed that DATS did not induce any O_2^- radical production, since there was no fluorescent staining demonstrated after exposure for 2 h, 4 h, 6 h, 10 h, 24 h and 48 h in both cell lines. However, the positive control for this experiment, referring to cells exposed to a 1% H_2O_2 solution for 5 minutes, made using distilled water, displayed fluorescence indicating that the dye itself was working it was just that there was a lack of O_2^- present in the cells, this can be seen in figures 27 and 28.

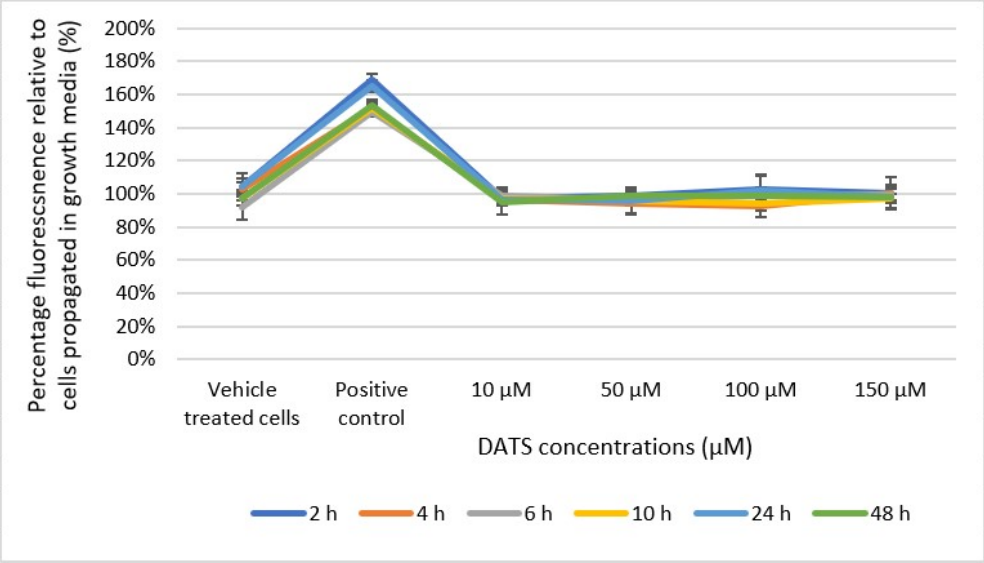

Figure 27: Fluorescent microscopy showing the dihydroethidium (DHE) staining results after the exposure of MDA-MB-231 cells to diallyl trisulfide (DATS) concentrations (10 µM, 50 µM, 100 µM and 150 µM) at various time intervals (2 h, 4 h, 6 h, 10 h, 24 h and 48 h). Statistical significance was calculated using an ANOVA test with a *p*-value < 0.05 indicating statistical significance of data compared to cells propagated in growth medium alone and is indicated by an *.

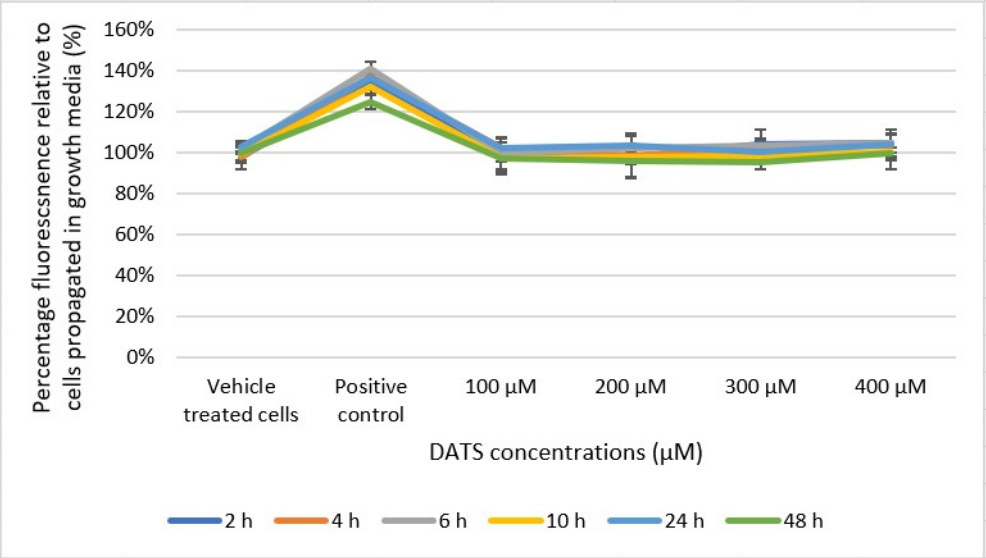

Figure 28: Fluorescent microscopy showing the dihydroethidium (DHE) staining results after the exposure of A549 cells to diallyl trisulfide (DATS) concentrations (100 µM, 200 µM, 300 µM and 400 µM) at various time intervals (2 h, 4 h, 6 h, 10 h, 24 h and 48 h). Statistical significance was calculated using an ANOVA test with a *p*-value < 0.05 indicating statistical significance of data compared to cells propagated in growth medium alone and is indicated by an *.

6.4 Cell Morphology (light Microscopy)

The effect of DATS on cell morphology was assessed using light microscopy in the presence and absence of 2 mM NAC after 24 h- and 48 h exposure to 10 µM, 50 µM, 100 µM and 150 µM DATS in the MDA-MB-231 cells and at 100 µM, 200 µM, 300 µM and 400 µM DATS in the A549 cells. The scavengers Carboxy-PTIO, DMTU, SA, Tiron, Mannitol and Trolox were chosen based on their effectiveness, as shown in the data of the cell proliferation assay, for 24 h- and 48 h exposure times.

Cell rounding increased significantly (*p*-value < 0.05) to 16, 46 and 55 after exposure to 50 µM-, 100 µM- and 150 µM DATS for 24 h in the MDA-MB-231 cell line when compared to 5 rounded cells in the negative control where cells were propagated in growth medium. Thus, an increase in cell rounding correlated to an increase in concentration after 24 h exposure to DATS, illustrated in figure 29 and table 4. However, cell rounding induced by DATS was significantly (*p*-value < 0.05) inhibited by co-exposure with 2 mM NAC where cell rounding was reduced to 6, 9 and 6 rounded cells after 24 h exposure to 50 µM-, 100 µM- and 150 µM DATS. After 48 h of exposure to DATS at 50 µM-, 100 µM- and 150 µM a significant increase in cell rounding was observed to 15, 20 and 29 rounded cells when compared to 3 rounded cells in the negative control where MDA-MB-231 cells were propagated in growth medium, this is observable in figure 30 and table 5. In addition, co-exposure

with 2 mM NAC greatly diminished the cell rounding induced by DATS to 4, 7 and 7 after exposure to DATS at 50 µM-, 100 µM- and 150 µM for 48 h indicating that the NAC was effective at reducing the effect of DATS exerts on the morphology of the cells after both 24 h- and 48 h of exposure.

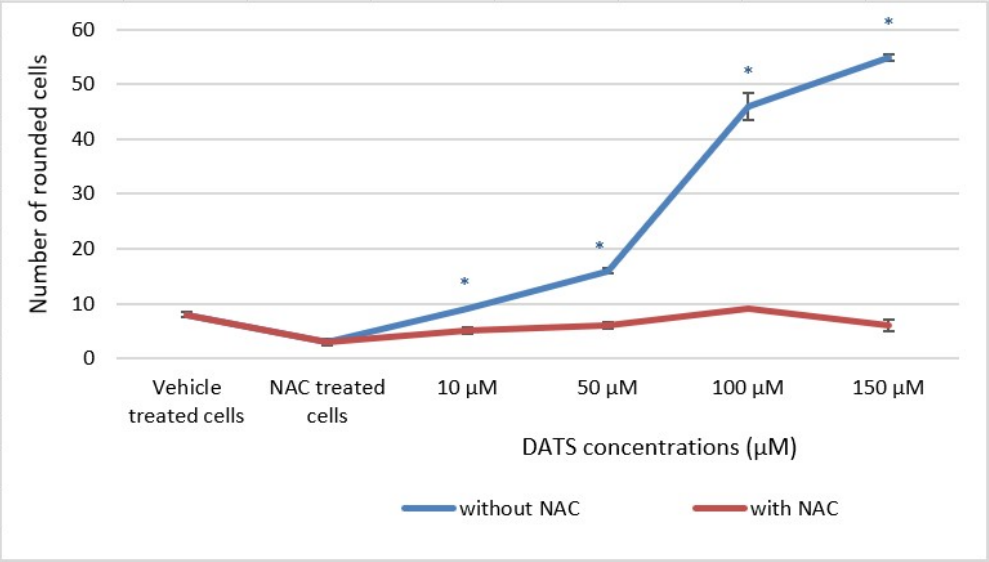

Figure 29: The number of rounded MDA-MB-231 cells after exposure for 24 h to diallyl trisulfide (DATS) (10 µM, 50 µM, 100 µM and 150 µM) in the presence and absence of N-acetyl cysteine (NAC) (2 mM). Statistical significance was calculated using an ANOVA test with a *p*-value < 0.05 indicating statistical significance of data compared to cells treated with DATS alone at 10 µM, 50 µM, 100 µM and 150 µM and is indicated by an *.

Table 4: Light microscopy representative images taken at **20X** magnification comparing the amount of cell rounding induced in MDA-MB-231 cells by diallyl trisulfide (DATS) (10 µM, 50 µM, 100 µM and 150 µM) in the presence and absence of N-acetyl cysteine (NAC) after 24 h of exposure. ↘ Indicates rounded cells.

	Cells propagated in growth medium	2 mM NAC-treated cells
Media only treated cells	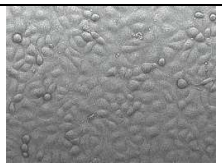	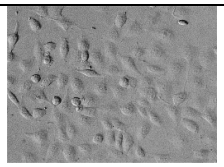
Vehicle-treated cells	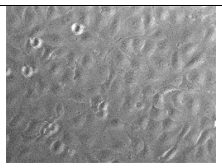	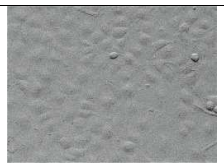
10 µM DATS-treated cells	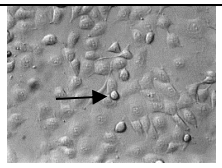	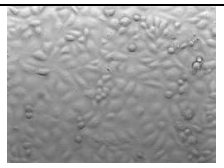
50 µM DATS-treated cells	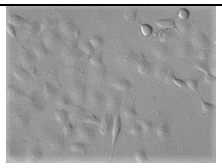	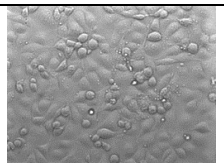
100 µM DATS-treated cells	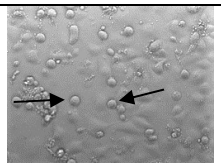	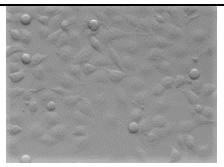
150 µM DATS-treated cells	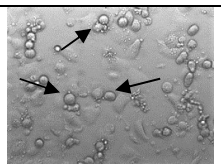	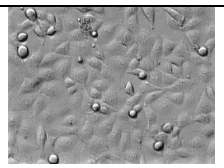

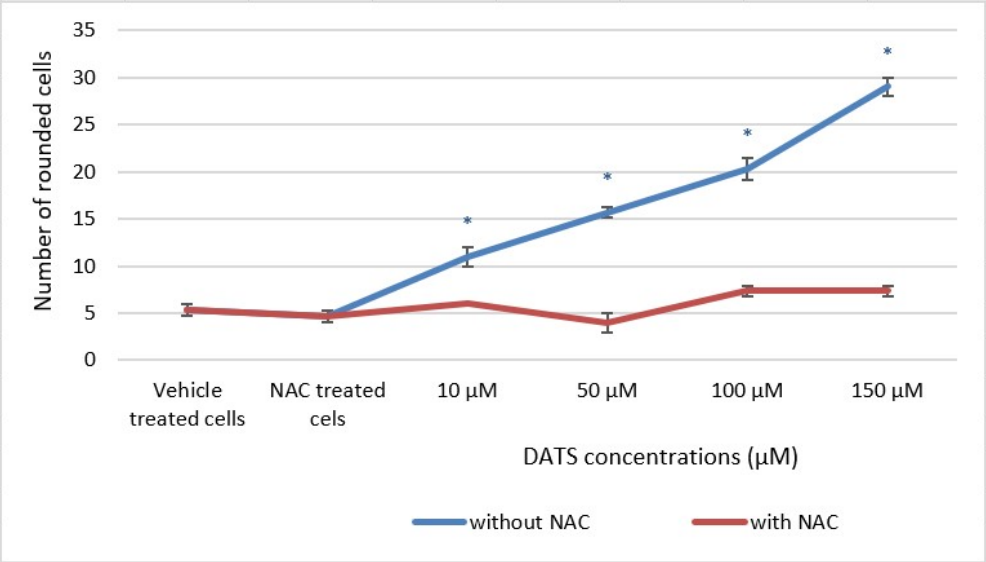

Figure 30: The number of rounded MDA-MB-231 cells after exposure for 48 h to diallyl trisulfide (DATS) (10 µM, 50 µM, 100 µM and 150 µM) in the presence and absence of N-acetyl cysteine (NAC) (2 mM). Statistical significance was calculated using an ANOVA test with a *p*-value < 0.05 indicating statistical significance of data compared to cells treated with DATS alone at 10 µM, 50 µM, 100 µM and 150 µM and is indicated by an *.

Table 5: Light microscopy representative images taken at **20X** magnification comparing the amount of cell rounding induced in MDA-MB-231 cells by diallyl trisulfide (DATS) (10 µM, 50 µM, 100 µM and 150 µM) in the presence and absence of N-acetyl cysteine (NAC) after 48 h of exposure. ↘ Indicates rounded cells

	Cells propagated in growth medium	2 mM NAC-treated cells
Media only treated cells	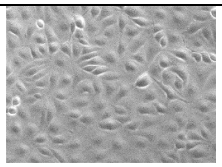	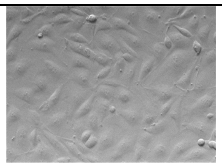
Vehicle-treated cells	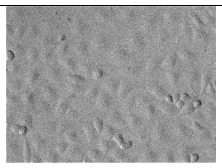	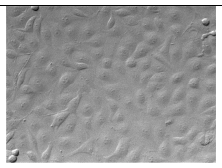
10 µM DATS-treated cells	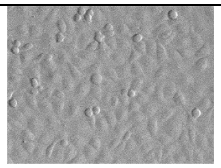	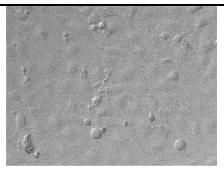
50 µM DATS-treated cells	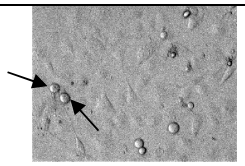	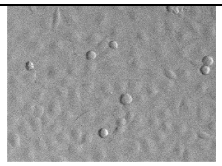
100 µM DATS-treated cells	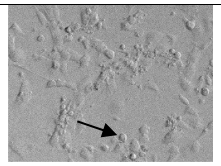	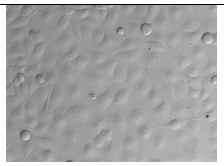
150 µM DATS-treated cells	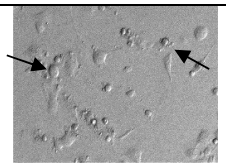	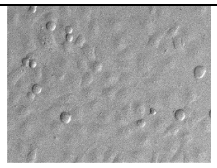

In order to evaluate the role of specific ROS on the cell rounding effects exerted by DATS, cells were exposed to DATS (10 µM, 50 µM, 100 µM and 150 µM) in the presence and absence of the ROS scavengers including SA (6mM), DMTU (8 mM), Carboxy-PTIO (8 µM), Mannitol (80 mM), Tiron (6 mM), and Trolox (40 µM) which scavenge the $O_2^{\bullet}$, H_2O_2, •NO, •OH, O_2^{-} and $HO_2^{\bullet}$, respectively for 24 h. Exposure to 50 µM-, 100 µM- and 150 µM DATS alone significantly (p-value < 0.05) increased cell rounding to 16, 46 and 55 compared to 5 cells when propagated in growth medium only. After co-

exposure to SA, cell rounding was significantly (*p*-value < 0.05) reduced at 50 µM, 100 µM and 150 µM DATS to only 6, 8- and 9 cells. After exposure to DATS in the presence of DMTU (8 mM), cell rounding was significantly reduced to 3, 5 and 28 rounded cells at 50 µM, 100 µM and 150 µM DATS. In addition, exposure to Mannitol (80 mM) partially but significantly reduced the cell rounding effects exerted by DATS with co-exposure to DATS 50 µM-, 100 µM- and 150 µM and Mannitol resulting in 7, 12 and 37 rounded cells, respectively. Exposure to Carboxy-PTIO (8 µM) also only partially but significantly reduced the cell rounding effects exerted by DATS with co-exposure to DATS 50 µM-, 100 µM- and 150 µM and Carboxy-PTIO resulting in 13, 16 and 20 rounded cells, respectively. Tiron displayed significant inhibition of the DATS effects on cell rounding at 50 µM, 100 µM, and 150 µM as well with 9, 10 and 14 rounded cells respectively as did Trolox to a lesser extent though with 24, and 43 cells rounded at 50 µM and 150 µM DATS. Data indicates that the scavengers partially inhibited the cell rounding effects induced by DATS with SA exhibiting the most prominent ability to reduce the amount of cell rounding induced by DATS and Trolox being the least effective at reducing the effect of DATS on cell rounding, this is illustrated in figure 31 and table 6.

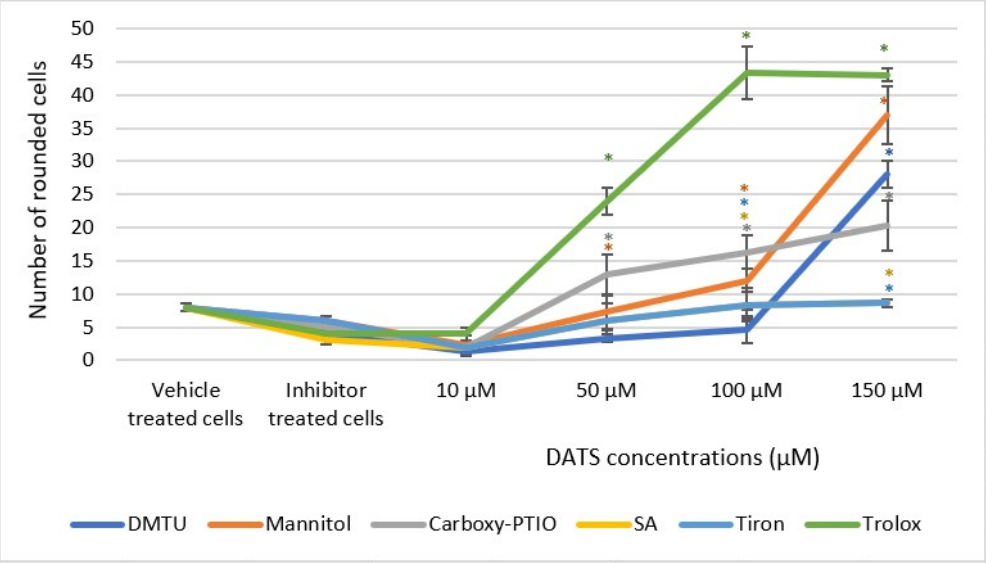

Figure 31: Figure illustrating the quantity of rounded MDA-MB-231 cells after exposure to diallyl trisulfide (DATS) (10 µM, 50 µM, 100 µM and 150 µM) in the presence and absence of the scavengers sodium azide (SA) (6mM), N, N-dimethyl thiourea (DMTU) (8 mM), 2-(4-Carboxyphenyl)-4,4,5,5-tetramethylimidazoline-1-oxyl-3-oxide (Carboxy-PTIO) (8 µM), D-Mannitol (Mannitol) (80 mM), Tiron (6 mM) and Trolox (40 µM) for 24 h. Statistical significance was calculated using an ANOVA test with a *p*-value < 0.05 indicating statistical significance of data compared to cells treated with DATS alone at and is indicated by an *.

Table 6: Light microscopy representative images taken at **20X** magnification comparing the amount of cell rounding induced in MDA-MB-231 cells by DATS (10 µM, 50 µM, 100 µM and 150 µM) in the presence of the scavengers sodium azide (SA), N, N-dimethyl thiourea (DMTU), D-Mannitol (Mannitol), 2-(4-Carboxyphenyl)-4,4,5,5-tetramethylimidazoline-1-oxyl-3-oxide (Carboxy-PTIO), Tiron and Trolox after 24 h of exposure. ↘ Indicates a rounded cell.

	Inhibitor-treated cells	**10 µM DATS-treated cells**	**50 µM DATS-treated cells**	**100 µM DATS-treated cells**	**150 µM DATS-treated cells**
6 mM SA-treated cells	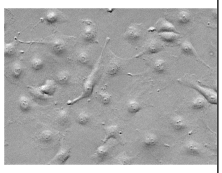	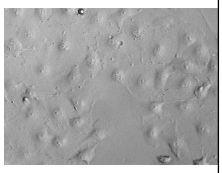	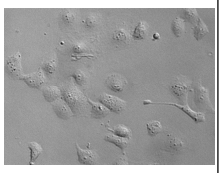	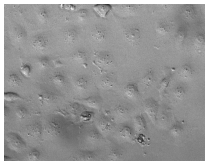	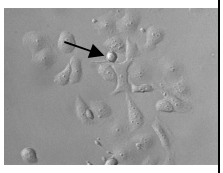
8 mM DMTU-treated cells	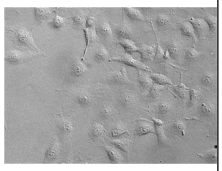	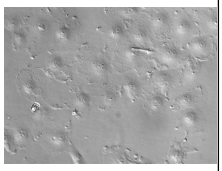	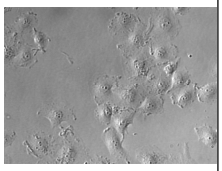	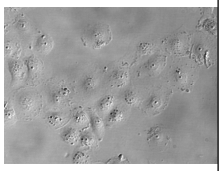	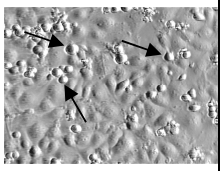
80 mM Mannitol-treated cells	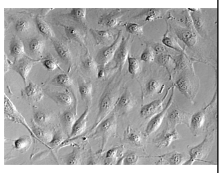	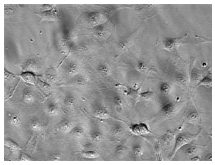	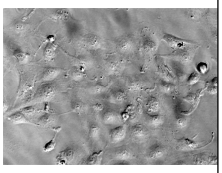	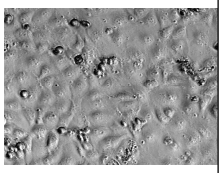	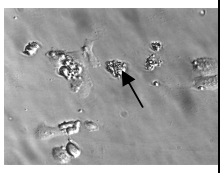
8 µM Carboxy-PTIO-treated cells	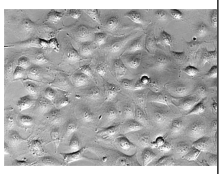	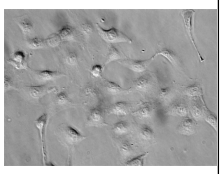	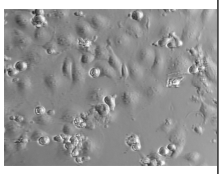	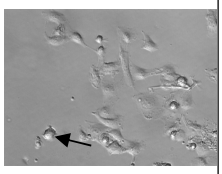	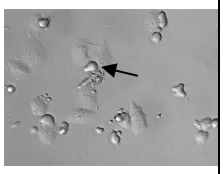
6 mM Tiron-treated cells	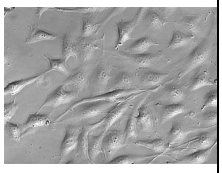	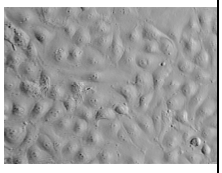	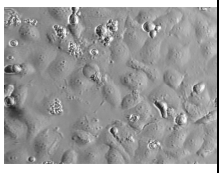	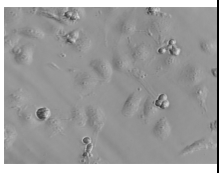	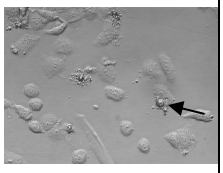

40 µM Trolox-treated cells	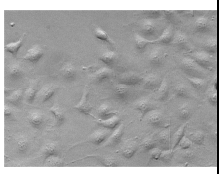	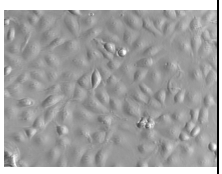	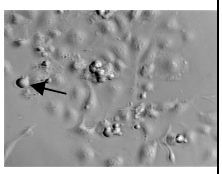	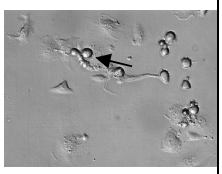	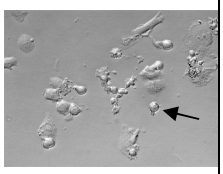

Light microscopy was also utilised to demonstrate the effect of DATS (10 µM, 50 µM, 100 µM and 150 µM) after exposure for 48 h in the MDA-MB-231 cell line in the presence and absence of Carboxy-PTIO (8 µM), Mannitol (100 mM) and Trolox (80 µM) to observe if the effects induced by DATS on morphology was dependent on oxidative stress. Data indicated that exposure to DATS (50 µM, 100 µM and 150 µM) resulted in a significant (p-value < 0.05) increase in cell rounding to 15, 20 and 29 rounded cells when compared to cells propagated in growth medium (2 rounded cells). The number of rounded cells after exposure to DATS (50 µM, 100 µM and 150 µM) in the presence of Carboxy-PTIO (8 µM) were 7, 11 and 12, and in the presence of Mannitol (100 mM) the number of rounded cells was significantly decreased only after exposure to 50 µM and 100 µM DATS to 6 and 12. Co-exposure to DATS and Trolox (80 µM) resulted in 8, 11 and 15 rounded cells at 50 µM, 100 µM- and 150 µM DATS respectively which was a significant decrease when compared to cells exposed to DATS alone. The amount of cell rounding caused by DATS alone at 10 µM and in the presence of the inhibitors at 10 µM DATS was not significantly different, this is shown in figure 32 and table 7.

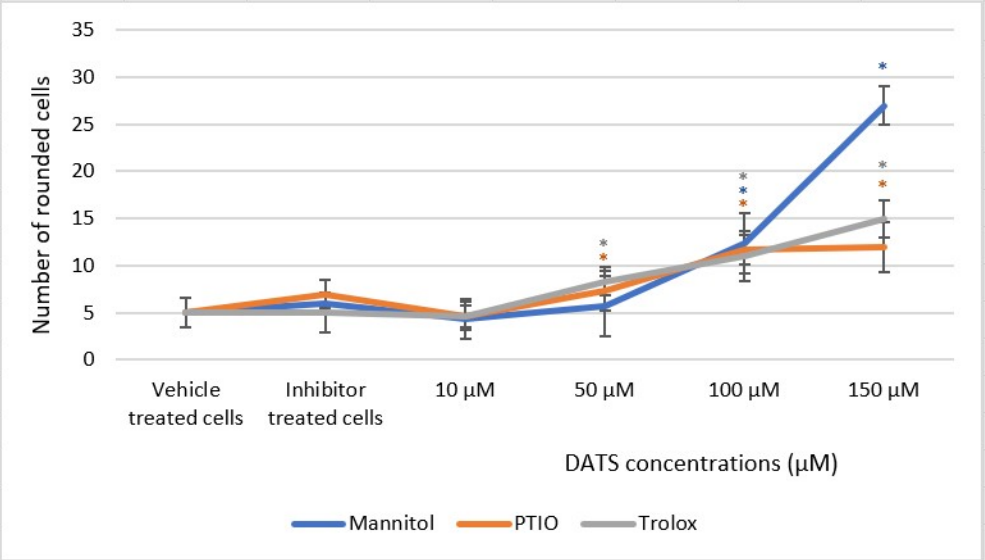

Figure 32: Figure illustrating the quantity of rounded MDA-MB-231 cells after exposure to DATS (10 µM, 50 µM, 100 µM, and 150 µM) in the presence of 2-(4-Carboxyphenyl)-4,4,5,5-tetramethylimidazoline-1-oxyl-3-oxide (Carboxy-PTIO) (8 µM), D-Mannitol (Mannitol) (100 mM), and Trolox (80 µM) for 48 h. Statistical significance was calculated using an ANOVA test with a *p*-value < 0.05 indicating statistical significance of data compared to cells treated with DATS alone at and is indicated by an *.

Table 7: Light microscopy representative images taken at **20X** magnification comparing the amount of cell rounding induced in MDA-MB-231 cells by DATS (10 µM, 50 µM, 100 µM and 150 µM) in the presence of the scavengers D-Mannitol (Mannitol) (100 mM), 2-(4-Carboxyphenyl)-4,4,5,5-tetramethylimidazoline-1-oxyl-3-oxide (Carboxy-PTIO) (8 µM), and Trolox after 48 h of exposure. ↘ Indicates rounded cells.

	Inhibitor-treated cells	**10 µM DATS-treated cells**	**50 µM DATS-treated cells**	**100 µM DATS-treated cells**	**150 µM DATS-treated cells**
100 mM Mannitol-treated cells	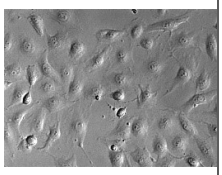	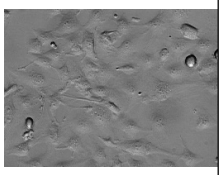	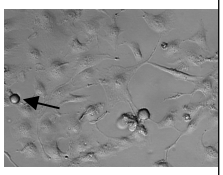	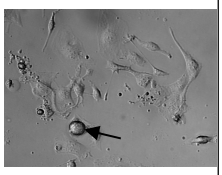	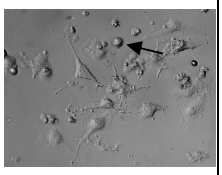
8 µM Carboxy-PTIO-treated cells	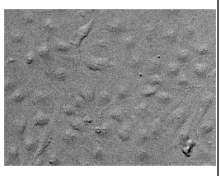	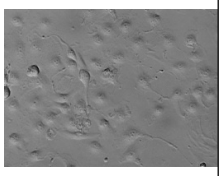	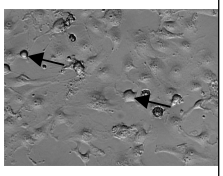	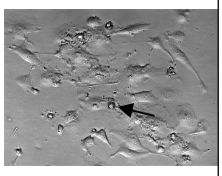	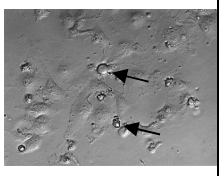
80 µM Trolox-treated cells	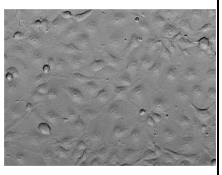	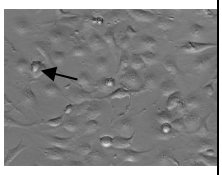	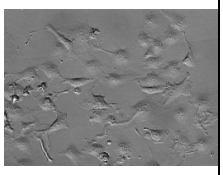	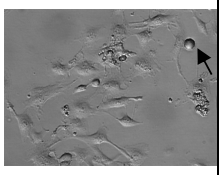	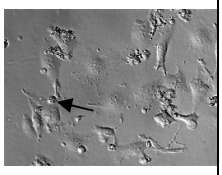

The A549 cells were also exposed to DATS (100 µM, 200 µM, 300 µM and 400 µM) in the presence and absence of NAC (2 mM) for 24- and 48 h in order to determine if the effect of DATS on cell morphology was dependent on an increase in ROS production. Cells treated with 100 µM, 200 µM, 300 µM and 400 µM DATS alone for 24 h demonstrated a significant (p-value < 0.05) increase in cell rounding to 15, 32, 45 and 54 rounded cells when compared to cells propagated in growth medium alone (4 rounded cells). However, co-exposure to 100 µM, 200 µM, 300 µM and 400 µM DATS in the presence of NAC (2 mM) demonstrated 3, 3, 3 and 6 rounded cells respectively, suggesting that NAC

effectively inhibited the effect DATS exerts on cell rounding, as illustrated in figure 33 and table 8. Exposure for 48 h to 200 µM, 300 µM and 400 µM DATS alone increased cell rounding significantly (*p*-value < 0.05) to 10, 17 and 32 cells compared to cells propagated in growth medium (3 rounded cells). DATS-treated cells (100 µM, 200 µM, 300 µM and 400 µM) in the presence of NAC (2 mM) demonstrated 4, 3, 3 and 5 rounded cells indicating that NAC successfully inhibited the effects of DATS after 48 h of exposure, depicted in figure 34 and table 9.

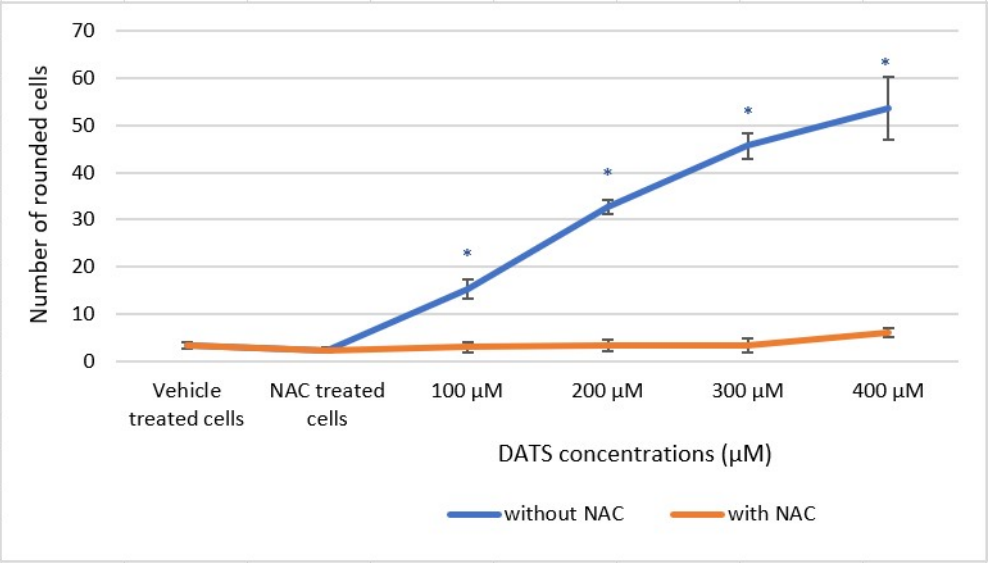

Figure 33: Figure illustrating the quantity of rounded A549 cells after exposure for 24 h to diallyl trisulfide (DATS) (100 µM, 200 µM, 300 µM and 400 µM) in the presence and absence of N-acetyl cysteine (NAC) (2 mM). Statistical significance was calculated using an ANOVA test with a *p*-value < 0.05 indicating statistical significance of data compared to cells propagated in growth medium and is indicated by an *.

Table 8: Light microscopy representative images taken at **20X** magnification comparing the amount of cell rounding induced in A549 cells by diallyl trisulfide (DATS) (100 µM, 200 µM, 300 µM and 400 µM) in the presence and absence of N-acetyl cysteine (NAC) after 24 h of exposure. ↘ Indicates rounded cells.

	Cells propagated in growth medium	2 mM NAC-treated cells
Media only treated cells	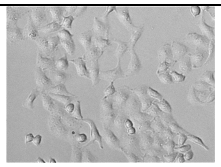	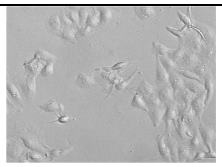
Vehicle-treated cells	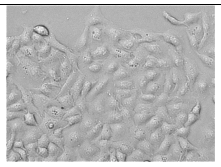	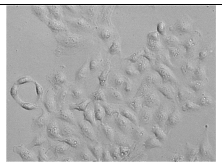
100 µM DATS-treated cells	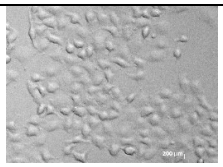	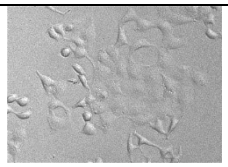
200 µM DATS-treated cells	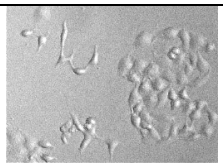	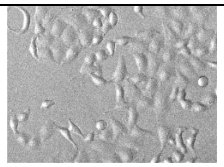
300 µM DATS-treated cells	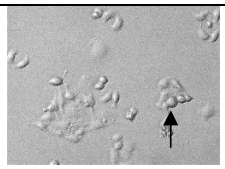	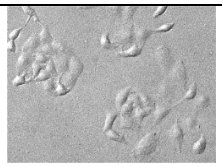
400 µM DATS-treated cells	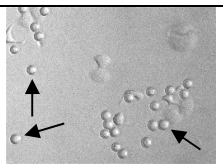	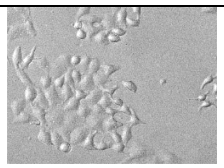

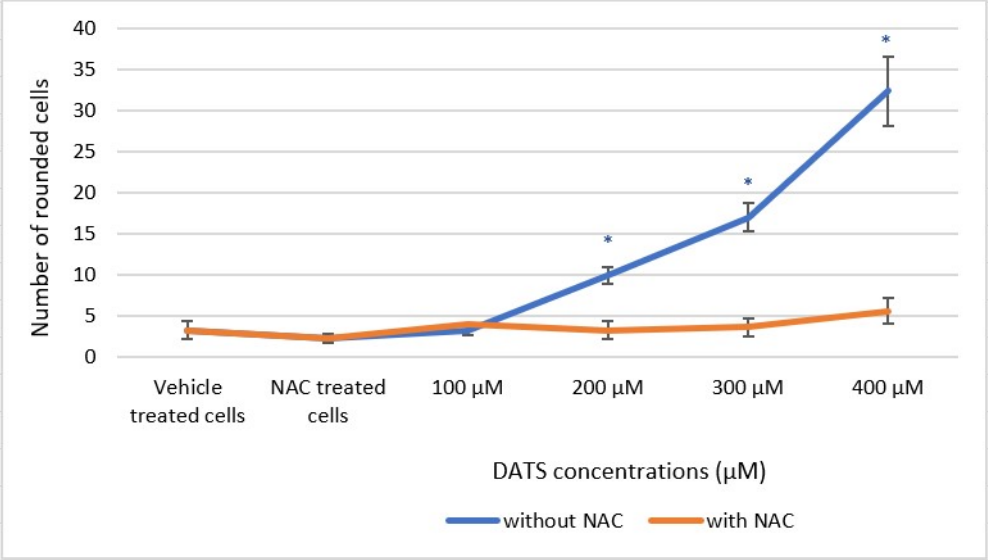

Figure 34: Figure illustrating the quantity of rounded A549 cells after exposure for 48 h to diallyl trisulfide (DATS) (100 µM, 200 µM, 300 µM and 400 µM) in the presence and absence of N-acetyl cysteine (NAC) (2 mM). Statistical significance was calculated using an ANOVA test with a *p*-value < 0.05 indicating statistical significance of data compared to cells propagated in growth medium alone at and is indicated by an *.

Table 9: Light microscopy representative images taken at **20X** magnification comparing the amount of cell rounding induced in A549 cells by DATS (100 µM, 200 µM, 300 µM and 400 µM) in the presence and absence of NAC after 48 h of exposure. ↘ Indicates rounded cells.

	Cells propagated in growth medium	2 mM NAC-treated cells
Media only treated cells	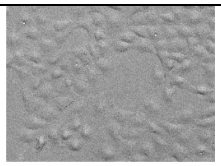	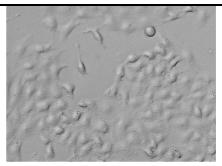
Vehicle-treated cells	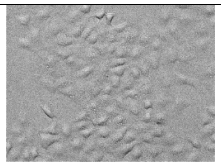	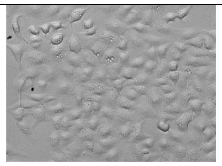
100 µM DATS-treated cells	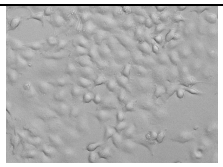	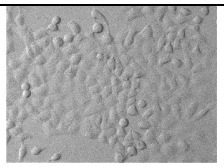
200 µM DATS-treated cells	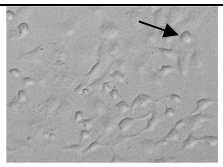	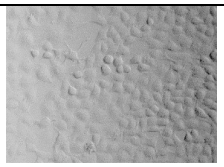
300 µM DATS-treated cells	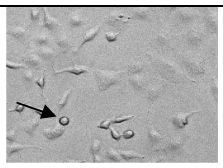	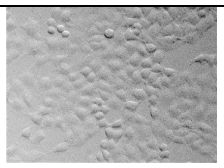
400 µM DATS-treated cells	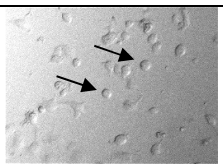	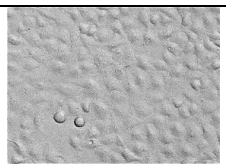

Furthermore, the crystal violet data indicated that the scavengers were sufficient at inhibiting the cell rounding effect exerted by DATS in the A549 cell line only after 24 h of exposure and from this, concentrations of the scavengers were selected including SA (10 mM), DMTU (8 mM), Carboxy-PTIO (6 µM), Mannitol (20mM), Tiron (2 mM) and Trolox (20 µM). To assess the effect of the scavengers in reducing the morphological effect of DATS the cells were exposed to the scavengers in the presence of DATS (100 µM, 200 µM, 300 µM and 400 µM). After exposure for 24 h cell rounding increased to 15, 32, 45 and 54 rounded cells after exposure to 100 µM-, 200 µM-, 300 µM- and 400 µM DATS,

respectively when compared to cells propagated in growth medium alone (4 rounded cells). After co-treatment of cells to DATS in the presence of SA the amount of cell rounding was significantly (*p*-value < 0.05) reduced at DATS concentrations of 200 µM, 300 µM and 400 µM (8, 9 and 11 rounded cells). Exposure to DATS (100 µM, 200 µM, 300 µM and 400 µM) in the presence of DMTU demonstrated a significant reduction in the number of cells rounded to 8, 18, 27 and 28 rounded cells respectively. Exposure to DATS (100 µM, 200 µM, 300 µM and 400 µM) in the presence of Mannitol displayed 6, 17, 38 and 39 rounded cells which was also significant. Exposure to DATS (100 µM, 200 µM, 300 µM and 400 µM) in the presence of Carboxy-PTIO showed a significant reduction in cell rounding to 6, 20, 33 and 38 rounded cells. Furthermore, exposure to DATS (100 µM, 200 µM, 300 µM and 400 µM) in the presence of Tiron also demonstrated a significant reduction in cell rounding to 8, 24, 23 and 26 rounded cells and treatment with DATS in the presence of Trolox resulted in 15, 24, 23 and 27 rounded cells, respectively which was also significant; this is depicted in figure 35 table 10. When compared to cells exposed to DATS alone with 15, 32, 45 and 54 cells rounded after exposure to 100 µM, 200 µM, 300 µM and 400 µM, respectively, the inhibitors were significantly effective at partially reducing the cell rounding effects induced by DATS, indicating that $O_2^{\bullet}$, H_2O_2, •NO, •OH, O_2^- and $HO_2^{\bullet}$ are involved in the mechanism by which DATS exerts its effect on cell rounding.

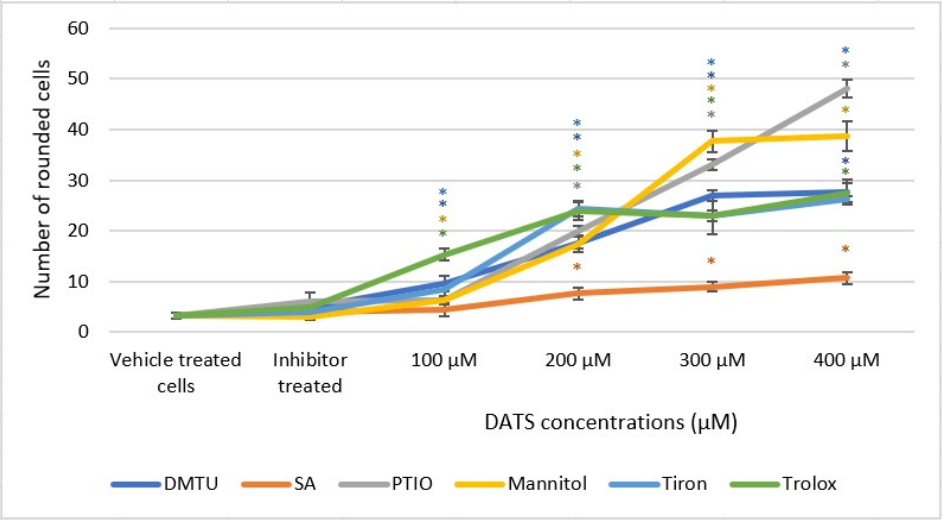

Figure 35: Figure illustrating quantity of rounded A549 cells after exposure to the scavengers sodium azide (SA), N, N-dimethyl thiourea (DMTU), D-Mannitol (Mannitol), 2-(4-Carboxyphenyl)-4,4,5,5-tetramethylimidazoline-1-oxyl-3-oxide (Carboxy-PTIO), Tiron and Trolox with diallyl trisulfide (DATS) (100 µM, 200 µM, 300 µM and 400 µM) for 24 h. Statistical significance was calculated using an ANOVA test with a *p*-value < 0.05 indicating statistical significance of data compared to cells treated with DATS alone and is indicated by an *.

Table 10: Light microscopy representative images taken at **20X** magnification demonstrating cell rounding and morphology in A549 cells after exposure to DATS (100 µM, 200 µM, 300 µM and 400 µM) in the presence of the scavengers sodium azide (SA) (10 mM), N, N-dimethyl thiourea (DMTU) (8 mM), 2-(4-Carboxyphenyl)-4,4,5,5-tetramethylimidazoline-1-oxyl-3-oxide (Carboxy-PTIO) (6 µM), D-Mannitol (Mannitol) (20mM), Tiron (2 mM) and Trolox (20 µM) after 24 h of exposure. ↘ Indicates rounded cells.

	Inhibitor-treated cells	100 µM DATS-treated cells	200 µM DATS-treated cells	300 µM DATS-treated cells	400 µM DATS-treated cells
10 mM SA-treated cells	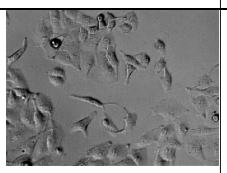	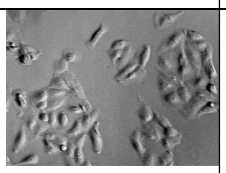	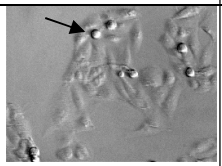	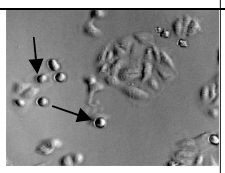	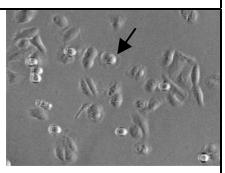
8 mM DMTU-treated cells		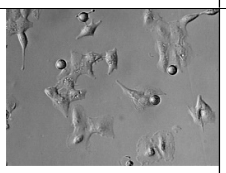	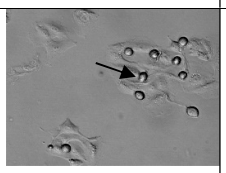	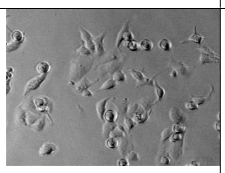	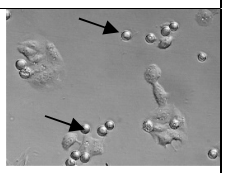
20 mM Mannitol-treated cells	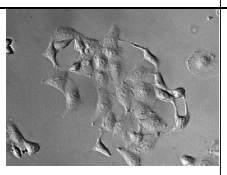	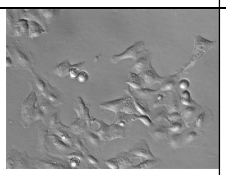	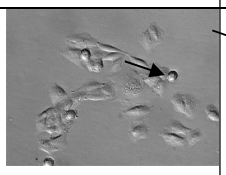	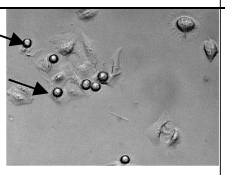	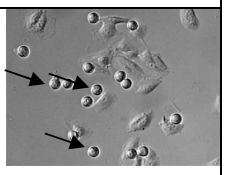
6 µM Carboxy-PTIO-treated cells		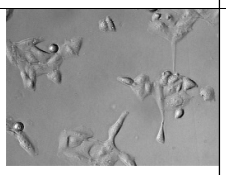	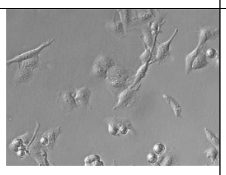	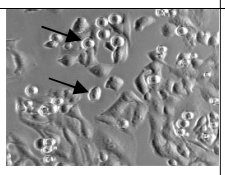	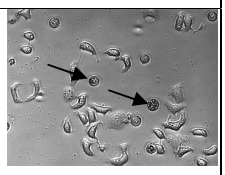
2 mM Tiron-treated cells	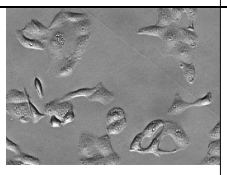	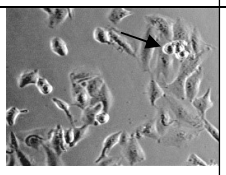	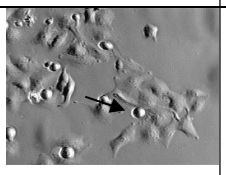	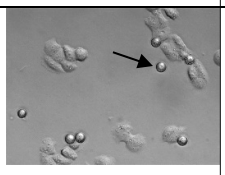	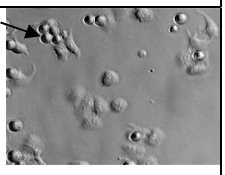
20 µM Trolox-treated cells	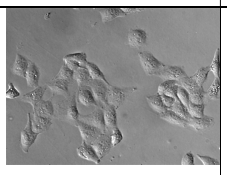	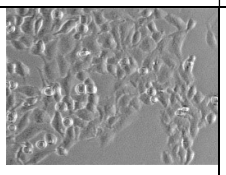	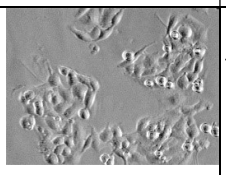	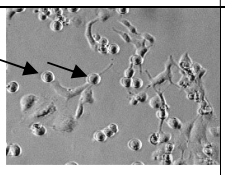	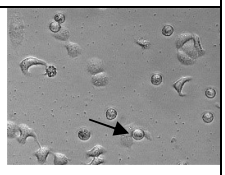

6.5 Cell cycle progression (ethanol fixation and PI): Flow cytometry

The effect of DATS on cell cycle progression and the induction of cell death was investigated using flow cytometry and PI staining in the presence and absence of NAC and the 6 scavengers of specific ROS. PI is a DNA intercalating agent, therefore the amount of PI within each cell can be quantified and correlates with the phase of the cell cycle phase the cell is occupying including G_1, S, G_2 and M which can be used to analyse cell cycle progression (76).

The MDA-MB-231 cells were exposed to DATS (10 µM, 50 µM, 100 µM and 150 µM) in the presence and absence of NAC for 24 h and 48 h to examine if the effect of DATS on cell cycle progression is dependent on ROS, the results of this are depicted in figure 36, figure 37, table 11 and table 12. After 24 h exposure to 100 µM- and 150 µM DATS in the presence of NAC (2 mM), cells presenting in the sub-G_1 phase significantly decreased to 9% and 7% compared to 25% and 26% after exposure to only DATS at 100 µM and 150 µM demonstrating that NAC inhibits the effect of DATS on the sub-G_1 phase. After 48 h of exposure to DATS 10 µM, 50 µM, 100 µM and 150 µM in the presence of NAC (2 mM) a significant decrease in the percentage of cells in the sub-G_1 phase was observed to be 9%, 8%, 8% and 8% from 11%, 18%, 30% and 29%, respectively that was observed in the cells treated with DATS alone. Cells occupying the sub-G_1 phase of the cell cycle is suggestive of cells that have undergone cell death. It was apparent however that NAC (2 mM) did inhibit the effect of DATS on the induction of an increase of cells occurring in the sub-G_1 phase therefore further studies were conducted in the presence of the 6 inhibitors of the individual ROS species in order to determine which ROS plays a role in the effect of DATS on the cell cycle.

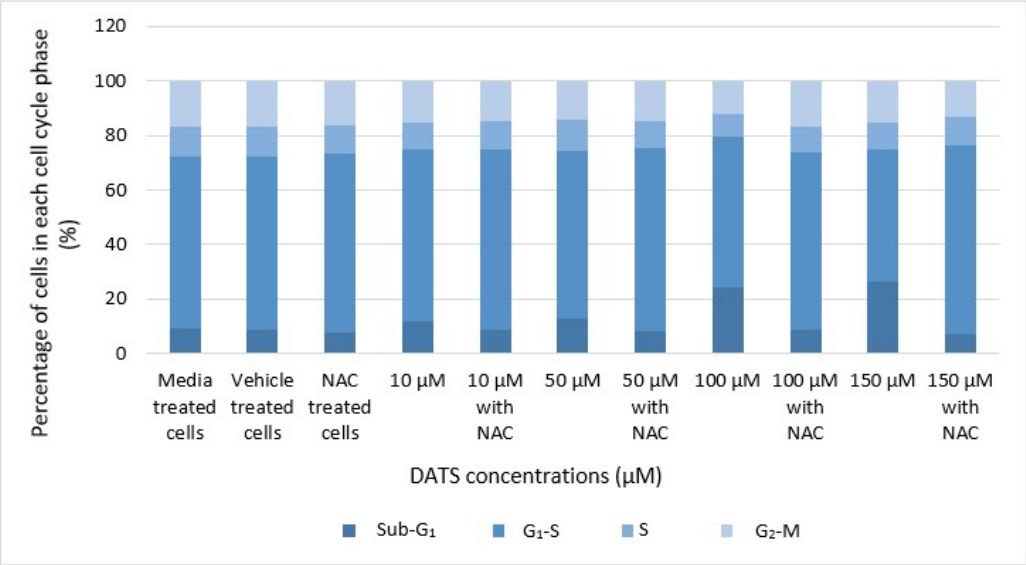

Figure 36: Figure illustrating the percentage of MDA-MB-231 cells in each phase of the cell cycle after 24 h of exposure to diallyl trisulfide (DATS) (10 µM, 50 µM, 100 µM and 150 µM) in the presence and absence of N-acetyl cysteine (NAC) (2 mM).

Table 11: The representative images of cell cycle progression in MDA-MB-231 cells after 24 h of exposure to diallyl trisulfide (DATS) (10 µM, 50 µM, 100 µM and 150 µM) in the presence and absence of N-acetyl cysteine (NAC) (2 mM).

	Cells treated with DATS alone	Cells treated in the presence of NAC (2 mM)
Cells propagated in growth medium	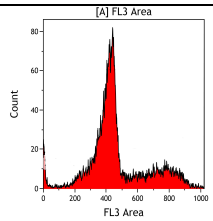	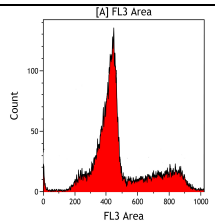
Vehicle-treated cells	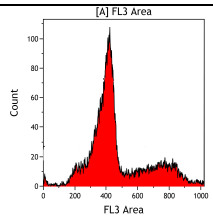	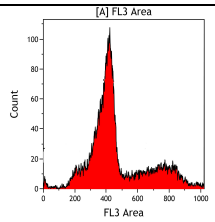
10 µM DATS-treated cells	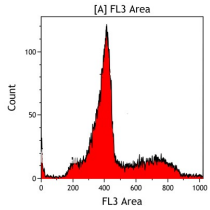	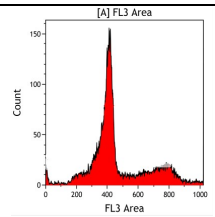
50 µM DATS-treated cells	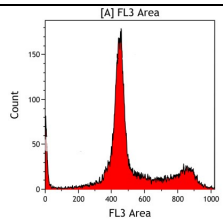	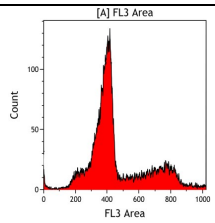
100 µM DATS-treated cells	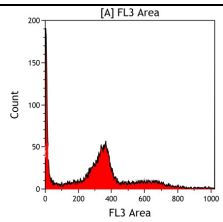	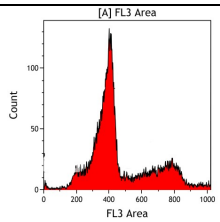
150 µM DATS-treated cells	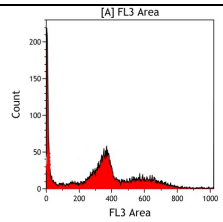	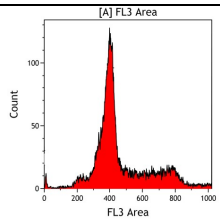

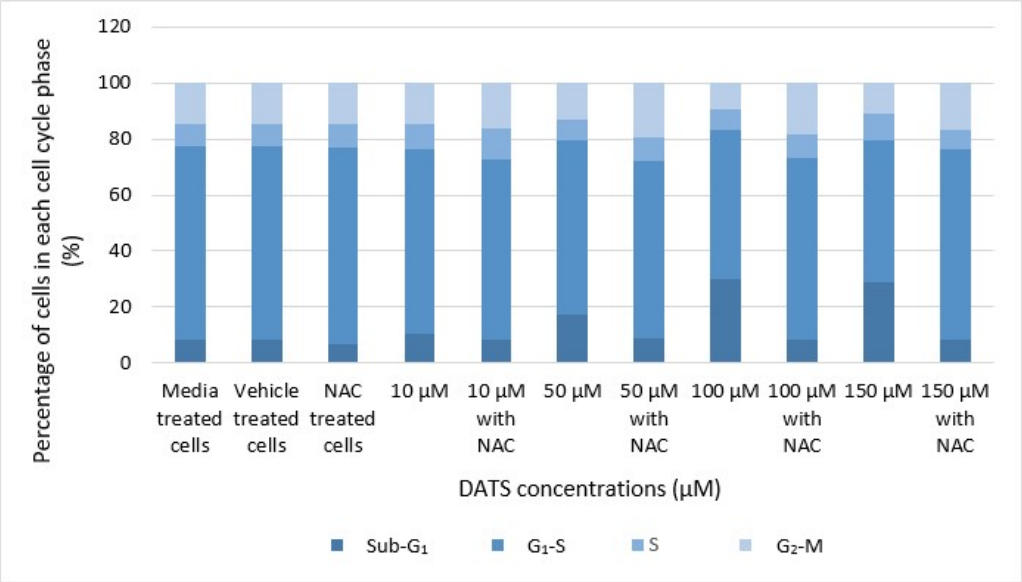

Figure 37: Figure illustrating the percentage of MDA-MB-231 cells in each phase of the cell cycle after 48 h of exposure to diallyl trisulfide (DATS) (10 µM, 50 µM, 100 µM and 150 µM) in the presence and absence of N-acetyl cysteine (NAC) (2 mM).

Table 12: The representative images of cell cycle progression in MDA-MB-231 cells after 48 h of exposure to diallyl trisulfide (DATS) (10 µM, 50 µM, 100 µM and 150 µM) in the presence and absence of N-acetyl cysteine (NAC) (2 mM).

	Cells treated with DATS alone	Cells treated in the presence of NAC (2 mM)
Cells propagated in growth medium	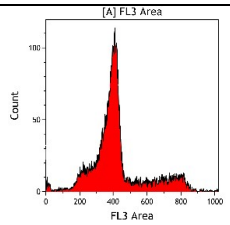	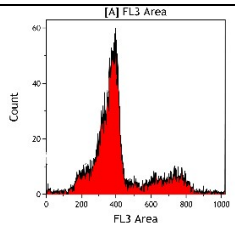
Vehicle-treated cells	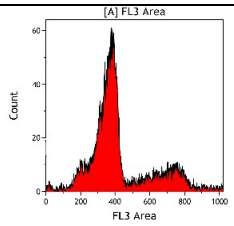	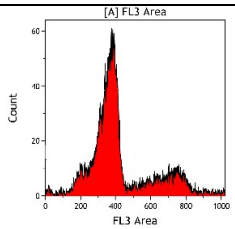
10 µM DATS-treated cells	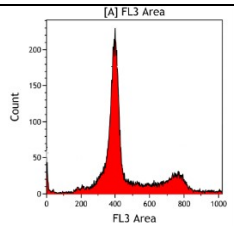	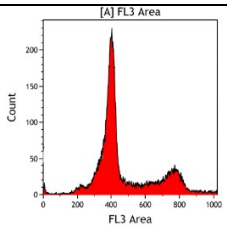
50 µM DATS-treated cells	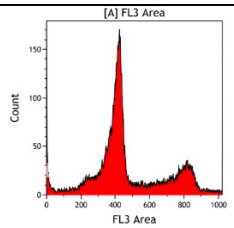	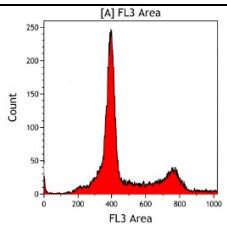
100 µM DATS-treated cells	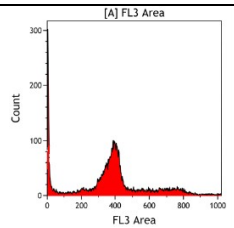	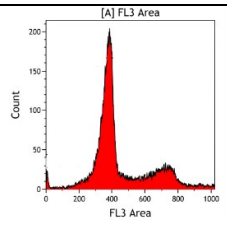
150 µM DATS-treated cells	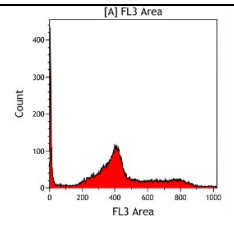	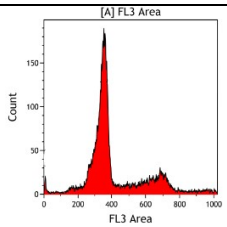

Data obtained by cell cycle studies indicated that exposure to 10 µM DATS alone resulted in insignificant aberrant cell cycle abnormalities compared to cells propagated in growth medium and the effect of DATS on cell cycle progression plateaued after 100 µM DATS treatment. Therefore, further cell cycle progression studies involving the scavengers for specific ROS was conducted only with cells exposed to 50 µM- and 100 µM DATS for the MDA-MB-231 cell line After 24 h of treatment to DATS (50 µM and 100 µM) with SA (6mM), DMTU (8 mM), Carboxy-PTIO (8 µM), Mannitol (80 mM), Tiron (6 mM) or Trolox (40 µM) which scavenge $O_2^{\bullet}$, H_2O_2, •NO, •OH, O_2^{-} and $HO_2^{\bullet}$ respectively, a significant change in the amount of cells in the G_2M phase of the cell cycle was observed when compared to the cells treated with 50 µM and 100 µM DATS alone which resulted in 14% and 12% of the cells being in the G_2M phase, this is illustrated in figures 38 and table 13. Exposure of the cells to SA (6mM) and 50 µM DATS resulted in an increase in the percentage of cells in the G_2M phase from 14% in the DATS-treated cells without SA to 18% in the cells with that were co-exposed to DATS and SA. However, exposure to SA and 100 µM DATS led to an increase in the percentage of cells in the G_2M phase of the cell cycle from 12% in the DATS-treated cells without SA to 25% in the DATS-treated cells with SA treatment. After exposure to DATS at 50 µM- and 100 µM in the presence of DMTU (8 mM) a significant increase in the percentage of cells in the G_2M phase of the cell cycle was seen from 14% and 12% in cells treated with DATS alone to 29% and 76% in cells treated with DATS in the presence of DMTU. After exposure to 50 µM- and 100 µM DATS in the presence of Mannitol (80 mM) an increase to 25% and 48% of cells in the G_2M phase of the cell cycle was observed from 14% and 12% in cells treated with 50 µM and 100 µM DATS alone, respectively. After exposure to 50 µM- and 100 µM DATS in the presence of Carboxy-PTIO (8 µM) the percentage of cells in the G_2M phase of the cell cycle increased to 20% and 70% respectively, from 14% and 12% that was observed in cells exposed to 50 µM- and 100 µM DATS alone. After treatment of cells to 50 µM- and 100 µM DATS with Tiron (6 mM), an increase in the percentage of cells in the G_2M phase of the cell cycle to 32% and 37%, respectively from 14% and 12% as was seen in the cells exposed to 50 µM- and 100 µM DATS. After exposure to 50 µM- and 100 µM DATS in combination with Trolox (40 µM) resulted in an increase in the percentage of cells in the G_2M phase of the cell cycle, from 14% and 12% in cells treated with 50 µM- and 100 µM DATS to 32% and 75%, respectively in co-treated cells. With the addition of the scavengers, DATS effected the G_2M phase of the cell cycle instead of the sub-G_1 phase suggesting that scavenging of $O_2^{\bullet}$, H_2O_2, •NO, •OH, O_2^{-}, and $HO_2^{\bullet}$ decreases the amount of time DATS takes to cause cell death and the cells remain in G_2M phase cell cycle arrest for a longer period of time.

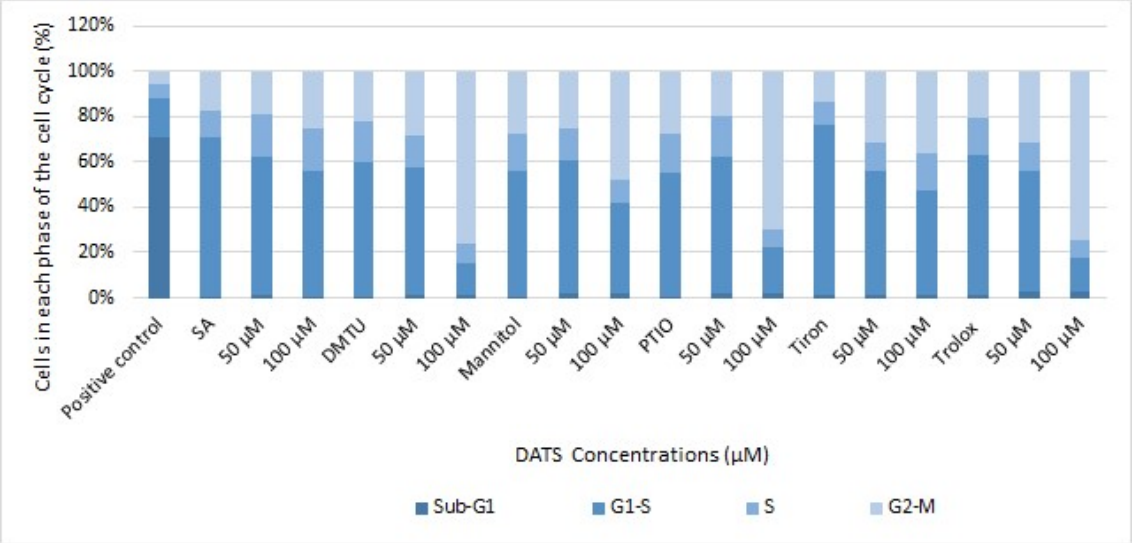

Figure 38: Figure illustrating the percentage of MDA-MB-231 cells in each phase of the cell cycle after 24 h of exposure to diallyl trisulfide (DATS) (50 µM and 100 µM) in the presence of the scavengers, including sodium azide (SA) (6mM), N, N-dimethyl thiourea (DMTU) (8 mM), 2-(4-Carboxyphenyl)-4,4,5,5-tetramethylimidazoline-1-oxyl-3-oxide (Carboxy-PTIO) (8 µM), D-Mannitol (Mannitol) (80 mM), Tiron (6 mM), and Trolox (40 µM) with data showing exposure to cells in the presence of the scavengers alone followed by co-exposure with DATS.

Table 13: The representative images of cell cycle progression in MDA-MB-231 cells after 24 h of exposure to DATS (50 µM and 100 µM) and sodium azide (SA) (6mM), N, N-dimethyl thiourea (DMTU) (8 mM), 2-(4-Carboxyphenyl)-4,4,5,5-tetramethylimidazoline-1-oxyl-3-oxide (Carboxy-PTIO) (8 µM), D-Mannitol (Mannitol) (80 mM), Tiron (6 mM) and Trolox (40 µM).

	Inhibitor-treated cells	50 µM DATS-treated cells	100 µM DATS-treated cells
6 mM SA-treated cells	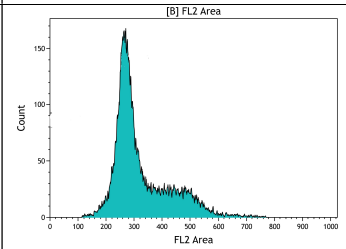	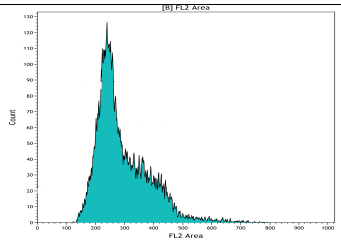	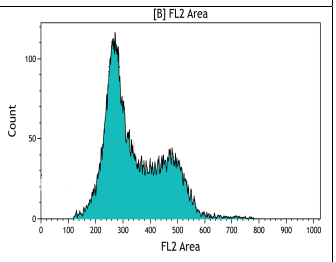
8 mM DMTU-treated cells	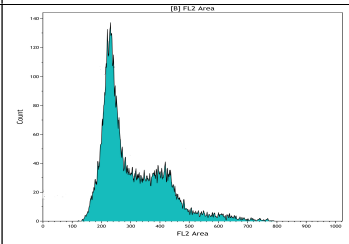	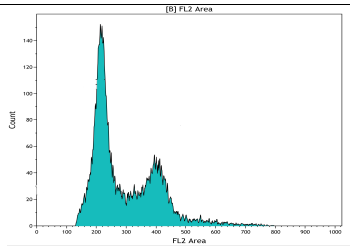	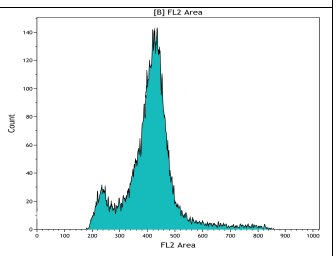
80 mM Mannitol -treated cells	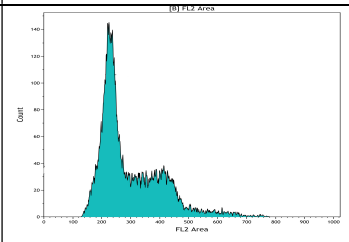	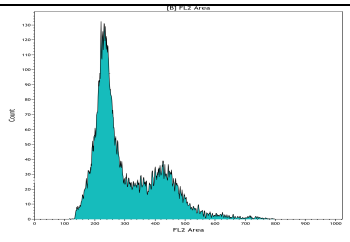	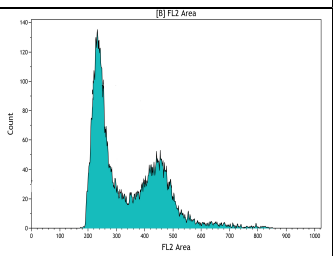
8 µM Carboxy-PTIO-treated cells	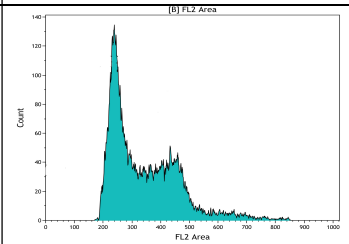	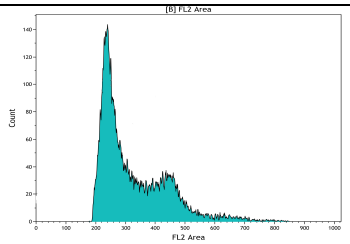	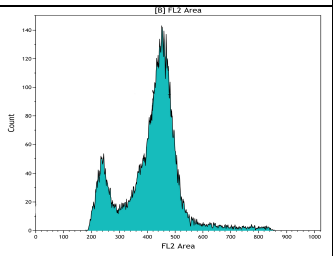
6 mM Tiron-treated cells	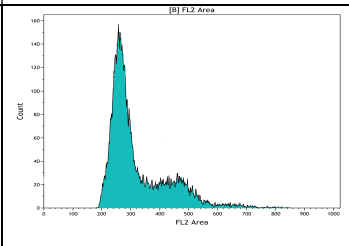	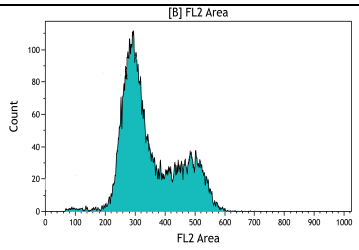	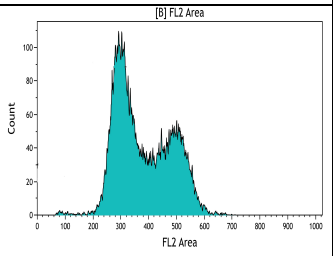

40 µM Trolox-treated cells	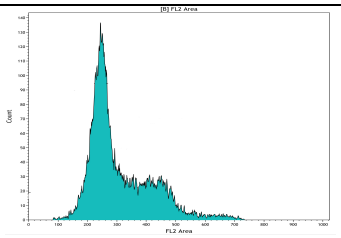	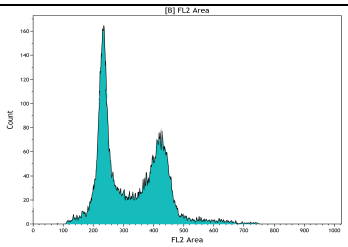	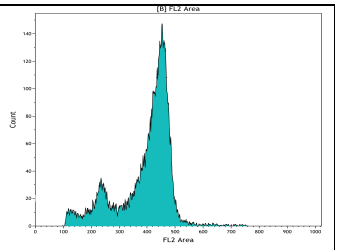

The A549 cells were exposed to DATS (100 µM, 200 µM, 300 µM and 400 µM) in the presence and absence of NAC (2 mM) for 24- and 48 h to examine if the effect exerted by DATS on cell cycle progression was dependent on ROS, these results are illustrated in figures 39 and 40 and table 14 and 15. After 24 h of exposure to DATS alone a significant increase in the number of cells in the G_2M phase of the cell cycle was observed for cells exposed to 200 µM, 300 µM and 400 µM DATS, the percentage of cells in the G_2M phase increased from 22%, as seen in cells propagated in growth medium alone, to 41%, 56% and 56% in 200 µM-, 300 µM- and 400 µM DATS-treated cells. By comparison, DATS exposure (200 µM, 300 µM and 400 µM) in the presence of NAC (2 mM) demonstrated decreased the percentage of cells present in the G_2M phase to 24%, 19% and 24% respectively, when compared to cells exposed to DATS alone (41%, 56% and 56%). Thus, NAC inhibited the effect exerted by DATS on cell cycle progression in the A549 cell line after 24 h of exposure. After 48 h of exposure to 100 µM, 200 µM, 300 µM and 400 µM DATS there was a significant increase in the percentage of cells in the sub-G_1 phase of the cell cycle from 1% in cells propagated in growth medium alone to 3%, 20%, 47% and 22%, respectively. In addition, after exposure to 400 µM DATS alone for 48 h a significant increase in the percentage of cells occupying the G_2M phase was observed to 31% compared to 15% in cells propagated in growth medium alone. Effects of exposure to DATS at 100 µM, 200 µM, 300 µM and 400 µM in the presence of NAC (2 mM) reduced the number of cells occupying the sub-G_1 phase of the cell cycle to 1%, 1%, 1% and 2% from 3%, 20%, 47% and 22% respectively. In addition the effect of 400 µM DATS on the G_2M phase in the presence of NAC was also reduced from 31% when treated with DATS alone to 18%.

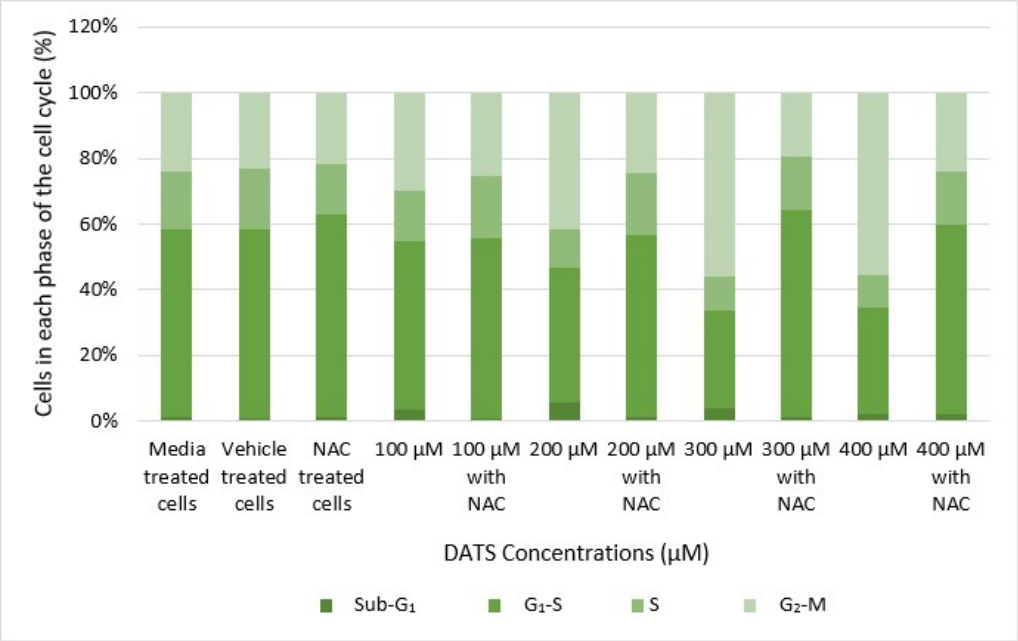

Figure 39: Figure illustrating the percentage of A549 cells in each phase of the cell cycle after 24 h of exposure to diallyl trisulfide (DATS) (100 µM, 200 µM, 300 µM and 400 µM) in the presence and absence of N-acetyl cysteine (NAC) (2 mM).

Table 14: Table displaying the representative images of cell cycle progression in A549 cells after 24 h of exposure to diallyl trisulfide (DATS) (100 µM, 200 µM, 300 µM and 400 µM) in the presence and absence of N-acetyl cysteine (NAC) (2 mM).

	Cells treated with DATS alone	Cells treated in the presence of NAC (2 mM)
Cells propagated in complete growth medium	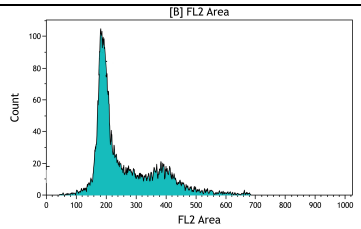	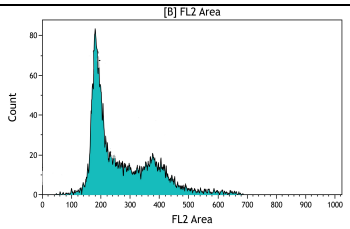
Vehicle-treated cells	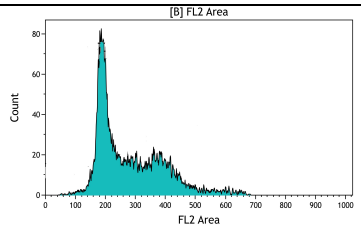	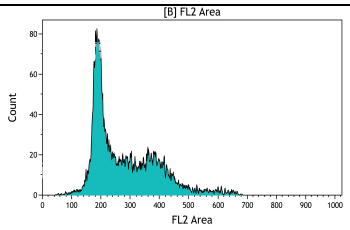
100 µM DATS-treated cells	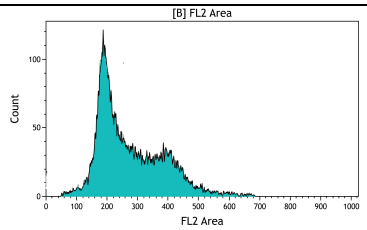	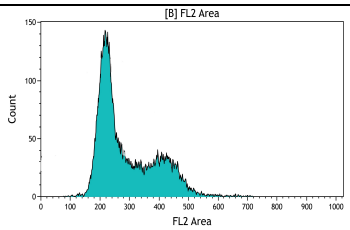
200 µM DATS-treated cells	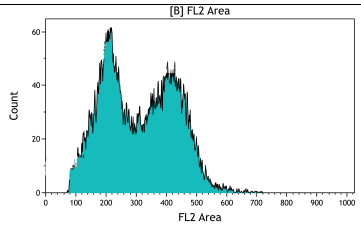	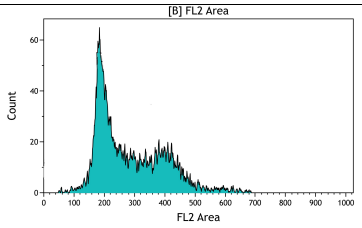
300 µM DATS-treated cells	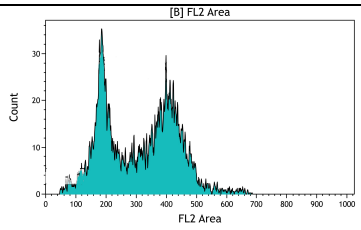	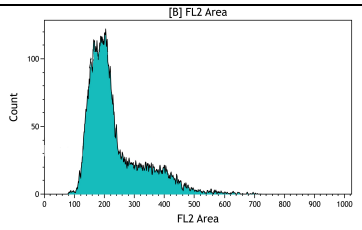
400 µM DATS-treated cells	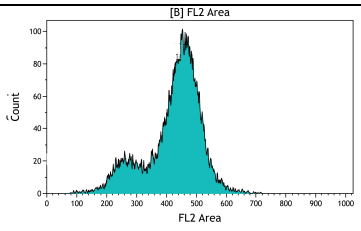	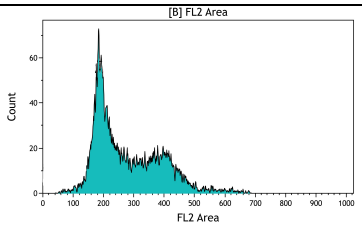

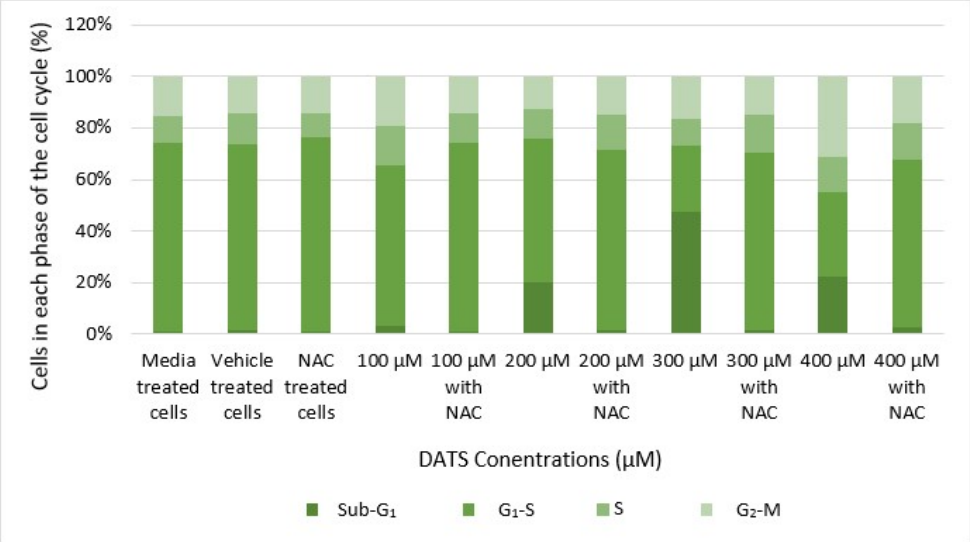

Figure 40: Figure illustrating the percentage of A549 cells in each phase of the cell cycle after 48 h of exposure to diallyl trisulfide (DATS) (100 µM, 200 µM, 300 µM and 400 µM) in the presence and absence of N-acetyl cysteine (NAC) (2 mM).

Table 15: Table displaying the representative images of cell cycle progression in A549 cells after 48 h of exposure to diallyl trisulfide (DATS) (100 µM, 200 µM, 300 µM and 400 µM) in the presence and absence of N-acetyl cysteine (NAC) (2 mM).

	Cells treated with DATS alone	Cells treated in the presence of NAC (2 mM)
Cells propagated in complete growth medium	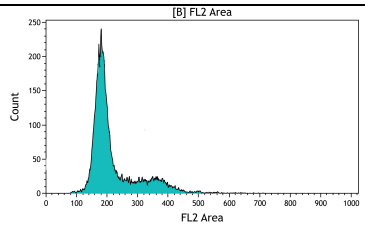	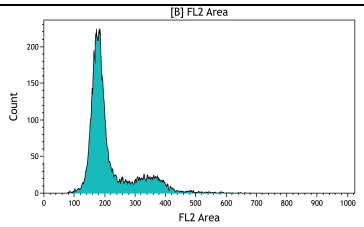
Vehicle-treated cells	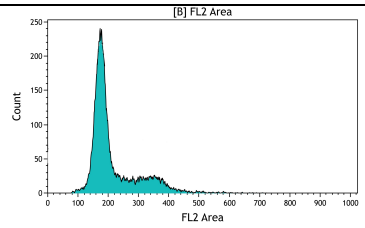	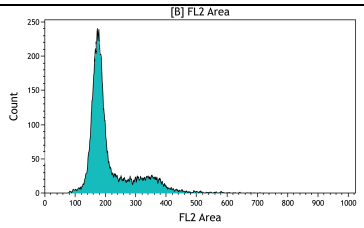
100 µM DATS-treated cells	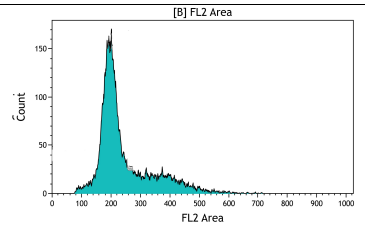	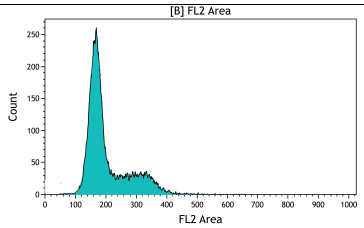
200 µM DATS-treated cells	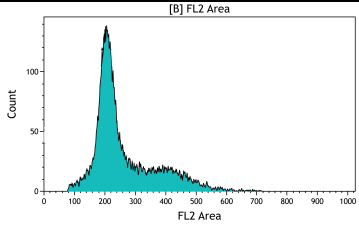	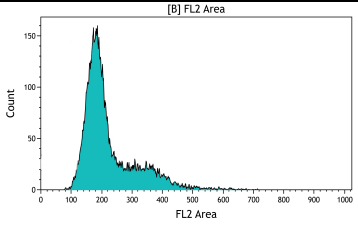
300 µM DATS-treated cells	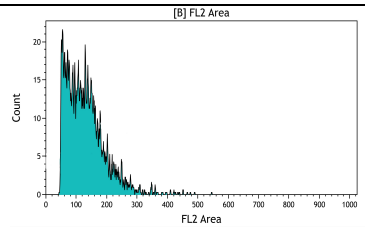	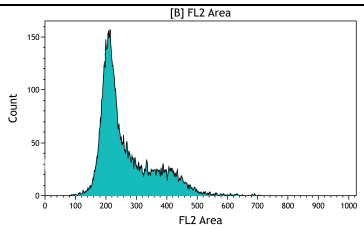
400 µM DATS-treated cells	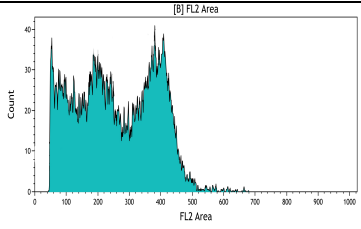	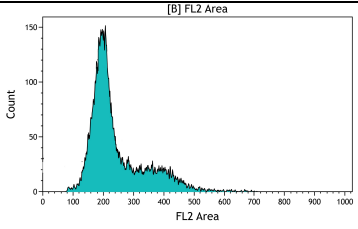

Due to the efficacy of NAC (2 mM) at significantly reducing the effect DATS exerts on cell cycle progression in the A549 cell line after 24- and 48 h exposure, experiments were conducted where cells were exposed to 100 µM and 300 µM DATS for 24 h in the presence and absence of the scavengers including SA (10 mM), DMTU (8 mM), Carboxy-PTIO (6 µM), Mannitol (20mM), Tiron (2 mM) and Trolox (20 µM) which scavenge $O_2^{\bullet}$, H_2O_2, •NO, •OH, O_2^{-} and $HO_2^{\bullet}$ respectively, as indicated in figures 41 and Table 16. After treatment with 100 µM- and 300 µM DATS in the presence of SA (10 mM) no significant change in the G_2M phase of the cell cycle was observed when compared to cells propagated in growth medium (22%) thus demonstrating a significant decrease when compared to cells exposed to 100 µM and 300 µM DATS alone (29% and 54%). In the presence of DMTU (8 mM) however, there was an increase to 37% and 67% after exposure to 100 µM- and 300 µM DATS respectively. This is a more prominent increase than cells exposed to DATS alone (29% and 54%) and correlates with a decrease in the percentage of cells in the G_1-S phase of the cell cycle. Cells treated with 100 µM- and 300 µM DATS in the presence of Mannitol (20mM) also demonstrated an increase in the percentage of cells in the G_2-M phase of the cell cycle to 34% and 79% from 29% and 54% respectively as seen in cells treated with just DATS alone. Cells exposed to 100 µM- and 300 µM DATS in the presence of Carboxy-PTIO (6 µM) experienced a significant increase in the percentage of cells in the G_2-M phase of the cell cycle to 81% at 300 µM only when compared to cells exposed to 300 µM DATS alone (54%). after treatment with DATS 100 µM and 300 µM in the presence of Tiron (2 mM) an increase in the percentage of cells in the G_2-M phase of the cell cycle was observed to 49% and 75% from 29% and 54% in cells treated with DATS alone. After treatment of cells with 100 µM- and 300 µM DATS in the presence of Trolox (20 µM) an increase in the percentage of cells in the G_2-M phase of the cell cycle was observed from 29% and 54% in cells treated with DATS alone to 52% and 75% respectively. All increases in the percentage of cells in the G_2-M phase of the cell cycle with regards to the A549 cell line were correlated with a decrease in the percentage of cells in the G_1-S phase of the cell cycle. This indicated that the scavengers did not reduce the effect of DATS on causing a G_2M phase cell cycle arrest but instead increased this effect with the exception of SA, after 24 h of treatment in the A549 cell line.

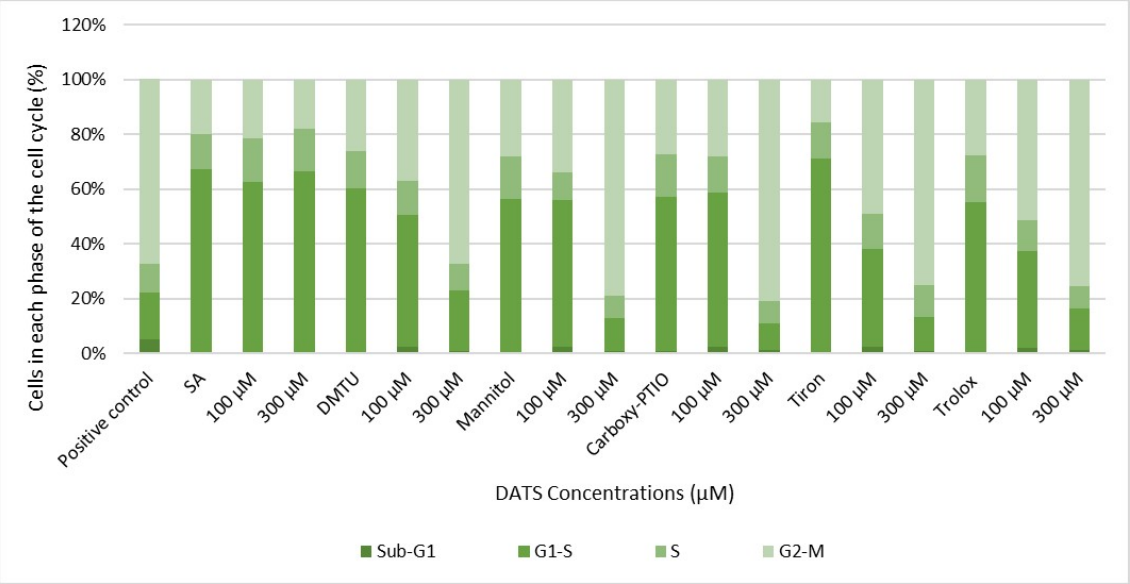

Figure 41: Figure illustrating the percentage of A549 cells in each phase of the cell cycle after 24 h of exposure to diallyl trisulfide (DATS) (100 µM, 300 µM) in the presence of the inhibitors, sodium azide (SA) (10 mM), N, N-dimethyl thiourea (DMTU) (8 mM), 2-(4-Carboxyphenyl)-4,4,5,5-tetramethylimidazoline-1-oxyl-3-oxide (Carboxy-PTIO) (6 µM), D-Mannitol (Mannitol) (20 mM), Tiron (2 mM) and Trolox (20 µM) with data showing exposure to cells in the presence of the scavengers alone followed by co-exposure with DATS.

Table 16: The representative images of cell cycle progression in A549 cells after 24 h of exposure to DATS (100 µM, 300 µM) and sodium azide (SA) (10 mM), N, N-dimethyl thiourea (DMTU) (8 mM), 2-(4-Carboxyphenyl)-4,4,5,5-tetramethylimidazoline-1-oxyl-3-oxide (Carboxy-PTIO) (6 µM), D-Mannitol (Mannitol) (20 mM), Tiron (2 mM) and Trolox (20 µM).

	Inhibitor-treated cells	**100 µM DATS-treated cells**	**300 µM DATS-treated cells**
10 mM SA-treated cells	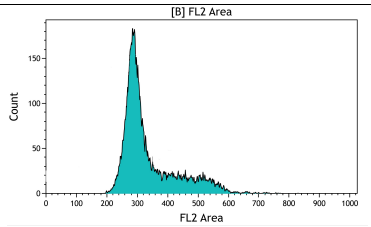	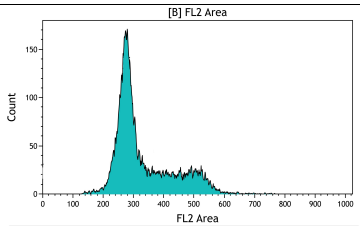	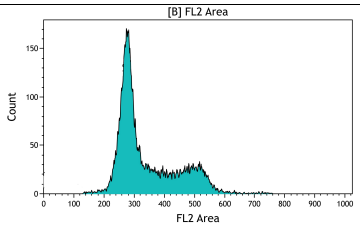
8 mM DMTU-treated cells	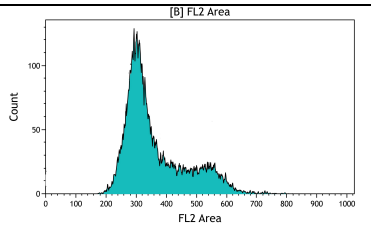	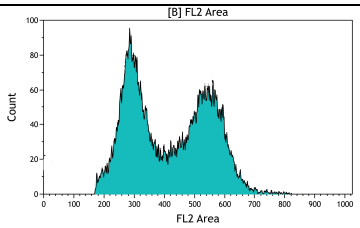	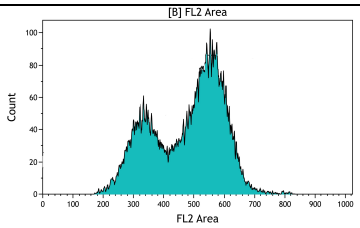
20 mM Mannitol-treated cells	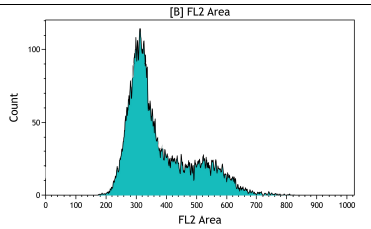	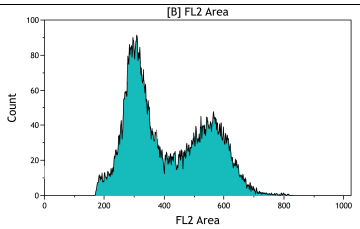	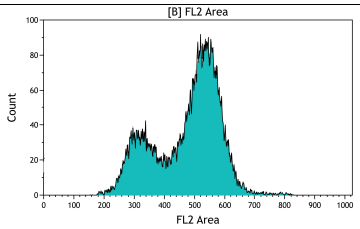
6 µM Carboxy-PTIO-treated cells	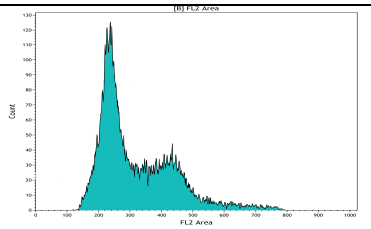	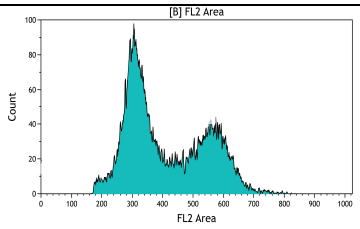	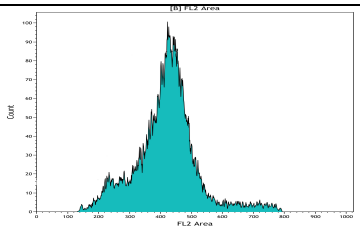
2 mM Tiron-treated cells	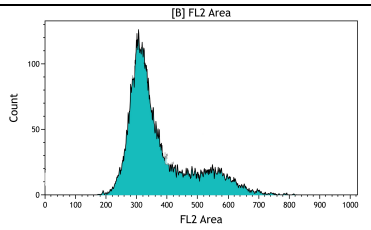	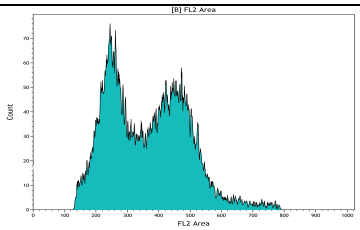	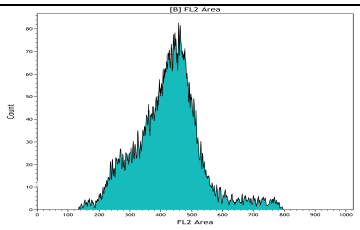

20 µM Trolox-treated cells	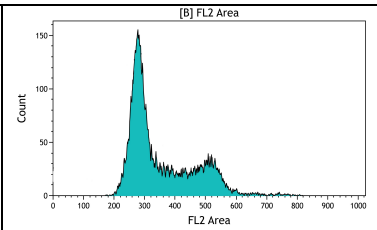	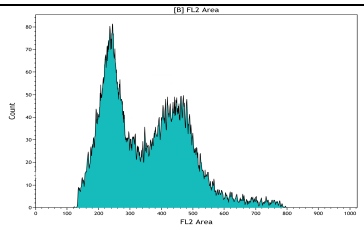	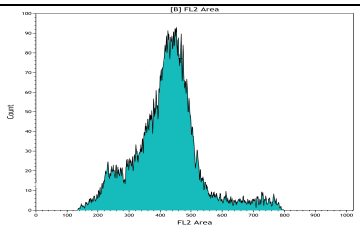

6.6 Mitochondrial membrane potential depolarisation (Mitocapture assay): flow cytometry

The influence of DATS on the mitochondrial membrane potential was evaluated by means of flow cytometry and 5',6,6'-tetrachloro-1,1',3,3'-tetraethylbenzimidazolylcarbocyanine iodide (JC-1), a fluorescent cyanine dye, which can distinguish between energized, disrupted and not disrupted mitochondrial membrane potentials. This is accomplished by the dye aggregating inside energized depolarized mitochondria. The aggregated dye emits an orange red fluorescent signal when compared to the JC-1 monomers found outside of the mitochondria which emit a green fluorescent signal (77).

The MDA-MB-231 cells were exposed for 24 h to DATS (10 µM, 50 µM, 100 µM, and 150 µM) alone or in the presence of NAC (2 mM) as well as DATS-treated cells (50 µM and 100 µM) in the presence of all the scavengers including SA (6mM), DMTU (8 mM), Carboxy-PTIO (8 µM), Mannitol (80 mM), Tiron (6 mM) and Trolox (40 µM) which scavenge the $O_2^{\bullet}$, H_2O_2, •NO, •OH, O_2^{-} and $HO_2^{\bullet}$, respectively, as depicted in figure 42, Table 17 and 18. Exposure to DATS resulted in a dose-dependent effect on the mitochondrial membrane potential exhibited by cells. Exposure to 10 µM- and 50 µM DATS resulted in a fold decrease in cells demonstrating mitochondrial depolarisation to 0.78 and 0.9 relative to cells propagated in growth medium. Furthermore, cells exposed to 100 µM- and 150 µM DATS resulted in an increase in cells demonstrating mitochondrial depolarisation to 1.75- and 1.8-fold relative to cells propagated in growth medium. Exposure to 10 µM-, 50 µM-, 100 µM- and 150 µM DATS in the presence of NAC (2 mM) resulted in an significant increase (p-value < 0.05) in cells demonstrating mitochondrial depolarisation to 1.4-, 1.87-, 1.68- and 1.40 fold relative to cells in media, indicating that in the presence of NAC, cells exposed to 10 µM- and 50 µM DATS demonstrated mitochondrial depolarisation that was increased in the presence of NAC when compared to cells exposed to DATS alone; however, cells exposed to higher concentrations of DATS (100 µM and 150 µM), demonstrated that the mitochondrial depolarisation was partially decreased by the presence of NAC.

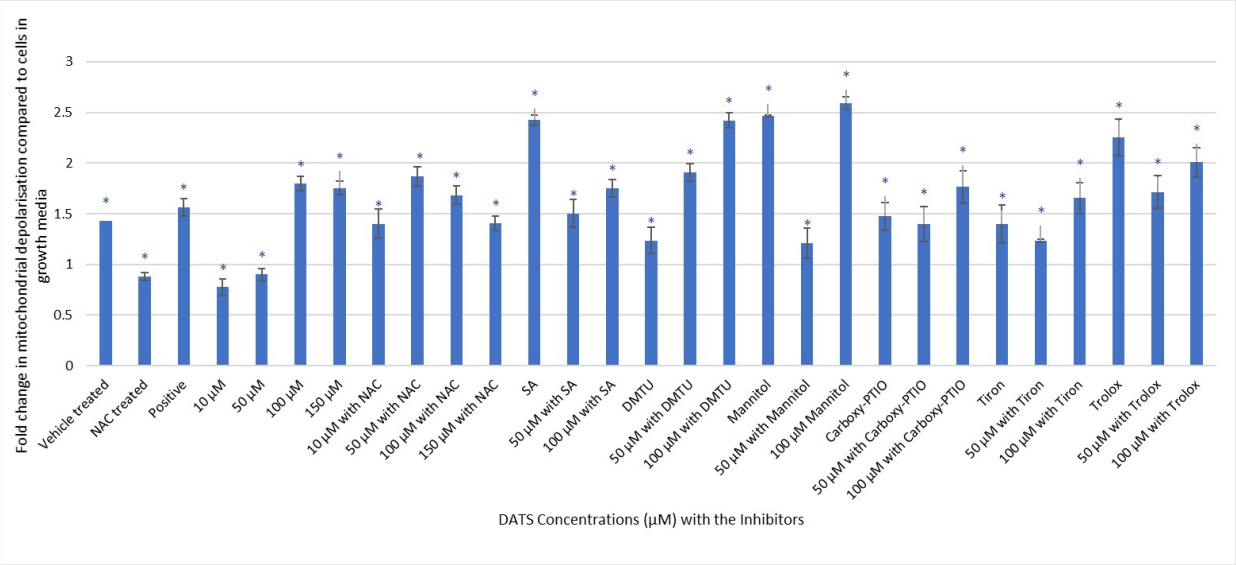

Figure 42: Figure illustrating the fold increase in mitochondrial depolarisation for the MDA-MB-231 cell line after exposure to diallyl trisulfide (DATS) (50 µM and 100 µM) in the presence of sodium azide (SA) (6mM), N, N-dimethyl thiourea (DMTU) (8 mM), 2-(4-Carboxyphenyl)-4,4,5,5-tetramethylimidazoline-1-oxyl-3-oxide (Carboxy-PTIO) (8 µM), D-Mannitol (Mannitol) (80 mM), Tiron (6 mM) and Trolox (40 µM). Statistical significance was calculated using an ANOVA test with a *p*-value < 0.05 indicating statistical significance of data compared to cells propagated in growth medium alone and is indicated by an *.

Table 17: Representative images displaying the amount of green fluorescence demonstrating mitochondrial membrane potential after 24 h exposure of MDA-MB-231 cells to diallyl trisulfide (DATS) (10 µM, 50 µM, 100 µM and 150 µM) in the presence and absence of N-acetyl cysteine (NAC) (2 mM).

	Cells treated with DATS alone	**Cells treated in the presence of NAC (2 mM)**
Cells propagated in growth medium	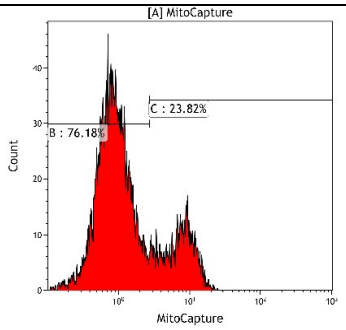	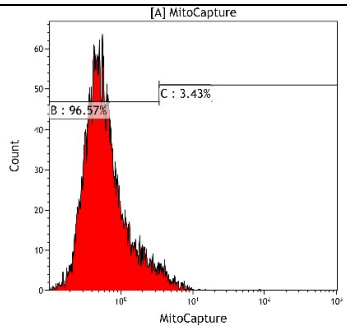

Vehicle-treated cells	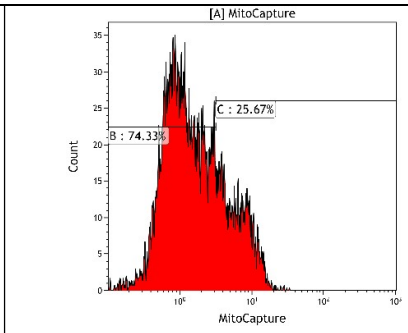	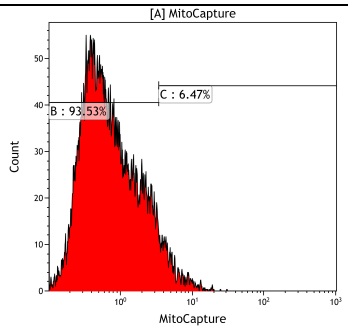
10 µM DATS-treated cells	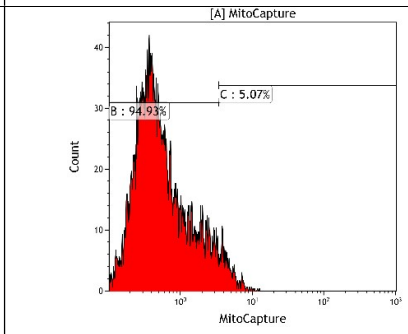	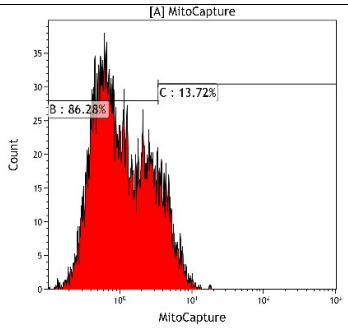
50 µM DATS-treated cells	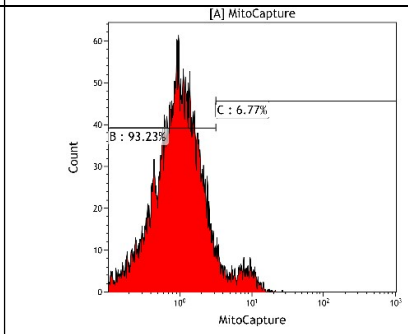	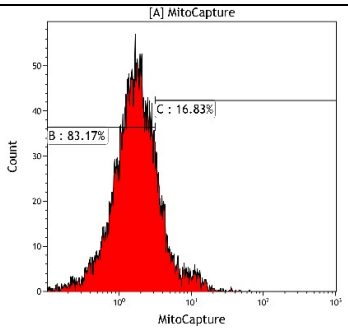
100 µM DATS-treated cells	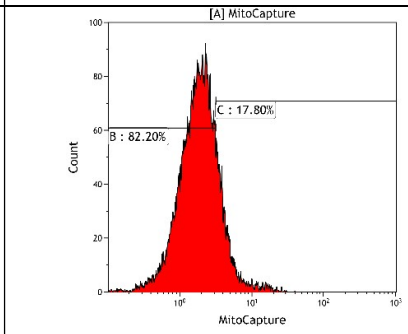	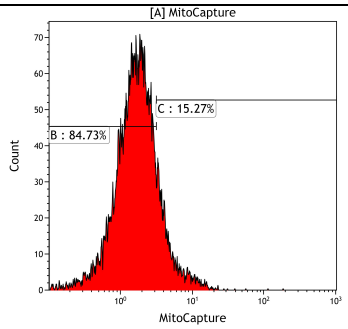
150 µM DATS-treated cells	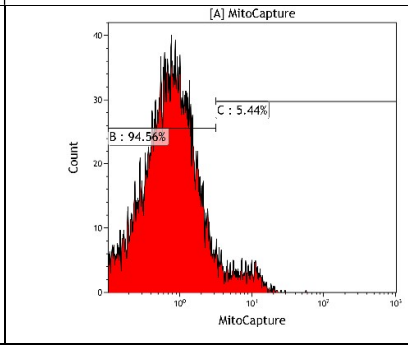	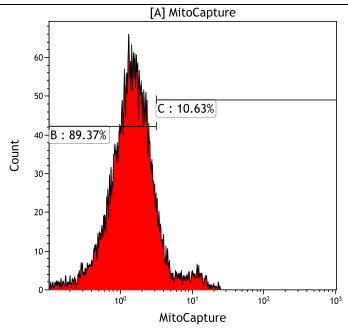

Table 18: Representative images displaying the amount of green fluorescence demonstrating mitochondrial membrane potential after 24 h exposure of MDA-MB-231 cells to diallyl trisulfide (DATS) (10 µM, 50 µM, 100 µM and 150 µM) in the presence of sodium azide (SA) (6mM), N, N-dimethyl thiourea (DMTU) (8 mM), 2-(4-Carboxyphenyl)-4,4,5,5-tetramethylimidazoline-1-oxyl-3-oxide (Carboxy-PTIO) (8 µM), D-Mannitol (Mannitol) (80 mM), Tiron (6 mM) and Trolox (40 µM).

	Inhibitor treated cells	50 µM DATS treated cells	100 µM DATS treated cells
6 mM SA-treated cells	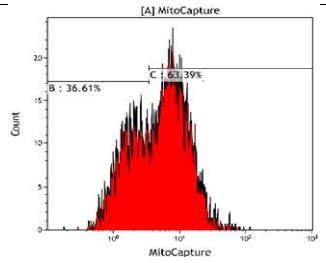	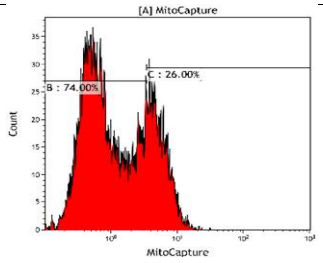	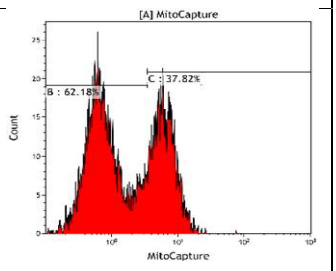
8 mM DMTU-treated cells	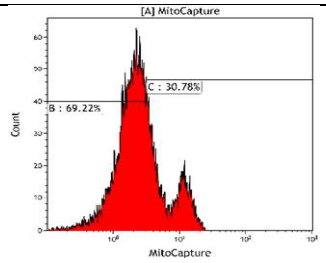	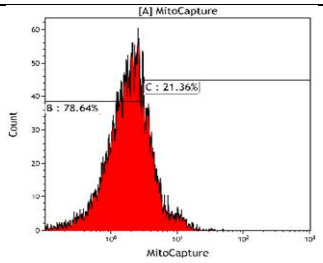	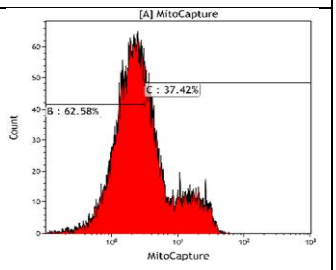
80 mM Mannitol-treated cells	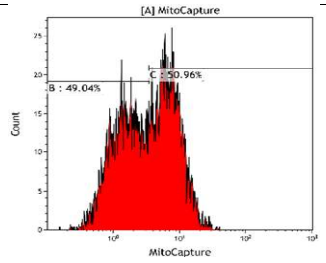	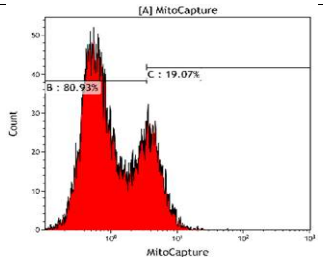	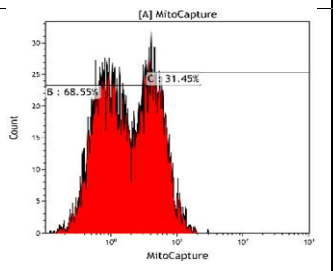
8 µM Carboxy-PTIO-treated cells	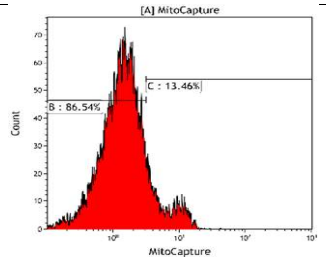	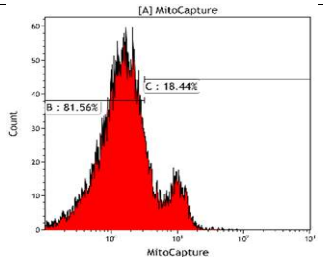	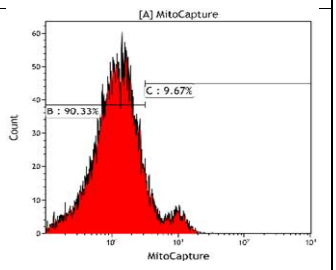
6 mM Tiron-treated cells	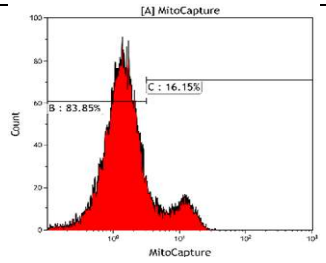	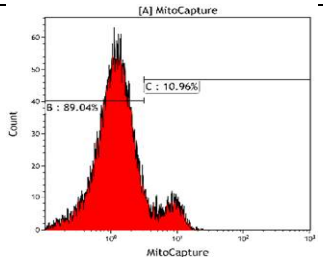	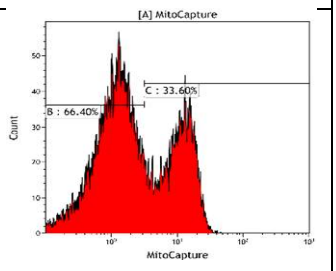

Exposure to 50 µM DATS alone resulted in a decrease in cells demonstrating mitochondrial depolarisation to 0.9-fold; however, exposure to 100 µM DATS resulted in an increase in cells demonstrating mitochondrial depolarisation to 1.75-fold compared to cells propagated in growth medium. Exposure to DATS (50 µM and 100 µM) in the presence of SA (6mM) for 24 h resulted in an increase in cells demonstrating mitochondrial depolarisation to 1.5- and 1.75-fold relative to cells propagated in complete growth medium. However, exposure to only SA demonstrated a significant increase in cells demonstrating mitochondrial depolarisation to 2.4 fold relative to cells propagated in growth medium. This indicates that exposure to only SA increased cells demonstrating mitochondrial depolarisation. Cells exposed to DMTU (8 mM) alone exhibited a significant increase in cells displaying mitochondrial depolarisation to 1.23 fold relative to cells propagated in growth medium alone and cells co-exposed to 50 µM- or 100 µM DATS and DMTU displayed a further increase in cells possessing mitochondrial depolarisation to 1.9- and 2.4 fold relative to cells propagated in growth medium. This was also a significant increase in cells demonstrating mitochondrial depolarisation when compared to cells exposed to 50 µM- and 100 µM DATS alone (0.9- and 1.75 fold), suggesting that DMTU increases the effect of DATS on mitochondrial depolarisation. Cells co-exposed to mannitol and DATS (50 µM and 100 µM) displayed an increase in cells possessing mitochondrial depolarisation of 1.21- and 2.6 fold respectively. Exposure of cells to 8 µM Carboxy-PTIO resulted in an increase in cells demonstrating mitochondrial depolarisation to 1.47 fold relative to cells propagated in media alone, cells co-exposed to 50 µM- and 100 µM DATS resulted in a significant increase in cells demonstrating mitochondrial depolarisation to 1.39- and 1.76 fold, compared to cells exposed to 50 µM- and 100 µM DATS alone (0.9- and 1.75 fold). In addition, a significant increase in cells demonstrating mitochondrial depolarisation was observed when cells were exposed to Carboxy-PTIO and 50 µM DATS but not at 100 µM DATS; indicating that Carboxy-PTIO caused an increase in the effects of DATS at lower concentrations and increases the amount of mitochondrial depolarisation by the cells on its own. After exposure of cells to Tiron (6 mM) cells demonstrated increased mitochondrial depolarisation by 1.4 fold relative to cells propagated in growth medium alone and co-treatment with 50 µM and 100 µM DATS resulted in a significant increase in cells demonstrating mitochondrial depolarisation to 1.24- and 1.65 fold when compared to cells treated with DATS alone (0.9 and 1.75), suggesting that Tiron also caused cells to demonstrate decreased mitochondrial depolarisation in the presence of 50 µM DATS and increased mitochondrial depolarisation at 100 µM DATS. Exposure to Trolox resulted in a significant increase in cells demonstrating mitochondrial depolarisation to 2.25 fold relative to cells propagated in growth medium. Co-exposure to DATS (50 µM and 100 µM) and Trolox resulted in a significant increase in cells demonstrating mitochondrial depolarisation to 1.71- and 2 fold, however, mitochondrial

depolarisation increased less prominently when cells were exposed to DATS alone (0.9- and 1.75 fold). It was observed that in the MDA-MB-231 cell line, exposure to the inhibitors alone increased the amount of mitochondrial depolarisation demonstrated by the cells more prominently compared to cells exposed to only 50 µM DATS. However, co-exposure to 100 µM DATS in the presence of the scavengers resulted in more extensive mitochondrial depolarisation. This corelates with the data obtained when cells were treated with DATS alone, as it indicated that at the lower concentrations of DATS (10 µM and 50 µM) the amount of cells demonstrating mitochondrial depolarisation was significantly less than that of cells propagated in media alone (0.78- and 0.9 fold) indicating that at low concentrations DATS could be inhibiting the amount of mitochondrial depolarisation displayed by the cells and at higher concentrations (100 µM and 150 µM DATS) cells displayed increased mitochondrial depolarisation, indicated by an increase in red fluorescence relative to cells propagated in growth medium (1.75- and 1.8 fold respectively).

The A549 cells were also exposed to DATS (100 µM, 200 µM, 300 µM and 400 µM) for 24 h in the presence and absence of NAC (2 mM) as well as in the presence of all the scavengers including SA (10 mM), DMTU (8 mM), Carboxy-PTIO (6 µM), Mannitol (20 mM), Tiron (2 mM) and Trolox (20 µM) which scavenge $O_2^{\bullet}$, H_2O_2, •NO, •OH, O_2^{-}, and $HO_2^{\bullet}$ respectively. After which they were assessed for the amount of depolarisation of their mitochondrial matrix potential relative to cells propagated in growth medium, this is illustrated in figure 42, Table 19 and 20. Cells exposed to 100 µM, 200 µM, 300 µM and 400 µM DATS alone exhibited a significant (p-value < 0.05) dose-dependent increase in cells demonstrating mitochondrial depolarisation, which was indicted by a significant fold-increase to 1.35-, 2.72-, 2.71- and 3.2 fold respectively, relative to cells propagated in growth medium only. In the presence of NAC, the cells possessing mitochondrial depolarisation decreased to 1.13-, 1.13-, 1.22- and 1.31 fold. However, even though the amount of mitochondrial depolarisation was decreased after exposure to 300 µM- and 400 µM DATS in the presence of NAC, the amount of mitochondrial depolarisation demonstrated by the cells was still significantly more prominent compared to cells propagated in growth medium alone.

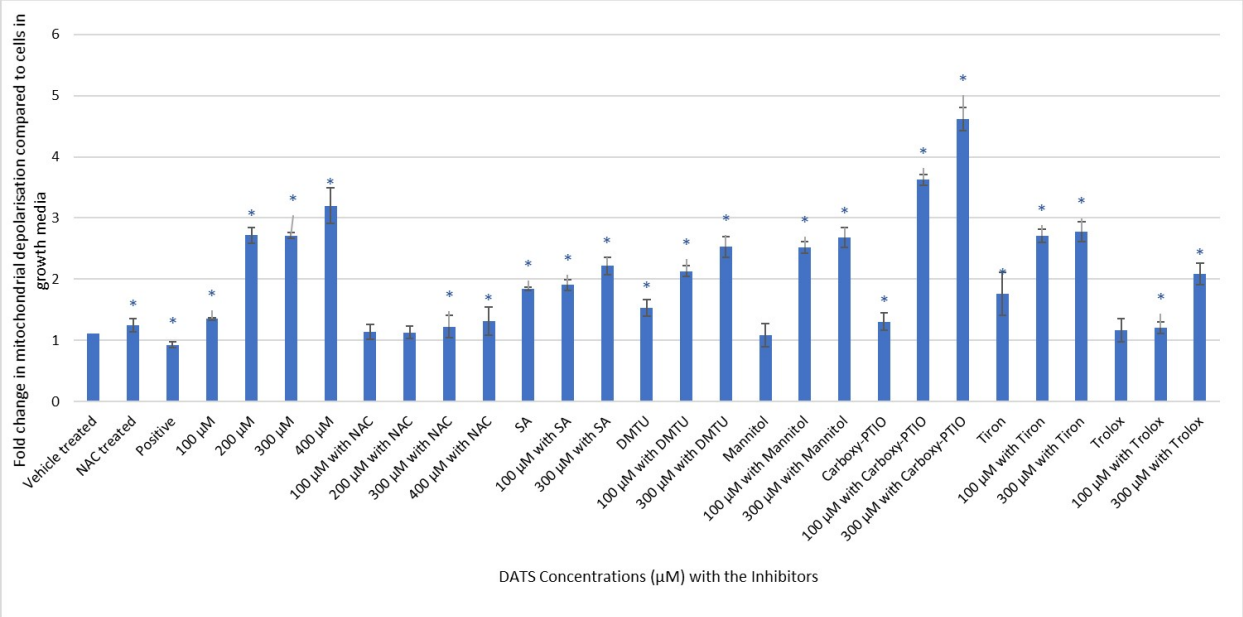

Figure 43: Figure illustrating the fold increase in mitochondrial depolarisation for the A549 cell line after exposure to DATS (100 µM, 200 µM, 300 µM and 400 µM) in the presence and absence of NAC (2 mM) as well as the scavengers including sodium azide (SA) (10 mM), N, N-dimethyl thiourea (DMTU) (8 mM), 2-(4-Carboxyphenyl)-4,4,5,5-tetramethylimidazoline-1-oxyl-3-oxide (Carboxy-PTIO) (6 µM), D-Mannitol (Mannitol) (20mM), Tiron (2 mM) and Trolox (20 µM) for 24 h. Statistical significance was calculated using an ANOVA test with a *p*-value < 0.05 indicating statistical significance of data compared to cells propagated in growth medium alone and is indicated by an *.

Table 19: Representative images displaying the amount of green fluorescence as a result of the mitocapture assay after 24 h exposure of the A549 cells to diallyl trisulfide (DATS) (100 µM, 200 µM, 300 µM and 400 µM) in the presence and absence of N-acetyl cysteine (NAC).

	Cells treated with DATS alone	**Cells treated in the presence of NAC (2 mM)**
Cells propagated in growth medium	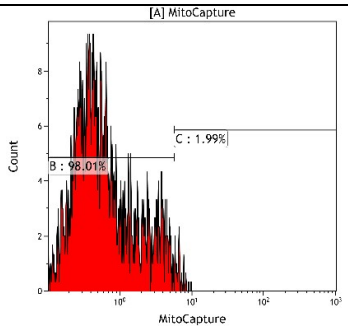	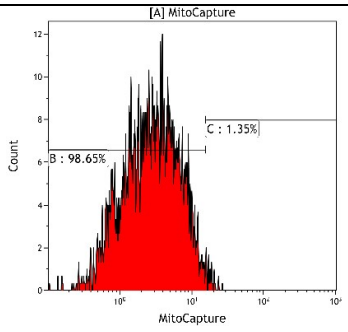

Vehicle-treated cells	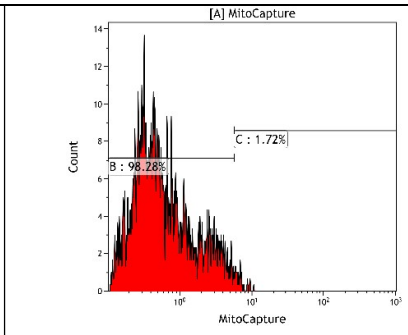	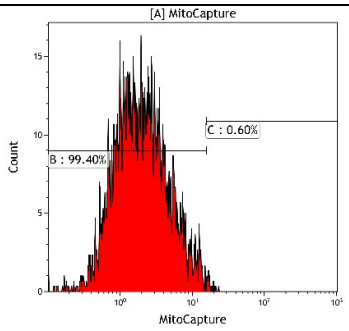
100 µM DATS-treated cells	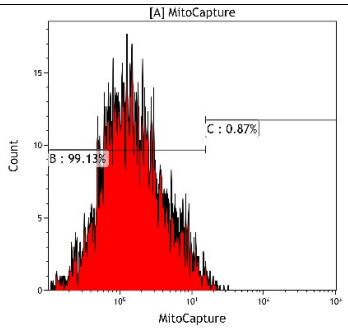	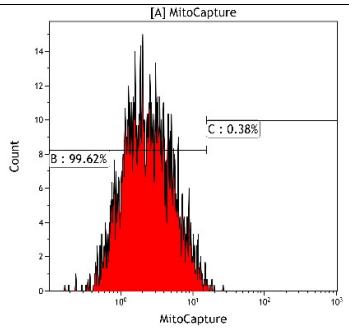
200 µM DATS-treated cells	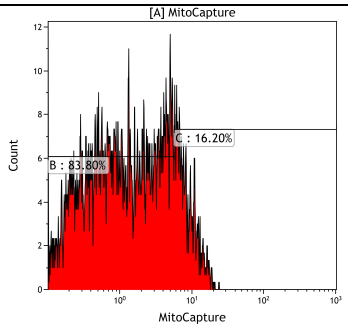	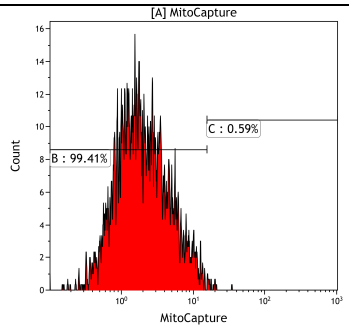
300 µM DATS-treated cells	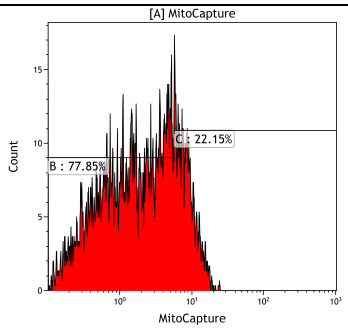	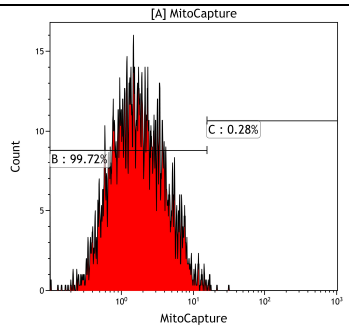
400 µM DATS-treated cells	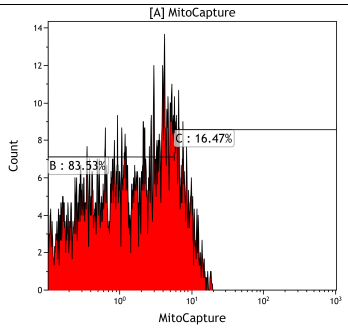	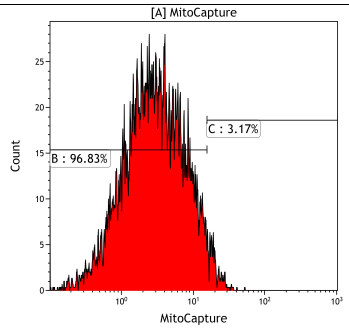

Table 20: Representative images displaying the amount of green fluorescence as a result of the mitocapture assay after 24 h exposure of A549 cells to diallyl trisulfide (DATS) (100 µM, 200 µM, 300 µM and 400 µM) in the presence and absence of N-acetyl cysteine (NAC) (2 mM).

	Inhibitor treated cells	100 µM DATS treated cells	300 µM DATS treated cells
10 mM SA-treated cells	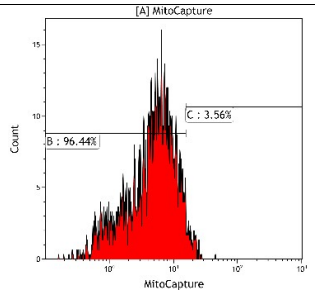	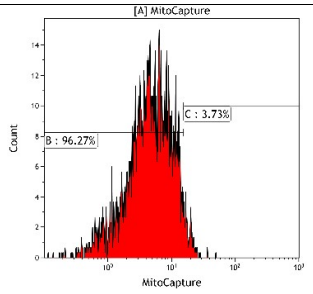	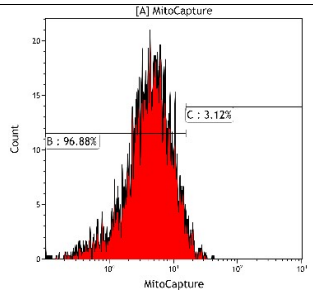
8 mM DMTU-treated cells	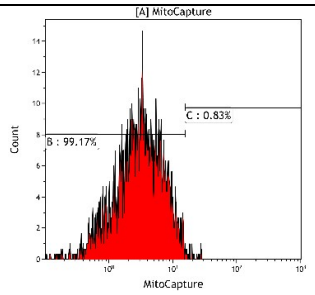	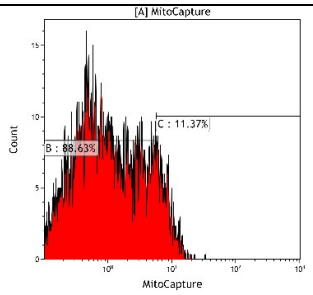	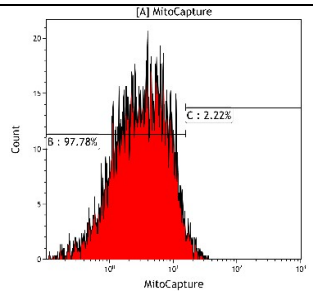
20 mM Mannitol-treated cells	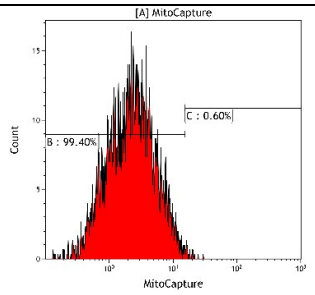	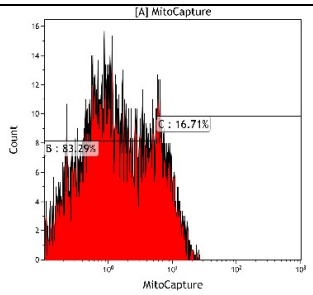	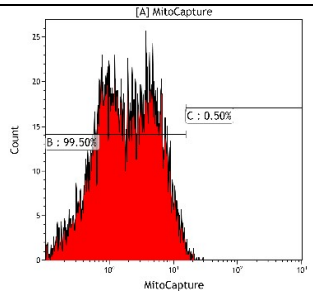
6 µM Carboxy-PTIO-treated cells	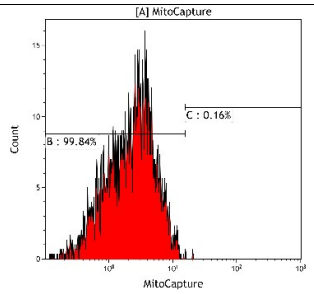	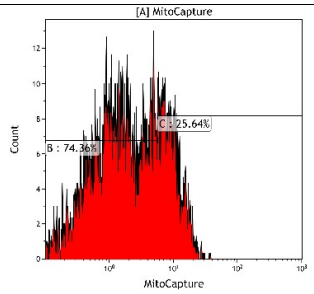	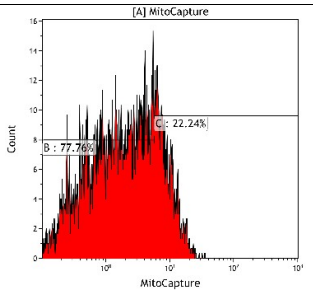

2 mM Tiron-treated cells	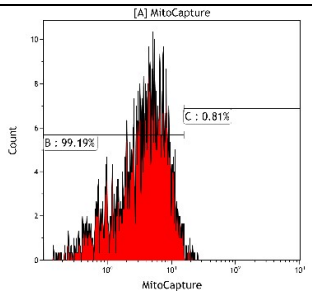	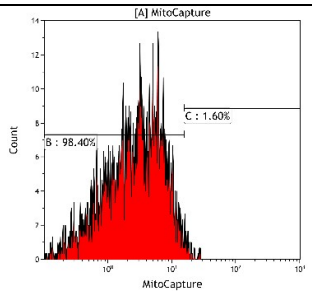	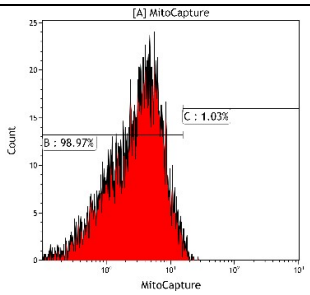
20 µM Trolox-treated cells	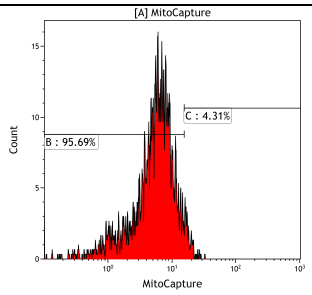	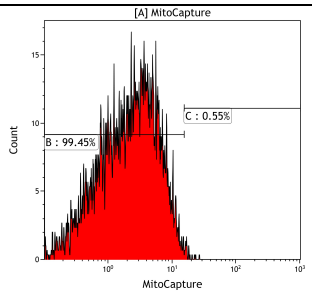	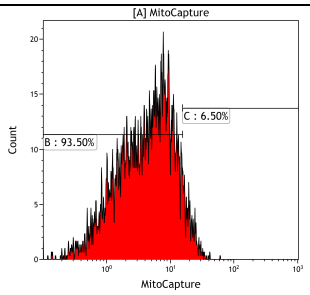

After exposure of cells to SA (10 mM) alone, a significant increase was observed in cells demonstrating mitochondrial depolarisation to 1.84 fold relative to cells in media only. Exposure to 100 µM- and 300 µM DATS in the presence of SA, increased cells demonstrating mitochondrial depolarisation to 1.9- and 2.22 fold respectively, compared to cells exposed to DATS alone (1.35- and 2.71 fold). This suggests that SA itself increases the amount of mitochondrial depolarisation that the cells demonstrated, but it is also further increased in the presence of DATS in a dose-dependent manner. Exposure of cells to DMTU (8 mM) resulted in a significant increase in cells demonstrating mitochondrial depolarisation to 1.53 fold relative to cells propagated in growth medium indicating that DMTU also causes mitochondrial depolarisation, this was further increased in the presence of 100 µM- and 300 µM DATS in a dose dependant manner to 2.13- and 2.53 fold respectively which is higher than the effects of DATS alone (1.35- and 2.71 fold respectively). After exposure of cells to Mannitol (20mM), no significant increase in cells demonstrating mitochondrial depolarisation was established, however co-treatment with 100 µM- and 300 µM DATS resulted in a significant dose-dependent fold-increase in cells demonstrating mitochondrial depolarisation to 2.52- and 2.67 fold relative to cells propagated in growth medium, which is more prominent than when cells were exposed to 100 µM- and 300 µM DATS alone (1.35- and 2.71 fold). Exposure of cells to Carboxy-PTIO (6 µM) resulted in a significant increase in cells demonstrating mitochondrial depolarisation to 1.31 fold, relative to cells propagated in growth medium. This was further increased in a dose-dependent manner in the presence of 100 µM- and 300 µM DATS with Carboxy-PTIO to 3.62- and 4.61 fold. After exposure of cells to Tiron (2 mM), a significant increase was observed in the amount of

mitochondrial depolarisation demonstrated by the cells to 1.76 fold relative to cells propagated in growth medium. Co-treatment of cells with Tiron and 100 µM- and 300 µM DATS resulted in a further increase to 2.71- and 2.77 fold respectively. Exposure of cells to Trolox (20 µM) alone resulted in an insignificant increase in cells demonstrating mitochondrial depolarisation to 1.16 fold relative to cells propagated in growth medium. Co-treatment of cells with Trolox and 100 µM and 300 µM DATS resulted in a significant increase in cells demonstrating mitochondrial depolarisation to 1.21- and 2.08 fold compared to cells exposed DATS alone (1.35- and 2.71 fold). After exposure of the A549 cells to 100 µM DATS in the presence of the inhibitors only Trolox caused a decrease in cells demonstrating mitochondrial depolarisation when compared to cells exposed to 100 µM DATS alone (1.35 fold increase); and after 300 µM DATS exposure only in the presence of SA, DMTU, Mannitol and Trolox was there a decrease in the amount of mitochondrial depolarisation demonstrated by the cells when compared to cells exposed to DATS alone (2.71 fold increase) this was most pronounced in the presence of Trolox.

6.7. Superoxide dismutase activity (SOD assay)

The influence of DATS on SOD activity was assessed as an indicator of the effect DATS exerts on the innate antioxidant defence mechanism of the cells. SOD is an endogenous enzyme responsible for converting the superoxide radical (O_2^-) and the singlet oxygen radical ($O_2^{\bullet}$) into H_2O_2. This assay provided data as represented by values referring to the inhibition percentage applied by SOD enzyme by means of quantifying the amount of O_2^- that is produced by the enzyme xanthine oxidase which is subsequently reduced by SOD. Therefore, the amount of O_2^- present in the cells correlates to the inhibition of SOD (30). The percentage of SOD inhibition was used as in indication regarding the effect of DATS on the antioxidant activity in MDA-MB-231- and A549 cells and whether aberrant ROS production is due to DATS modulating the SOD enzyme activity.

After 24 h of exposure to DATS (10 µM, 50 µM, 100 µM and 150 µM) in the MDA-MB-231 cell line it was observed that cells propagated in growth medium alone displayed a SOD inhibition percentage of 63% and vehicle-treated cells exhibited a SOD inhibition percentage of 66%. Cells exposed to 10 µM-, 50 µM-, 100 µM- and 150 µM DATS demonstrated a SOD inhibition percentage of 61%, 77%, 73% and 68% respectively, which was a significant increase only after exposure to 50 µM- and 100 µM DATS. However, after 48 h of exposure to 10 µM-, 50 µM-, 100 µM- and 150 µM DATS, the SOD inhibition was decreased significantly (p-value < 0.05) when compared to cells propagated in growth medium (58%). SOD inhibition after exposure to DATS was 22%, 28%, 40% and 50% after exposure to 10 µM, 50 µM, 100 µM and 150 µM DATS for 48 h and this decrease in inhibition was significant when cells were exposed to 10 µM-, 50 µM- and 100 µM DATS. This indicates that after 24 h DATS

increased the inhibition of SOD inversely to DATS concentration and after 48 h of exposure DATS significantly decreased SOD inhibition inversely to DATS concentration, this is shown in figure 44.

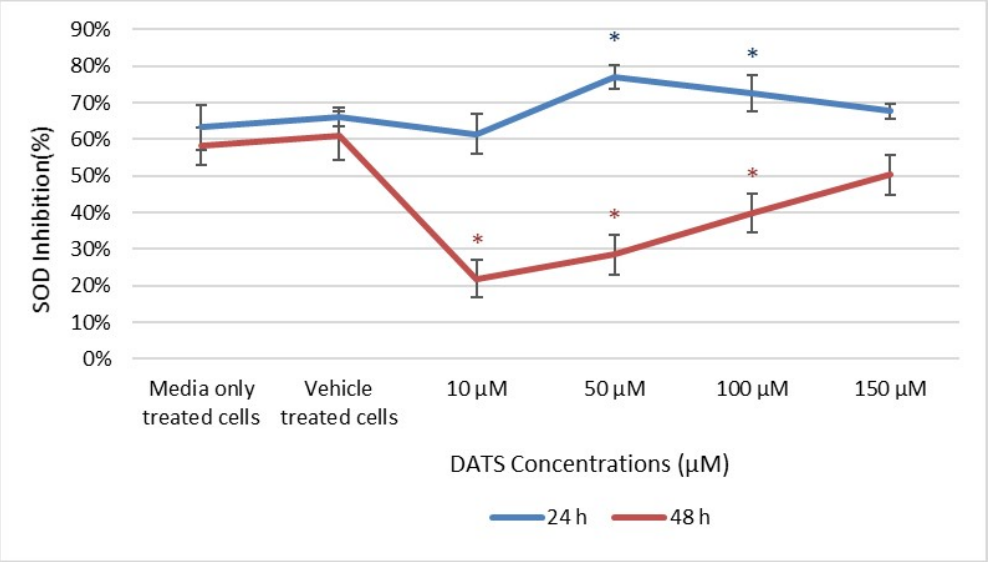

Figure 44: Figure illustrating the percentage of superoxide dismutase (SOD) inhibition in the MDA-MB-231 cell line after exposure to diallyl trisulfide (DATS) (10 µM, 50 µM, 100 µM and 150 µM) for 24 h and 48 h. Statistical significance was calculated using an ANOVA test with a *p*-value < 0.05 indicating statistical significance of data compared to cells propagated in media only and is indicated by an *.

The A549 cell line was exposed to 100 µM-, 200 µM-, 300 µM- and 400 µM DATS for 24 h, subsequently the SOD enzyme inhibition percentage was recorded at 79%, 82%, 79% and 83% compared to cells propagated in growth medium (85%). Thus, DATS (100 µM and 300 µM) exposure for 24 h resulted in a significant decrease in SOD inhibition after exposure to DATS. Exposure to 100 µM-, 200 µM-, 300 µM- and 400 µM DATS for 48 h resulted in a SOD inhibition percentage that was recorded as being 79%, 79%, 88%, and 90% respectively, but when compared to cells propagated in growth medium alone (91%) a significant decrease in SOD inhibition was observed only after exposure to 100 µM- and 200 µM DATS for 48 h, illustrated in figure 45. This indicates after 24 h and 48 h of exposure to DATS a significant decrease in SOD inhibition was observed and therefore DATS induced an increase in SOD activity particularly at the lower concentrations of DATS.

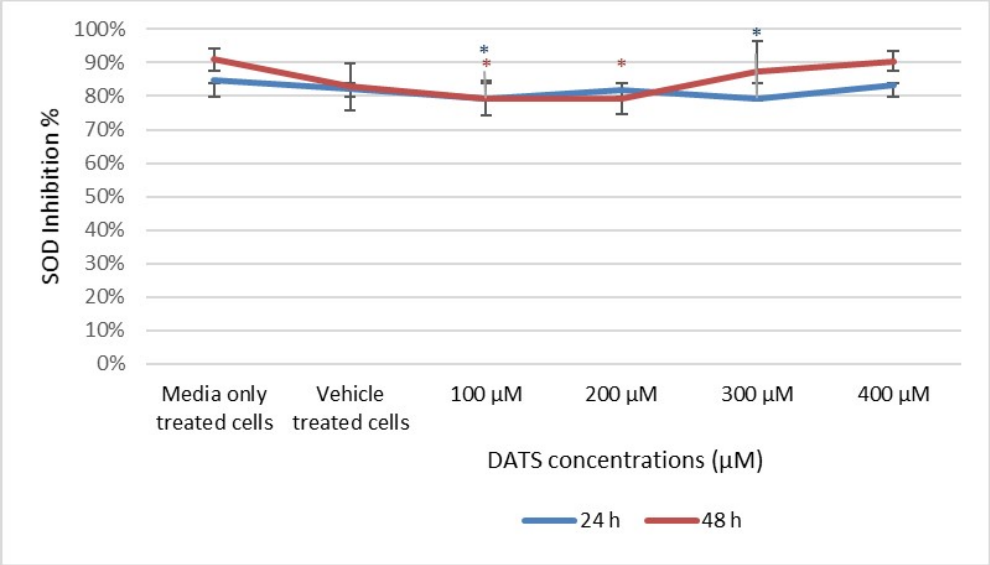

Figure 45: Figure illustrating the percentage of superoxide dismutase (SOD) inhibition for the A549 cell line after exposure to diallyl trisulfide (DATS) (100 µM, 200 µM, 300 µM and 400 µM) for 24 h and 48 h relative to cells propagated in growth medium. Statistical significance was calculated using an ANOVA test with a *p*-value < 0.05 indicating statistical significance of data compared to cells propagated in media only and is indicated by an *.

6.8 Catalase enzyme activity (catalase assay)

The effect of DATS on the antioxidant activity of the cells was assessed further by means of catalase protein quantification within the cells. Catalase is responsible for the conversion of H_2O_2 produced by SOD into water and oxygen (30). Therefore, quantification of catalase was used as an indication of the effect of DATS on antioxidant activity within the cells and whether an increase in ROS due to DATS is due to reduced activity of the catalase enzyme. In this assay, the concentration of catalase enzyme was calculated relative to the catalase concentration present in cells propagated in growth medium.

Exposure to DATS (10 µM, 50 µM, 100 µM and 150 µM) in the MDA-MB-231 cell line for 24 h demonstrated a decrease in the amount of catalase enzyme to 89%, 64%, 60% and 61% relative to cells propagated in growth medium, which was only significant (*p*-value < 0.05) after exposure to 50 µM, 100 µM and 150 µM DATS (64%, 60% and 61%). After 48 h of treatment with 10 µM, 50 µM, 100 µM and 150 µM DATS, it was observed that the amount of catalase enzyme present decreased to 88%, 74%, 74% and 84% relative to cells propagated in growth medium, which was also only a significant reduction (*p*-value < 0.05) after exposure to 50 µM, 100 µM and 150 µM DATS (74%, 74% and 84%). This Indicated that after 48 h of treatment with DATS the amount of catalase enzyme was

decreased when compared to cells propagated in growth medium alone, however, the decrease in the amount of the enzyme was more prominent after 24 h than 48 h of exposure to DATS, these results can be seen in figure 46.

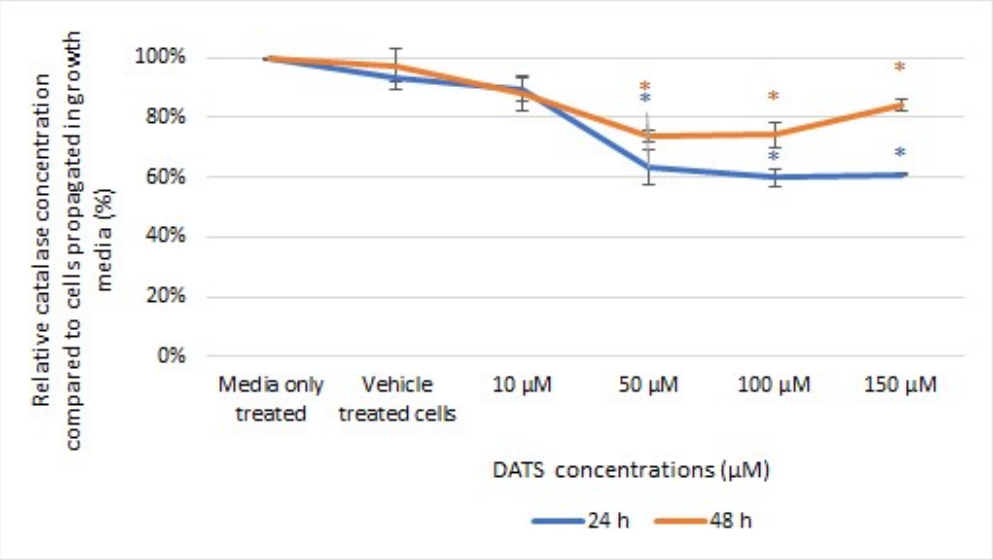

Figure 46: Figure illustrating the amount of catalase enzyme present in the MDA-MB-231 cell line after exposure to diallyl trisulfide (DATS) (10 µM, 50 µM, 100 µM and 150 µM) for 24 h and 48 h relative to cells propagated in growth medium. Statistical significance was calculated using an ANOVA test with a *p*-value < 0.05 indicating statistical significance of data compared to cells propagated in media alone and is indicated by an *.

Exposure to DATS (100 µM, 200 µM, 300 µM and 400 µM) for 24 h in the A549 cell line resulted in a significant (*p*-value < 0.05) decrease in catalase concentration to 75%, 75%, 76% and 55% when compared to cells propagated in growth medium alone. However, exposure to 100 µM-, 200 µM-, 300 µM- and 400 µM DATS for 48 h led to an increase in catalase concentration to 115%, 105%, 113% and 110% when compared to cells propagated to media only which was significant after 100 µM-, 300 µM- and 400 µM DATS exposure, as illustrated in figure 47. This indicates that after 24 h of exposure to DATS in the A549 cell line there was a dose-dependent decrease in the amount of catalase, however, after 48 h an exposure to DATS also resulted in an increase in the amount of catalase present relative to cells propagated in growth medium.

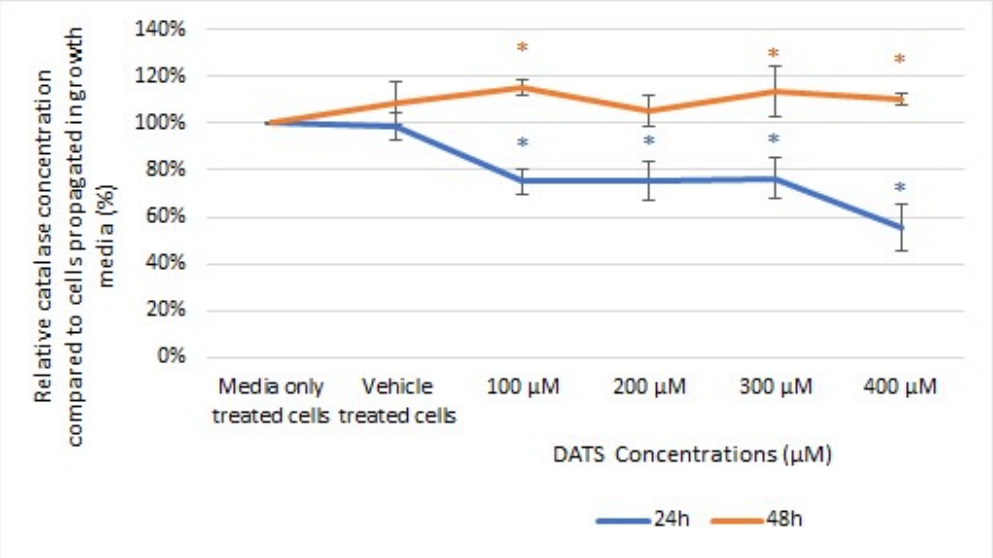

Figure 47: Figure illustrating the amount of catalase enzyme present in the A549 cell line after exposure to diallyl trisulfide (DATS) (100 µM, 200 µM, 300 µM and 400 µM) for 24 h and 48 h relative to cells propagated in growth medium. Statistical significance was calculated using an ANOVA test with a *p*-value < 0.05 indicating statistical significance of data compared to cells propagated in media alone and is indicated by an *.

7. Discussion

Lung cancer is the leading cause of cancer-related deaths worldwide while breast cancer is the leading cause of cancer-associated mortality in women (3, 4). Literature indicates that garlic posesses antiproliferative-and antimitotic activity on cancer cells possibly due to the prescence of organosulfur compounds including diallyl trisulphide (DATS) (12, 13, 15, 16). However, the possible role of reactive oxygen species (ROS) in the antiproliferative-and antimitotic effects exerted by DATS remains elusive. The current study was conducted in order to unravel the role of oxidative stress in the effects exerted by DATS in the MDA-MB-231 triple negative metastatic breast cancer cell line and the A549 lung cancer cell line on cell proliferation, morphology, cell cycle progression and mitochondrial membrane potential. In addition, the role of some possible sources of oxidative stress induced by DATS including dysregulation of SOD and catalase were also investigated. The experiments were conducted in the presence and absence of the ROS scavanger, N-acetyl cystein (NAC) and the specific ROS scavengers SA, DMTU, Carboxy-PTIO, Mannitol, Tiron, and Trolox which scavenge $O_2^{\bullet}$, H_2O_2, •NO, •OH, O_2^{-}, and $HO_2^{\bullet}$ to determine the dependency of the effects of DATS on these specific ROS with the exception of the SOD and catalase enzyme assays.

Data obtained from the crystal violet assay indicated that DATS exerted a dose-and time-dependent inhibition of cell growth that was also cell line dependant. DATS induced antiproliferative activity in both cell lines; however, the MDA-MB-231 cell line was more prominently affected by DATS. Furthermore, the antiproliferative activity in this cell line is supported in other studies which described reduced viability by 53% in the MDA-MB-231 cell line after exposure to 40 µM DATS for 24 h (21, 57). Furthermore, cell growth was also reduced to 50% after exposure to 75 µM DATS for 24 h, exposure to 50 µM DATS for 48 h or exposure to 50 µM DATS for 16 h (66, 79). However, in the current study, cell proliferation decreased to 60% and 51% after 24 h and 48 h of exposure to 100 µM DATS in the MDA-MB-231 cell line. Moreover, DATS exhibited less prominent effects in the A549 cell line, and therefore, this study required exposure to higher concentrations of DATS (10 µM-300 µM) to achieve optimal antiproliferative activity in the A549 cell line when compared to the triple negative metastatic MDA-MB-231 cell line. This could possibly be due to the upregulation of the NRF2 transcription factor gene present in the A549 cell line as a result of a mutation in Kelch-like ECH-associated protein 1 (Keap1) gene, which results in the subsequent upregulation of the genes producing antioxidant enzymes such as GSTs and drug metabolising enzymes including NQO (60-62). The current study found that exposure to 100 µM DATS for 48 h reduced cell growth to 83% when compared to cells propagated in growth medium. However, a previous study found that 48 h exposure to 100 µM DATS reduced cell growth to 57% in the A549 cell line when compared to cells propagated in growth medium (20). In addition, another study reported that exposure of the A549

cells with 10 µM DATS for 24 h resulted in 47% growth inhibition (79). The current study also demonstrates that NAC inhibits the antiproliferative activity exerted by DATS in both cell lines which is supported by previous studies as well (39). The latter suggests that the mechanism of action utilised by DATS resulting in reduced cell growth is dependent on increased generation of ROS since NAC is a precursor molecule of L-cysteine which promotes the formation of glutathione and therefore reduces ROS quantities since NAC possesses a thiol-disulphide bond which reacts with and reduces ROS thereby preventing the depletion of glutathione (80). Furthermore, this is the first study to report on findings regarding antiproliferative assays where both cell lines were exposed to DATS in the presence and absence of various scavengers for specific ROS. It was observed that SA, DMTU, Carboxy-PTIO, Mannitol, Tiron, and Trolox completely inhibited the antiproliferative effects of DATS in both cell lines after 24 h exposure indicating that $O_2^{\bullet}$, H_2O_2, •NO, •OH, O_2^-, and $HO_2^{\bullet}$ is involved in the effect of DATS on proliferation and this is reported for the first time in this current project.

Data in the current study obtained by means of fluorescent microscopy also confirmed that exposure to DATS resulted in a dose-dependent significant increase in H_2O_2 production after 24 h of exposure to DATS in the MDA-MB-231 cell line and a significant increase in H_2O_2 production was observed after 48 h of exposure to DATS in both cell lines. The increase in H_2O_2 production was more prominent in the MDA-MB-231 cell line when compared to the A549 cell line after exposure to DATS, this was likely due to the increased oxidative stress resistance conferred to the A549 cell line due to increased Nrf2 gene expression. In addition, the effects of DATS on H_2O_2 production in the A549 cell line has not been reported previously (60-62). Moreover, the increase in H_2O_2 production after 24 h of exposure to DATS in the MDA-MB-231 cell line is supported by another study that reported similar findings after exposure for 24 h exposure to 50 µM DATS (54). In addition, exposure to 32.96 µM DATS for 48 h also a 15 fold increase in H_2O_2 production as demonstrated by DCFDA staining when compared to cells propagated in growth medium in the MDA-MB-231 cell line (81). However, oxidative stress due to O_2^- was not observed to be induced by DATS in either cell line. Data obtained by means of SOD activity assays supported these findings since DATS induced a significant decrease in SOD inhibition and thus an increase in SOD activity which results in decreased O_2^- (30, 37). However, studies conducted using a MitoSOX red assay to detect O_2^- in the mitochondria indicated a significant increase in fluorescence after 24 h of exposure to 50 µM DATS in the MDA-MB-231 cell line indicating that the mitochondria are involved in the mechanism of action of DATS (54). Another study found that after 6 h of exposure to 40 µM DATS in the MDA-MB-231 cell line the amount of fluorescence detected by a MitoSOX red assay increased by 1.75 fold compared to cells propagated in growth medium (82).

Light microscopy showed that following DATS exposure there was a time-dependent increase observed in rounded cells that correlated to an increase in DATS concentration in both cell lines. However, the effects on cell rounding was more prominent after 24 h compared to 48 h of exposure. The effect of DATS on cell rounding has previously been confirmed in the MDA-MB-231 cell line after 24 h exposure to 50 µM DATS; however, the data was only reported in a qualitative manner (54) Moreover, the effect DATS exerts on cell rounding in both cell lines was negated by NAC (2 mM) and thus, further studies in the presence of the inhibitors was conducted. Data indicated that the scavengers partially inhibited the cell rounding effects induced by DATS after 24 h of exposure with SA exhibiting the most prominent ability to reduce the amount of cell rounding induced by DATS and Trolox being the least effective. This data suggests that $O_2^{\bullet}$, H_2O_2, •NO, •OH, O_2^{-}, and $HO_2^{\bullet}$ are all involved in the effect of DATS on cell rounding; however, $O_2^{\bullet}$ is involved the most prominently in the mechanism of action exerted by DATS to in induce cell rounding and $HO_2^{\bullet}$ the least. After 48 h of exposure to the scavengers including Carboxy-PTIO (8 µM), Mannitol (100 mM), and Trolox (80 µM) in the MDA-MB-231 cell line it was determined that these inhibitors were partially effective at reducing the effect of DATS on cell rounding after 48 h of exposure indicating that after 48 h •OH, •NO, and $HO_2^{\bullet}$ were involved in the mechanism of DATS to induce cell rounding. The various scavengers reduced cell rounding induced by DATS (100 µM, 200 µM, 300 µM and 400 µM) in the A549 cell line with SA again being the most effective. This is the first study to demonstrate effects of DATS on cell rounding in the presence of various scavengers that is specific for certain ROS species that could potentially indicate which ROS is involved in the mechanism of action exerted by DATS.

The current study also evaluated the effect DATS exerts on cell cycle progression using flow cytometry. It was observed that exposure to DATS in the MDA-MB-231 cell line for 24 h and 48 h resulted in a dose-dependent increase in the percentage of cells occupying the sub-G_1 phase of the cell cycle indicating that cell death is induced by DATS. Studies have demonstrated exposure to 20 µM DATS for 24 h in the MDA-MB-231 cell line resulted in a significant increase in the percentage of cells in the G_2M phase of the cell cycle was observed to 33% when compared to cells propagated in growth medium (83). After exposure to DATS alone for 24 h in the A549 cell line; however, there was a dose-dependent increase in the percentage of cells arrested in the G_2M phase of the cell cycle and after 48 h of exposure there was a significant increase in the percentage of cells in the sub-G_1 phase of the cell cycle. In addition, another study which reported that exposure of the A549 cells to 50 µM DATS for 24 h lead to a 4 fold increase in the percentage of cells in the G_2M phase of the cell cycle was observed (84). Since data suggests that the effects of DATS on the cell cycle progression is time-dependent it is possible that cells which had arrested in the G_2M phase after 24 h of exposure to DATS transitioned to cell death after 48 h of exposure. Nevertheless, the effects caused by DATS on

cell cycle progression was negated in the presence of NAC (2 mM) in both cell lines, therefore 24 h treatment of cells in the presence of the inhibitors continued and is reported for the first time in these cell lines in this current study. Exposure of the MDA-MB-231 cells to DATS in the presence of the inhibitors for 24 h resulted in a dose-dependent increase in the percentage of cells in the G_2M phase of the cell cycle instead of the sub-G_1 phase as displayed after treatment with DATS alone, with the exception of cells exposed in the presence of SA which mostly negated the effects of DATS on cell cycle progression indicating that DATS is dependent on $O_2^{\bullet}$ to exert its effect on cell cycle progression this effect by SA also occurred in the A549 cell line confirming the dependency of DATS on $O_2^{\bullet}$ to exert its effects on cell cycle progression. In the A549 cell line the co-exposure with DATS and the inhibitors of H_2O_2, •NO, •OH, O_2^- and $HO_2^{\bullet}$ caused a G_2M phase cell cycle arrest after 24 h and this may be the reason a G_2M phase increase was seen in the MDA-MB-231 cell line as well instead of a sub-G_1 phase increase after 24 h of exposure in the presence of the inhibitors, the effect of DATS may have been partially mitigated by the inhibitors which allowed the detection of the G_2M phase cell cycle arrest before the cells moved to the sub-G_1 phase.

The effect of DATS on mitochondrial membrane depolarisation was also investigated in this study using flow cytometry. In this current study it was found that there was a dose-dependent increase cells exhibiting mitochondrial membrane depolarisation caused by treatment with DATS alone for 24 h in the A549 cell line which was abolished in the presence of NAC indicating the dependency of DATS on ROS to cause mitochondrial depolarisation. Mitochondrial membrane depolarisation by DATs is supported by another study which demonstrated that exposure of the A549 cells to 100 µM DATS for 3 h resulted in a significant decrease in mitochondrial membrane depolarisation (84). The effects of DATS on mitochondrial depolarisation in the presence of the inhibitors were investigated for the first time in these cell lines in this study. After exposure of the A549 cells to 100 µM DATS for 24 h in the presence of the inhibitors only Trolox caused a decrease in mitochondrial depolarisation when compared to cells exposed to 100 µM DATS alone; and after 300 µM DATS exposure only in the presence of SA, DMTU, Mannitol and Trolox was there a decrease in the amount of mitochondrial depolarisation when compared to cells exposed to DATS alone indicating that $O_2^{\bullet}$, H_2O_2, •OH, and $HO_2^{\bullet}$ are partially involved in the effect of DATS on mitochondrial depolarisation in the A549 cell line with $HO_2^{\bullet}$ having the most involvement.

The possibility of DATS influencing the innate intracellular antioxidant enzymes resulting in the increased ROS production and subsequent oxidative stress was also investigated in this study by means of evaluating SOD and catalase. After 24 h exposure to DATS, the MDA-MB-231 cell line displayed increased SOD inhibition that was inversely related to DATS concentration and after 48 h

of exposure DATS SOD inhibition was significantly decreased inversely to the DATS concentration. The involvement of SOD in the mechanism of action of DATS has been confirmed in a previous study where 24 h of exposure to 40 µM DATS in the MDA-MB-231 cell line led to a 36 fold increase in SOD expression observed by a western blot analysis (84). Following DATS exposure for 24 h and 48 h in the A549 cell line, a significant decrease in SOD inhibition was observed for the first time in this study. Regulation of the endogenous catalase enzyme was dysregulated by DATS exposure for 24 h and 48 h in the MDA-MB-231 cell line, resulting in a dose-dependent- and time-dependant decrease in catalase activity that was more prominent after 24 h of exposure than 48 h. Similarly, in the A549 cell line exposure to DATS for 24 h resulted in a dose-dependent- and time-dependant decrease in catalase activity, however, after 48 h of exposure catalase activity was significantly increased compared to cells propagated in growth medium. The increase in catalase activity seen in both cell lines after 48 h of exposure to DATS is likely due to the cells recovering from the effects of DATS. The effect of DATS on the activity of the catalase enzyme in these cell lines is reported for the first time in this study.

8. Conclusion

In this study the influence of the ROS $O_2^{\bullet}$, H_2O_2, •NO, •OH, O_2^{-}, and $HO_2^{\bullet}$ in the effects exerted by DATS on cell proliferation, oxidative stress, morphology, cell cycle progression and mitochondrial depolarization was investigated as well as the effects of DATS on the activity of SOD and catalase. It was observed that the effects of DATS were dependent on ROS however the ROS that was observed to have the most prominent role in the effects of DATS was $O_2^{\bullet}$ even though the effects and the effective dose range was cell line specific. This study therefore provides insight into the oxidative stress-dependent mechanism of action exerted by DATS resulting in cell death; however, further research would still be required to fully comprehend the mechanism of action used by DATS and how the mechanism of action may differ for different cell lines. Additionally, this study provides insight into the role of oxidative stress in the mechanism of action of other small naturally occuring organosulfur compounds. This may assist with research into other potential phytomedicinal compounds or with the the synthesis of synthetic medicinal compounds that utilize a similar mechanism of action as small naturally occuring organosulfur compounds in order to reduce the side effects or decrease the effects of the body's natural metabolic processes on the efficacy of the synthetic drug. Research into DATS and other phytomedicinal compounds falls in line with sustainable development goal 3 as proposed by the United Nations; this goal aims to ensure healthy living and to promote well-being for all ages (85). Sustainable development goal 3 includes research into the treatment of non-communicable diseases like cancer, additionally, the potential to reduce the severe side effects of many conventional treatment regimens which may be provided by phytomedicinal compounds like DATS can improve overall patient well being. In addition, the lower cost of naturally sourced medicine compared to synthetic medicine will allow for more accessible treatment (6-10).

9. Ethical Consideration

The project received ethical approval (716/2019) from the Research Ethics Committee of the Faculty of Health Sciences (University of Pretoria, Pretoria, South Africa).

10. Acknowledgements

This project was supported by grants awarded to Prof Joubert from the Department of Physiology, by the Cancer Association of South Africa and the Medical Research Council. The project was also funded from grants received from the Struwig Germeshuysen Trust, School of Medicine Research Committee of the University of Pretoria and grants from the South African National Research Foundation awarded to Prof A.M. Joubert and Dr M.H. Visagie.

11. References

1. DeSantis C, Bray F, Ferlay J, Lortet-Tieulent J, Anderson B, Jemal A. International variation in female breast cancer incidence and mortality rates. Cancer Epidemiol Biomarkers Prev. 2015;24(10):1495-1506.
2. Ngwa W, Addai B, Adewole I, Ainsworth V, Alaro J, Alatise O et al. Cancer in sub-Saharan Africa: a Lancet Oncology Commission. Lancet Oncol. 2022;23(6):e251-e312.
3. Hercules S, Alnajar M, Chen C, Mladjenovic S, Shipeolu B, Perkovic O, et al. Triple-negative breast cancer prevalence in Africa: a systematic review and meta-analysis. BMJ Open. 2022;12(5):1-11.
4. Bhardwaj A, Tiwari A. Breast cancer diagnosis using genetically optimized neural network model. Expert Syst Appl. 2015; 42(10):4611-4620.
5. Pilleron S, Soto-Perez-de-Celis E, Vignat J, Ferlay J, Soerjomataram I, Bray F et al. Estimated global cancer incidence in the oldest adults in 2018 and projections to 2050. Int J Cancer Res. 2020;148(3):601-608.
6. Gandhi L, Rodríguez-Abreu D, Gadgeel S, Esteban E, Felip E, De Angelis F, et al. Pembrolizumab plus chemotherapy in metastatic non–small-cell lung cancer. N Engl J Med. 2018;378(22):2078-2092.
7. Rehman J, Zahra, Ahmad N, Khalid M, Noor ul Huda Khan Asghar H, Gilani Z, et al. Intensity modulated radiation therapy: a review of current practice and future outlooks. JRRAS. 2018;11(4):361-367.
8. Rutqvist L, Rose C, Cavallin-stahl E. A systematic overview of radiation therapy effects in breast cancer. Acta Oncol. 2003;42(5-6):532-545.
9. Sirzén F, Kjellén E, Sörenson S, Cavallin-ståhl E. A systematic overview of radiation therapy effects in non-small cell lung cancer. Acta Oncol. 2003;42(5-6):493-515.
10. Bonam S, Wu Y, Tunki L, Chellian R, Halmuthur M, Muller S, Pandy V. What has come out from phytomedicines and herbal edibles for the treatment of cancer? Chem Med Chem. 2018;13(18):1854-1872.
11. Goncharov N, Orekhov A, Voitenko N, Ukolov A, Jenkins R, Avdonin P. Organosulfur compounds as nutraceuticals. Nutraceuticals 2016;1(1):555-568.
12. Puccinelli M, Stan S. Dietary bioactive diallyl trisulfide in cancer prevention and treatment. Int J Mol. Sci. 2017;18(8):1645-1663.
13. Li Z, Ying X, Shan F, Ji J. The association of garlic with Helicobacter pylori infection and gastric cancer risk: A systematic review and meta-analysis. Helicobacter. 2018;23(5):12532-12547.
14. Balasenthil S, Arivazhagan S, Nagini S. Garlic enhances circulatory antioxidants during 7,12-dimethylbenz[a]anthracene–induced hamster buccal pouch carcinogenesis. J Ethnopharmacol. 2000;72(3):429-433.
15. Xiao D, Choi S, Johnson D, Vogel V, Johnson C, Trump D et al. Diallyl trisulfide-induced apoptosis in human prostate cancer cells involves c-Jun N-terminal kinase and extracellular-signal regulated kinase-mediated phosphorylation of Bcl-2. Oncogene. 2004;23(33):5594-5606.
16. Sumiyoshi H, Wargovich M. Garlic (Allium sativum): A review of its relationship to cancer. Curr Cancer Drug Targets. 2021;4(2):133-140.
17. Singh S, Pan S, Srivastava S, Xia H, Hu X, Zaren H et al. Differential Induction of NAD(P)H:Quinone Oxidoreductase by Anti-Carcinogenic Organosulfides from Garlic. Biochem Biophys Res Commun. 1998;244(3):917-920.
18. Thomson M, Ali M. Garlic [Allium sativum]: A review of its potential use as an anti-cancer agent. Curr Cancer Drug Targets. 2003;3(1):67-81.

19. Amagase H, Petesch BL, Matsuura H, Kasuga S, Itakura Y. Intake of garlic and its bioactive components. JN. 2001;131:955S–962S.
20. Li W, Tian H, Li L, Li S, Yue W, Chen Z et al. Diallyl trisulfide induces apoptosis and inhibits proliferation of A549 cells in vitro and in vivo. ABBS. 2012;44(7):577-583.
21. Kiesel V, Stan S. Diallyl trisulfide, a chemopreventive agent from *Allium* vegetables, inhibits alpha-secretases in breast cancer cells. Biochem Biophys Res Commun. 2017;484(4):833-838.
22. Liu Y, Zhao Y, Wei Z, Tao L, Sheng X, Wang S et al. Targeting Thioredoxin System with an Organosulfur Compound, Diallyl Trisulfide (DATS), Attenuates Progression and Metastasis of Triple-Negative Breast Cancer (TNBC). Cell Physiol and Biochem. 2018;50(5):1945-1963.
23. Lai K, Hsu S, Yang J, Yu C, Lein J, Chung J. Diallyl trisulfide inhibits migration, invasion and angiogenesis of human colon cancer HT-29 cells and umbilical vein endothelial cells and suppresses murine xenograft tumour growth. J Cell Mol Med. 2015;19(2):474-484.
24. Liu M, Wu L, Montaut S, Yang G. Hydrogen sulfide signaling axis as a target for prostate cancer therapeutics. Prostate Cancer Prostatic Dis. 2016;2016(1):1-9.
25. Choi Y. Diallyl trisulfide induces apoptosis and mitotic arrest in AGS human gastric carcinoma cells through reactive oxygen species-mediated activation of AMP-activated protein kinase. Biomed. Pharmacother. 2017;94(1):63-71.
26. Wang J, Chen J, Jiang Y, Shi Y, Zhu J, Xie C, et al. Wnt/β-catenin modulates chronic tobacco smoke exposure-induced acquisition of pulmonary cancer stem cell properties and diallyl trisulfide intervention. Toxicol Lett. 2018;291(1):70-76.
27. Hwang J, Lee Y, Lee D, Kwon K. DATS sensitizes glioma cells to TRAIL-mediated apoptosis by up-regulation of death receptor 5 via ROS. Food Chem Toxicol. 2017;106(1):514-521.
28. Wu C, Chung J, Tsai S, Yang J, Sheen L. Differential effects of allyl sulfides from garlic essential oil on cell cycle regulation in human liver tumor cells. Food Chem Toxicol. 2004;42(12):1937-1947.
29. Wu C, Sheen L, Chen H, Kuo W, Tsai S, Lii C. Differential effects of garlic oil and its three major organosulfur components on the hepatic detoxification system in rats. J Agric. Food Chem. 2002;50(2):378-383.
30. Poljsak B, Šuput D, Milisav I. Achieving the balance between ROS and antioxidants: when to use the synthetic antioxidants. Oxid Med Cell. Longev. 2013;2013(1):1-11.
31. Chao W, Deng J, Li P, Liang Y, Huang G. 3,4-Dihydroxybenzalactone suppresses human non-small cell lung carcinoma cells metastasis via suppression of epithelial to mesenchymal transition, ROS-mediated PI3K/AKT/MAPK/MMP and NFκB signaling pathways. Molecules. 2017;22(4):537-546.
32. Schumacker P. Reactive oxygen species in cancer: a dance with the devil. Cancer Cell. 2015;27(2):156-157.
33. Scialò F, Sriram A, Fernández-Ayala D, Gubina N, Lõhmus M, Nelson G, et al. Mitochondrial ROS produced via reverse electron transport extend animal lifespan. Cell Metab. 2016;23(4):725-734.
34. Ježek J, Cooper K, Strich R. Reactive oxygen species and mitochondrial dynamics: The yin and yang of mitochondrial dysfunction and cancer progression. Antioxidants. 2018;7(1):1-24.
35. Kumari S, Badana A, G M, G S, Malla R. Reactive Oxygen Species: A Key Constituent in Cancer Survival. Biomark. 2018;13(1):117727191875539.
36. Porporato P, Filigheddu N, Pedro J, Kroemer G, Galluzzi L. Mitochondrial metabolism and cancer.ECR. 2017;28(3):265-280.

37. Ighodaro O, Akinloye O. First line defence antioxidants-superoxide dismutase (SOD), catalase (CAT) and glutathione peroxidase (GPX): their fundamental role in the entire antioxidant defence grid. AJM. 2018;54(4):287-293.
38. Glasauer A, Chandel NS. Targeting antioxidants for cancer therapy. Biochem Pharmacol. 2014;92(1):90-101.
39. Gupta SC, Hevia D, Patchva S, Park B, Koh W, Aggarwal BB. Upsides and downsides of reactive oxygen species for cancer: the roles of reactive oxygen species in tumorigenesis, prevention, and therapy. Antioxid Redox Signal. 2012;16(11):1295-1322.
40. Chaabane W, User SD, El-Gazzah M, Jaksik R, Sajjadi E, Rzeszowska-Wolny J, et al. Autophagy, apoptosis, mitoptosis and necrosis: interdependence between those pathways and effects on cancer. Arch Immunol Ther. Exp. 2013;61(1):43-58
41. Collins K, Jacks T, Pavletich N. The cell cycle and cancer. PNAS. 1997;94(7):2776-2778.
42. Leal-Esteban L, Fajas L. Cell cycle regulators in cancer cell metabolism. Biochim Biophys Acta Mol Basis Dis. 2020;1866(5):1-10.
43. Borkowska A, Sielicka-Dudzin A, Herman-Antosiewicz A, Wozniak M, Fedeli D, Falcioni G et al. Diallyl trisulfide-induced prostate cancer cell death is associated with Akt/PKB dephosphorylation mediated by P-p66shc. Eur J Nutr. 2011;51(7):817-825.
44. Borkowska A, Sielicka-Dudzin A, Herman-Antosiewicz A, Halon M, Wozniak M, Antosiewicz J. P66Shc mediated ferritin degradation—A novel mechanism of ROS formation. Free Radic Biol Med. 2011;51(3):658-663.
45. Westphal D, Dewson G, Czabotar PE, Kluck RM. Molecular biology of Bax and Bak activation and action. Biochim Biophys Acta. 2011;1813(4):521-531.
46. Herman-Antosiewicz A, Stan S, Hahm E, Xiao D, Singh S. Activation of a novel ataxia-telangiectasia mutated and Rad3 related/checkpoint kinase 1–dependent prometaphase checkpoint in cancer cells by diallyl trisulfide, a promising cancer chemopreventive constituent of processed garlic. Mol Cancer Ther. 2007;6(4):1249-1261.
47. Xiao D, Zeng Y, Singh S. Diallyl trisulfide-induced apoptosis in human cancer cells is linked to checkpoint kinase 1-mediated mitotic arrest. Mol Carcinog. 2009;48(11):1018-1029.
48. Abou-Ghali M, Stiban J. Regulation of ceramide channel formation and disassembly: Insights on the initiation of apoptosis. Saudi J Biol Sci. 2015;22(6):760-772.
49. Ouyang L, Shi Z, Zhao S, Wang FT, Zhou TT, Liu B, et al. Programmed cell death pathways in cancer: a review of apoptosis, autophagy and programmed necrosis. Cell Prolif. 2012;45(6):487-498.
50. Park M-R, Kim S-G, Cho I-A, Oh D, Kang K-R, Lee S-Y, et al. Licochalcone-A induces intrinsic and extrinsic apoptosis via ERK1/2 and p38 phosphorylation-mediated TRAIL expression in head and neck squamous carcinoma FaDu cells. Food Chem Toxicol. 2015;77:34-43.
51. Burke P. Mitochondria, Bioenergetics and Apoptosis in Cancer. Trends Cancer. 2017;3(12):857-870.
52. Elmore S. Apoptosis: A Review of Programmed Cell Death. Toxicol. Pathol. 2007;35(4):495-516.
53. Dhanasekaran D, Reddy E. JNK signaling in apoptosis. Oncogene. 2008;27(48):6245-6251.
54. Lee B, Park B, Kim S, Lee Y. Role of Bim in diallyl trisulfide-induced cytotoxicity in human cancer cells. J Cell Biochem. 2011;112(1):118-127.
55. Na H, Kim E, Choi M, Park J, Kim D, Surh Y. Diallyl trisulfide induces apoptosis in human breast cancer cells through ROS-mediated activation of JNK and AP-1. Biochem Pharmacol. 2012;84(10):1241-1250.

56. Wang S, El-Deiry W. TRAIL and apoptosis induction by TNF-family death receptors. Oncogene.2003;22(53):8628-8633.
57. Liu Y, Zhu P, Wang Y, Wei Z, Tao L, Zhu Z, et al. Antimetastatic therapies of the polysulfide diallyl trisulfide against triple-negative breast cancer (TNBC) via suppressing MMP2/9 by blocking NF-κB and ERK/MAPK signaling pathways. Plos One. 2015;10(4):1-18.
58. Holliday DL, Speirs V. Choosing the right cell line for breast cancer research. Breast Cancer Res. 2011;13(4):215-225.
59. Visagie MH, van den Bout I, Joubert AM. A bis-sulphamoylated estradiol derivative induces ROS-dependent cell cycle abnormalities and subsequent apoptosis. PloS One. 2017;12(4):1-19.
60. Foster K, Oster C, Mayer M, Avery M, Audus K. Characterization of the A549 cell line as a type ii pulmonary epithelial cell model for drug metabolism. Exp Cell Res. 1998;243(2):359-366.
61. Zhang H, Chen Y, Xu R, He Q. Nrf2 mediates the resistance of human A549 and HepG2 cancer cells to boningmycin, a new antitumor antibiotic, in vitro through regulation of glutathione levels. Acta Pharmacol. Sin. 2018;39(10):1661-1669.
62. Ma Q. Role of Nrf2 in oxidative stress and toxicity. Annu Rev Pharmacol Toxicol. 2013;53(1):401-426.
63. Marais S, Mqoco TV, Stander A, Van Papendorp DH, Joubert AM. The *in vitro* effects of a sulphamoylated derivative of 2-methoxyestradiol on cell number, morphology and alpha-tubulin disruption in cervical adenocarcinoma (HeLa) cells. Biomed Res Int. 2012;23(3):357-362.
64. Potrich E, Amaral L. Determination of kinetic parameters of the crystal violet reaction with sodium hydroxide applying absorbance technique and the laws of lambert-beer and arrhenius. Encyclopaedia Bios. 2017;14(25):1852-1861.
65. Sigma-Aldrich. Spectrophotometry handbook. 1st ed. Buckinghamshire: GE healthcare; 2012.
66. Zhang Y, Xie W, Zhang Y, Chen Y, Wang D, Li G, et al. Experimental study of inhibitory effects of diallyl trisulfide on the growth of human osteosarcoma Saos-2 cells by down-regulating expression of glucose-regulated protein 78. Onco Targets Ther. 2018;11(1):271-277.
67. Kelly S, Patel N, Eccardt A, Fisher J. Glucose-dependent trans-plasma membrane electron transport and p70S6k phosphorylation in skeletal muscle cells. Redox Biol. 2018:1-10.
68. Rowlands J, Casida J. NADH: Ubiquinone oxidoreductase inhibitors block induction of ornithine decarboxylase activity in MCF-7 human breast cancer cells. Pharmacol Toxicol. 1998;83(5):214-219.
69. Kaushik N, Uddin N, Sim G, Hong Y, Baik K, Kim C, et al. Responses of solid tumor cells in DMEM to reactive oxygen species generated by non-thermal plasma and chemically induced ROS systems. Sci Rep. 2015;5(1):1-11.
70. Zhao X, Cai A, Peng Z, Liang W, Xi H, Li P, et al. JS-K induces reactive oxygen species-dependent anti-cancer effects by targeting mitochondria respiratory chain complexes in gastric cancer. J Cell Mol Med. 2019;0(0):1-16.
71. Sîrbu A, Palamarciuc O, Babak M, Lim J, Ohui K, Enyedy E, et al. Copper(ii) thiosemicarbazone complexes induce marked ROS accumulation and promote nrf2-mediated antioxidant response in highly resistant breast cancer cells. Dalton Trans. 2017;46(12):3833-3847.
72. Lee S, Hwang H, Shin J, Ahn J. Enhancement of cytotoxic effect on human head and neck cancer cells by combination of photodynamic therapy and sulforaphan. Gen Physiol Biophys. 2015;34(01):13-21.

73. Kutuk O, Aytan N, Karakas B, Kurt A, Acikbas U, Temel S, et al. Biphasic ROS production, p53 and BIK dictate the mode of cell death in response to DNA damage in colon cancer cells. PloS One. 2017;12(8):1-12.
74. Stander BA, Marais S, Vorster CJJ, Joubert AM. *In vitro* effects of 2-methoxyestradiol on morphology, cell cycle progression, cell death and gene expression changes in the tumorigenic MCF-7 breast epithelial cell line. J Steriod Biochem. Mol. Biol. 2010;119(3):149-60.
75. Peshavariya H, Dusting G, Selemidis S. Analysis of dihydroethidium fluorescence for the detection of intracellular and extracellular superoxide produced by NADPH oxidase. Free Radic Res. 2007;41(6):699-712.
76. Pietkiewicz S, Schmidt J, Lavrik I. Quantification of apoptosis and necroptosis at the single cell level by a combination of imaging flow cytometry with classical Annexin V/propidium iodide staining. J Immunol Methods. 2015;423:99-103.
77. Perelman A, Wachtel C, Cohen M, Haupt S, Shapiro H, Tzur A. JC-1: alternative excitation wavelengths facilitate mitochondrial membrane potential cytometry. Cell Death Dis. 2012;3(11):1-7.
78. Kanga K, Mendonca P, Soliman K, Ferguson D, Darling-Reed S. Effect of Diallyl Trisulfide on TNF-α-induced CCL2/MCP-1 Release in Genetically Different Triple-negative Breast Cancer Cells. Anticancer Res. 2021;41(12):5919-5933.
79. Sakamoto K, Lavvson L, Milner J. Allyl sulfides from garlic suppress the *in vitro* proliferation of human a549 lung tumor cells. Nutrition and Cancer. 1997;29(2):152-156.
80. Sun S. N-acetylcysteine, reactive oxygen species and beyond. Cancer Biol Ther. 2010;9(2):109-110.
81. Marni R, Kundrapu D, Chakraborti A, Malla R. Insight into drug sensitizing effect of diallyl disulfide and diallyl trisulfide from Allium sativum L. on paclitaxel-resistant triple-negative breast cancer cells. J Ethnopharmacol. 2022;296:1-13.
82. Chandra-Kuntal K, Lee J, Singh S. Critical role for reactive oxygen species in apoptosis induction and cell migration inhibition by diallyl trisulfide, a cancer chemopreventive component of garlic. Breast Cancer Res Treat. 2013;138(1):69-79.
83. Hahm E, Kim S, Mathan S, Singh R, Singh S. Mechanistic Targets of Diallyl Trisulfide in Human Breast Cancer Cells Identified by RNA-seq Analysis. J Cancer Prev. 2021;26(2):128-136.
84. Wu X, Hu Y, Lamy E, Mersch-Sundermann V. Apoptosis induction in human lung adenocarcinoma cells by oil-soluble allyl sulfides: Triggers, pathways, and modulators. Environ Mol Mutagen. 2009;50(3):266-275.
85. So WKW. Cancer nurses: A voice to lead—a vision for cancer care. Cancer Nursing. 2021Aug7;44(4):345–6.

12. Annexure A: University of Pretoria Faculty Day 2019 poster presented.

Oxidative-stress mediated cell death induced by a garlic constituent (diallyl trisulfide) in breast cancer cells

N. Surajlal, M.H. Visagie, Prof F. Wenhold, A.M. Joubert,

Background

Breast cancer is a significant health issue worldwide and is the leading cause of cancer-related mortality in women globally in addition to this the risk of developing it increases with age regardless of family history. Most current treatments include chemotherapy which may be harmful to the body. In order to reduce harmful side effects research into natural plant derived medicinal compounds or phytomedicine is occurring. In this study we look at the effect of garlic on breast cancer. Studies have shown that garlic has anti-proliferative and antimitotic effects on breast cancer cells due to the presence of its organosulphur compounds including diallyl trisulphide (DATS). Using DATS as an anti-proliferative compound, it's mechanism of action culminating in anti-proliferative activity in a triple negative breast cancer cell line (MDA-MB-231). This was investigated by demonstrating the dependency of the effects of DATS on reactive oxygen species (ROS). Furthermore, the effects of DATS were evaluated on proliferation (crystal violet staining and spectrophotometry), cell rounding (light microscopy), ROS production (2,7-dichlorofluoresceindiacetate (DCFDA) staining and fluorescent microscopy) cell cycle progression and cell death induction (flow cytometry, ethanol fixation and propidium iodide staining) in the presence and absence of the ROS scavenger, N-acetyl cystein (NAC 2mM) for 24 and 48 hours. This study demonstrated that the effects of DATS resulting in cell death is dependant on and induces ROS production in the MDA-MB-231 cell line.

Cell proliferation

Spectrophotometry (Crystal violet staining)

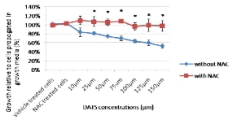

Spectrophotometry results demonstrating the effect of DATS after 24hrs on proliferation in the presence or absence of NAC.

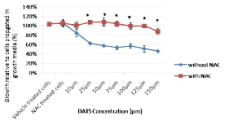

Spectrophotometry results demonstrating the effect of DATS after 48hrs on proliferation in the presence or absence of NAC.

Cell rounding

Light microscopy

Light microscopy indicated a dose dependant increase in cell rounding when cells were exposed to DATS. This was almost completely remediated in the presence of NAC for both 24 and 48 hours.

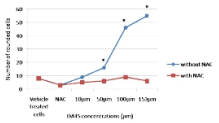

The amount of cell rounding observed after exposure to DATS for 24hrs in the presence or absence of NAC.

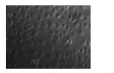

Cells propagated in growth media for 24hrs

Cells propagated in growth media for 48hrs

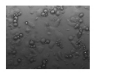

Cells exposed to DATS (150 µm) for 24hrs.

Cells exposed to DATS (150 µm) for 48hrs.

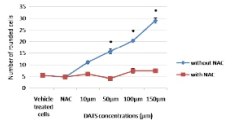

The amount of cell rounding observed after exposure to DATS for 24hrs in the presence or absence of NAC.

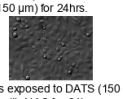

Cells exposed to DATS (150 µm) with NAC for 24hrs.

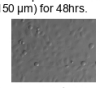

Cells exposed to DATS (150 µm) with NAC for 48hrs.

Cell death induction

Flow cytometry (Propidium iodide staining)

Flow cytometry results indicated a dose dependant increase in cell death when cells were exposed to DATS over 24hrs and 48hrs. This did not occur when cells were exposed in the presence of NAC for the same times.

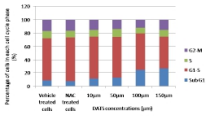

Flow cytometry results displaying the quantity of cells in each cell cycle phase after exposure to DATS for 24hrs.

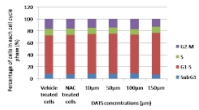

Flow cytometry results displaying the quantity of cells in each cell cycle phase after exposure to DATS in the presence of NAC for 24hrs.

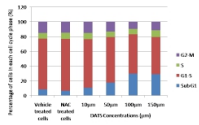

Flow cytometry results displaying the quantity of cells in each cell cycle phase after exposure to DATS for 48hrs.

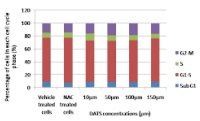

Flow cytometry results displaying the quantity of cells in each cell cycle phase after exposure to DATS in the presence of NAC for 48hrs.

ROS production

Fluorescent microscopy (DCFDA staining)

Fluorescent microscopy indicated a dose dependant increase in ROS production when cells were exposed to DATS.

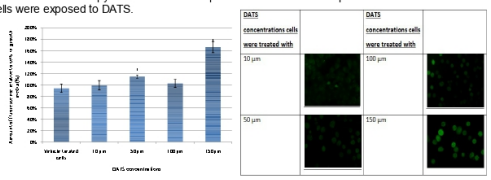

The amount of fluorescence observed after 24hrs of exposure to DATS.

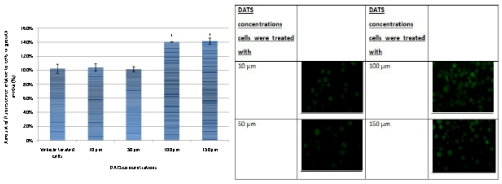

The amount of fluorescence observed after 48hrs of exposure to DATS.

Faculty of Health Sciences

13. Annexure B: University of Pretoria Faculty Day 2021 poster presented.

Effects of diallyl trisulfide-induced oxidative stress on proliferation, morphology and cell death in cancer cells

N. Surajlal[1], A.M. Joubert[1], F. Wenhold[2], M.H. Visagie[1]

1. Department of Physiology, School of Medicine, Faculty of Health Sciences, University of Pretoria, Pretoria, South Africa

2. Department of Human Nutrition, Faculty of Health Sciences, University of Pretoria.

Background

Breast cancer has become the most frequently diagnosed cancer worldwide accounting for 11.7% of new cancer diagnoses in 2020 followed by lung cancer (11.4%). Current cancer treatment strategies can have severe side effects which may result in treatment non-compliance and patient discomfort causing a shift towards phytomedicine. In this study we look at the effects of a garlic derived organosulphur compound called diallyl trisulphide (DATS) which has been shown to have antiproliferative and antimitotic effects on triple negative breast (MDA-MB-231) and lung (A549) cancer cells.

Materials and methods

The role of oxidative stress was investigated by means of a scavenger of reactive oxygen species (N-acetyl cystein (NAC)) and 6 inhibitors for specific ROS (table 1) for 24 and 48 hours in MDA-MB-231 and A549 cell lines, on proliferation (crystal violet staining and spectrophotometry), cell rounding (light microscopy), ROS production (2,7-dichlorofluoresceindiacetate (DCFDA) staining and fluorescent microscopy) and cell cycle progression and cell death induction (flow cytometry, ethanol fixation and propidium iodide staining).

Results

Table 1: Inhibitors for specific reactive oxygen species

Reactive oxygen species	Inhibitor
Hydrogen peroxide (H_2O_2)	N, N - dimethyl thiourea (DMTU)
Hydroxyl radical (•OH)	D – Mannitol
Nitric oxide (·NO)	2-(4-Carboxyphenyl)-4,4,5,5-tetramethylimidazoline-1-oxyl-3-oxide (Carboxy-PTIO)
Peroxyl radical (HO_2•)	Trolox
Singlet oxygen (O_2*)	Sodium azide
Superoxide anion (O_2^-)	Tiron

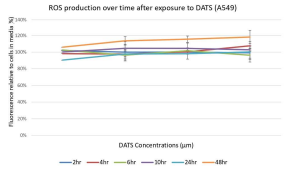

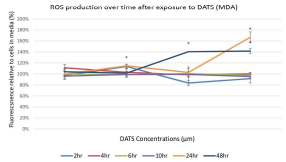

Figure 1: Fluorescent microscopy showing DCFDA staining results after exposure to DATS at various time intervals (2h, 4h, 6h, 10h, 24h, and 48h).

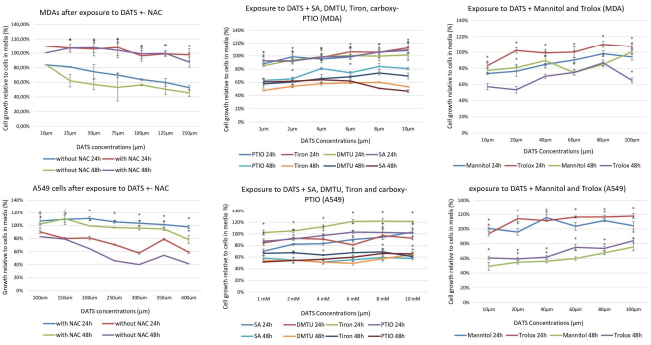

Figure 3: Crystal violet staining results showing proliferation relative to cells in growth media after exposure to DATS and the inhibitors for 24h. and 48h in both cell lines.

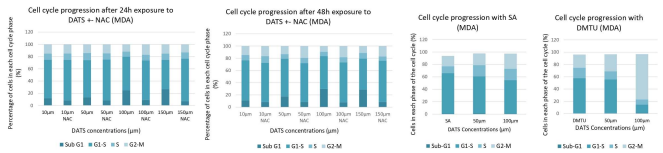

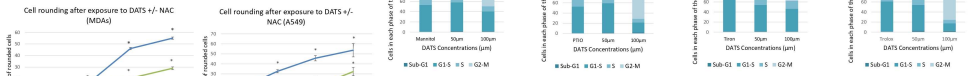

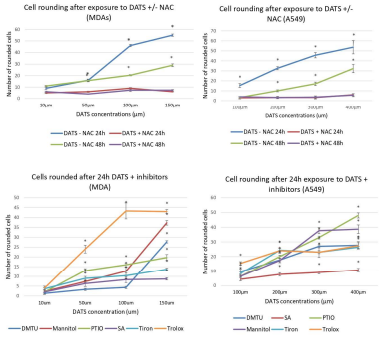

Figure 2: Light microscopy results showing the amount of cell rounding after exposure to DATS with the inhibitors for 24h, and 48h in both cell lines.

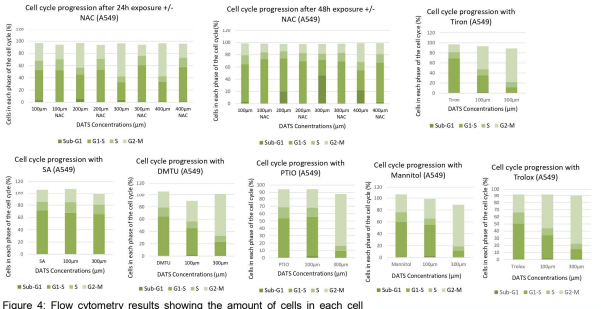

Figure 4: Flow cytometry results showing the amount of cells in each cell cycle phase after exposure to DATS with the inhibitors for 24h, and 48h in both cell lines.

Faculty of Health Sciences

14. Annexure C: University of Pretoria Faculty Day 2022 poster presented.

Oxidative stress-dependent effects exerted by diallyl trisulfide on proliferation and the activity of superoxide dismutase and catalase

Figure 1: Diallyl trisulfide (DATS)

N. Surajlal[1], A.M. Joubert[1], F. Wenhold[2], M.H. Visagie[1]

1. Department of Physiology, School of Medicine, Faculty of Health Sciences, University of Pretoria, Pretoria, South Africa

2. Department of Human Nutrition, Faculty of Health Sciences, University of Pretoria, Pretoria, South Africa

Background

Cancer is a global health concern with breast cancer being the most diagnosed cancer in sub-Saharan Africa accounting for 16.1% of the cancer incidences and 12.4% of the cancer related deaths, while lung cancer accounts for 2.8% of cancer incidences and 3.9% of cancer related deaths (1). The side effects of current treatment strategies may result in treatment non-compliance causing a shift towards plant-based medicinal compounds (2). In this study we investigate the effects of a garlic-derived organosulfur compound, diallyl trisulfide (DATS) which has been shown to have antiproliferative- and antimitotic effects on triple negative breast (MDA-MB-231) and lung (A549) cancer cells.

Materials and Methods

The role of oxidative stress was investigated by means of a scavenger of reactive oxygen species (ROS) N-acetyl cystein (NAC) and 6 inhibitors for specific ROS (Table 1) for 24 and 48 hours in MDA-MB-231 and A549 cell lines. The dependency of DATS on ROS and the specific ROS indicated in Table 1 with regards to its effect on proliferation (crystal violet staining and spectrophotometry) was investigated. In addition, dysregulation of the endogenous ROS modulating enzymes superoxide dismutase (SOD) and catalase was investigated using enzyme-linked immunosorbent assays (ELISA).

Results

This study demonstrated that DATS is dependent on ROS to exert its effect on breast and lung cancer cells. Furthermore, it is dependent on the presence of $O_2^{\bullet}$, H_2O_2, •NO, •OH, O_2^-, and $HO_2^{\bullet}$ to exert its effect (Figure 2 - 4).. Dysregulation of the endogenous enzymes SOD and catalase is a possible source of ROS. After 24 h increased SOD inhibition inversely related to DATS concentration was observed in the MDA-MB-231 cell line. After 48 h of exposure DATS SOD inhibition was decreased inversely to the DATS concentration (Figure 5 and 7). A significant decrease in SOD inhibition due to DATS was observed for the first time in this study in the A549 cell line. Catalase enzyme activity after DATS exposure for 24 h and 48 h in the MDA-MB-231 cell line, resulted in a dose-dependent- and time-dependant decrease in catalase activity. Similarly, in the A549 cell line a dose-dependent- and time-dependant decrease in catalase activity was observed (Figure 6 and 8).

Table 1: Inhibitors for specific reactive oxygen species

Reactive oxygen species	Inhibitor
Hydrogen peroxide (H_2O_2)	N, N - dimethyl thiourea (DMTU)
Hydroxyl radical (•OH)	D – Mannitol
Nitric oxide (-NO)	2-(4-Carboxyphenyl)-4,4,5,5-tetramethylimidazoline-1-oxyl-3-oxide (Carboxy-PTIO)
Peroxyl radical ($HO_2^{\bullet}$)	Trolox
Singlet oxygen ($O_2^{\bullet}$)	Sodium azide
Superoxide anion (O_2^-)	Tiron

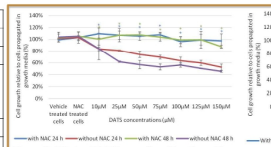

Figure 2: Effect of DATS on cell proliferation of the MDA-MB-231 cells in the presence and absence of NAC.

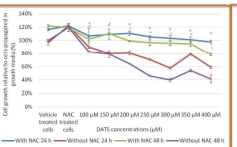

Figure 3: Effect of DATS on cell proliferation of the A549 cells in the presence and absence of NAC.

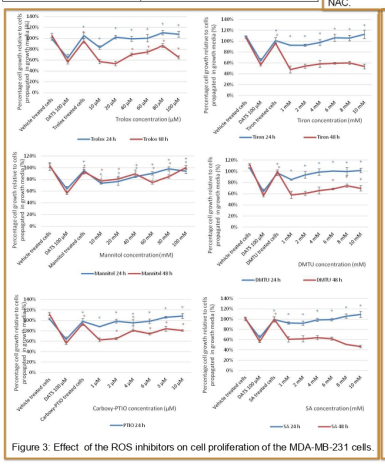

Figure 3: Effect of the ROS inhibitors on cell proliferation of the MDA-MB-231 cells.

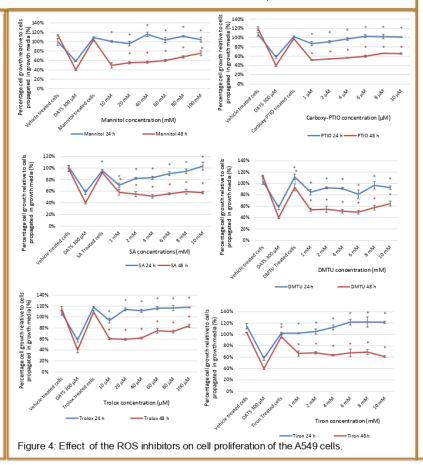

Figure 4: Effect of the ROS inhibitors on cell proliferation of the A549 cells.

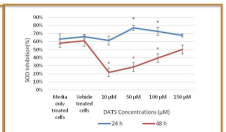

Figure 5: Effect of DATS on SOD inhibition of the MDA-MB-231 cells.

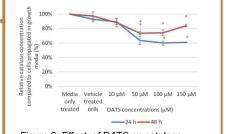

Figure 6: Effect of DATS on catalase concentration in the MDA-MB-231 cells.

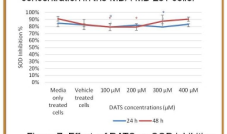

Figure 7: Effect of DATS on SOD inhibition of the A549 cells.

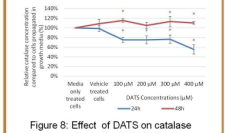

Figure 8: Effect of DATS on catalase concentration in the A549 cells.

Discussion and conclusion

Exposure to DATS with the inhibitors indicated that the effects of DATS were dependent on oxidative stress produced by $O_2^{\bullet}$, H_2O_2, •NO, •OH, O_2^- and $HO_2^{\bullet}$ particularly after 24 h in both cell lines. The effect of DATS to increase SOD inhibition and decrease catalase activity was more prominent after 24 h and the cells began recovering after 48 h in both cell lines. This study made the novel discovery that DATS modulates the endogenous ROS modulating enzymes SOD and catalase to exert its effects. This study therefore, provides new insight into the mechanism of action of DATS and other naturally occurring small sulfur containing compounds.

References

1. Ngwa W, Addai B, Adewole I, Ainsworth V, Alaro J, Alatise O et al. Cancer in sub-Saharan Africa: a Lancet Oncology Commission. Lancet Oncol. 2022;23(6):e251-e312.
2. Bonam S, Wu Y, Tunki L, Chellian R, Halmuthur M, Muller S, Pandy V. What has come out from phytomedicines and herbal edibles for the treatment of cancer? ChemMedChem. 2018;13(18):1854-1872.

Acknowledgements

RESCOM UNIVERSITY OF PRETORIA
SGKN (Trust) University of Pretoria
NRF National Research Foundation
MRC SOUTH AFRICAN MEDICAL RESEARCH COUNCIL
CANSA Research • Educate • Support
Faculty of Health Sciences